Fracture and Bending Mechanics

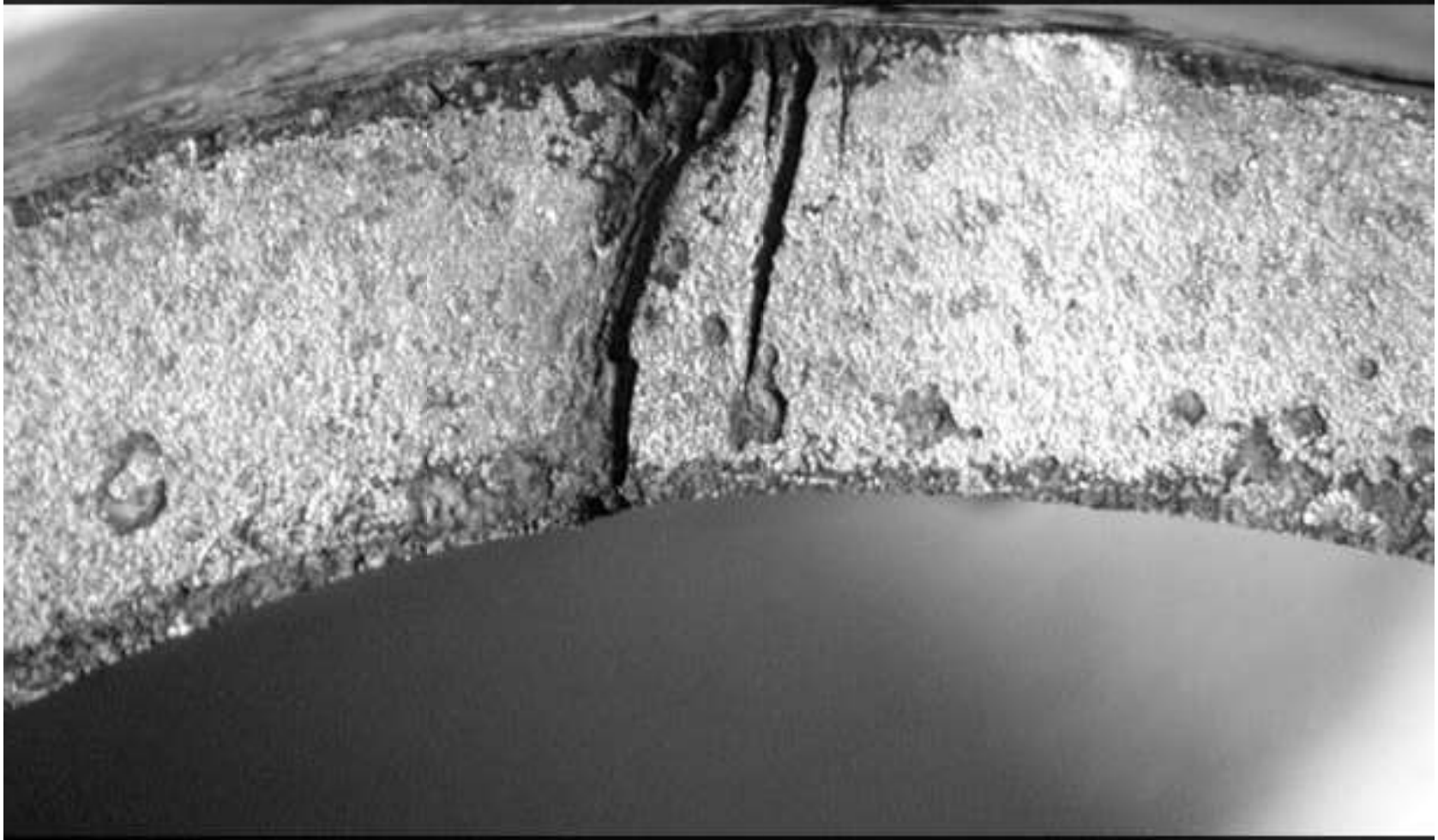

Erich Cavazos

Robert Khan

First Edition, 2012

ISBN 978-81-323-0884-3

Published by:
Academic Studio
4735/22 Prakashdeep Bldg,
Ansari Road, Darya Ganj,
Delhi - 110002
Email: info@wtbooks.com

Table of Contents

Chapter 1

Fracture Mechanics

Fracture mechanics is the field of mechanics concerned with the study of the propagation of cracks in materials. It uses methods of analytical solid mechanics to calculate the driving force on a crack and those of experimental solid mechanics to characterize the material's resistance to fracture.

In modern materials science, fracture mechanics is an important tool in improving the mechanical performance of materials and components. It applies the physics of stress and strain, in particular the theories of elasticity and plasticity, to the microscopic crystallographic defects found in real materials in order to predict the macroscopic mechanical failure of bodies. Fractography is widely used with fracture mechanics to understand the causes of failures and also verify the theoretical failure predictions with real life failures.

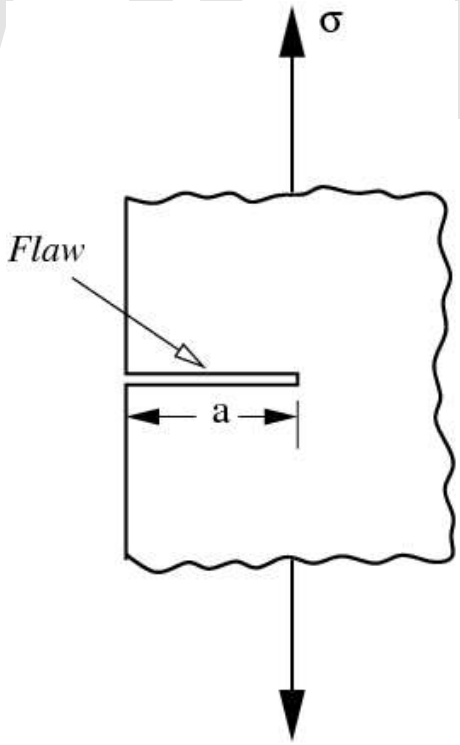

An edge crack (flaw) of length *a* in a material.

Linear elastic fracture mechanics

Griffith's criterion

Fracture mechanics was developed during World War I by English aeronautical engineer, A. A. Griffith, to explain the failure of brittle materials. Griffith's work was motivated by two contradictory facts:

- The stress needed to fracture bulk glass is around 100 MPa (15,000 psi).
- The theoretical stress needed for breaking atomic bonds is approximately 10,000 MPa (1,500,000 psi).

A theory was needed to reconcile these conflicting observations. Also, experiments on glass fibers that Griffith himself conducted suggested that the fracture stress increases as the fiber diameter decreases. Hence the uniaxial tensile strength, which had been used extensively to predict material failure before Griffith, could not be a specimen-independent material property. Griffith suggested that the low fracture strength observed in experiments, as well as the size-dependence of strength, was due to the presence of microscopic flaws in the bulk material.

To verify the flaw hypothesis, Griffith introduced an artificial flaw in his experimental specimens. The artificial flaw was in the form of a surface crack which was much larger than other flaws in a specimen. The experiments showed that the product of the square root of the flaw length (a) and the stress at fracture (σ_f) was nearly constant, which is expressed by the equation:

$$\sigma_f \sqrt{a} \approx C$$

An explanation of this relation in terms of linear elasticity theory is problematic. Linear elasticity theory predicts that stress (and hence the strain) at the tip of a sharp flaw in a linear elastic material is infinite. To avoid that problem, Griffith developed a thermodynamic approach to explain the relation that he observed.

The growth of a crack requires the creation of two new surfaces and hence an increase in the surface energy. Griffith found an expression for the constant C in terms of the surface energy of the crack by solving the elasticity problem of a finite crack in an elastic plate. Briefly, the approach was:

- Compute the potential energy stored in a perfect specimen under an uniaxial tensile load.
- Fix the boundary so that the applied load does no work and then introduce a crack into the specimen. The crack relaxes the stress and hence reduces the elastic energy near the crack faces. On the other hand, the crack increases the total surface energy of the specimen.
- Compute the change in the free energy (surface energy − elastic energy) as a function of the crack length. Failure occurs when the free energy attains a peak

value at a critical crack length, beyond which the free energy decreases by increasing the crack length, i.e. by causing fracture. Using this procedure, Griffith found that

$$C = \sqrt{\frac{2E\gamma}{\pi}}$$

where E is the Young's modulus of the material and γ is the surface energy density of the material. Assuming E = 62 GPa and γ = 1 J/m^2 gives excellent agreement of Griffith's predicted fracture stress with experimental results for glass.

Irwin's modification

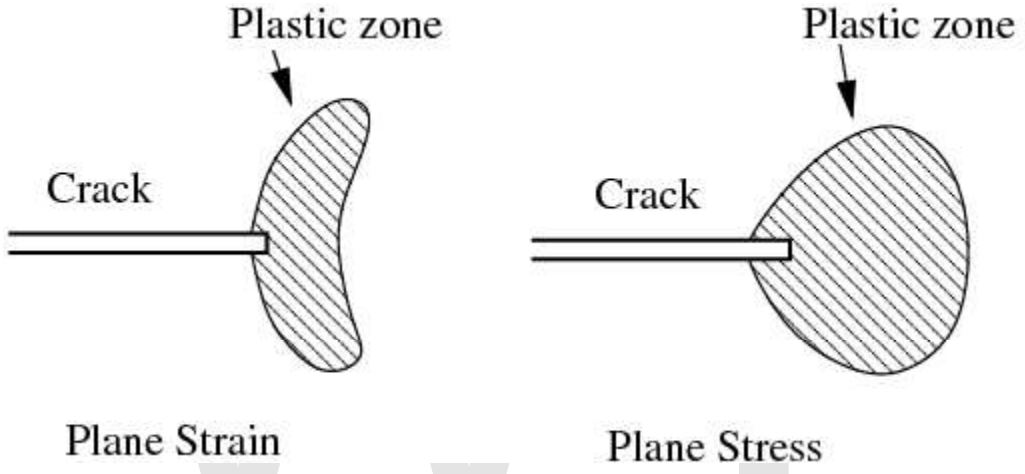

The plastic zone around a crack tip in a ductile material.

Griffith's work was largely ignored by the engineering community until the early 1950s. The reasons for this appear to be (a) in the actual structural materials the level of energy needed to cause fracture is orders of magnitude higher than the corresponding surface energy, and (b) in structural materials there are always some inelastic deformations around the crack front that would make the assumption of linear elastic medium with infinite stresses at the crack tip highly unrealistic. **F. Erdogan (2000)**

Griffith's theory provides excellent agreement with experimental data for brittle materials such as glass. For ductile materials such as steel, though the relation $\sigma_y\sqrt{a} = C$ still holds, the surface energy (γ) predicted by Griffith's theory is usually unrealistically high. A group working under G. R. Irwin at the U.S. Naval Research Laboratory (NRL) during World War II realized that plasticity must play a significant role in the fracture of ductile materials.

In ductile materials (and even in materials that appear to be brittle), a plastic zone develops at the tip of the crack. As the applied load increases, the plastic zone increases in size until the crack grows and the material behind the crack tip unloads. The plastic

loading and unloading cycle near the crack tip leads to the dissipation of energy as heat. Hence, a dissipative term has to be added to the energy balance relation devised by Griffith for brittle materials. In physical terms, additional energy is needed for crack growth in ductile materials when compared to brittle materials.

Irwin's strategy was to partition the energy into two parts:

- the stored elastic strain energy which is released as a crack grows. This is the thermodynamic driving force for fracture.
- the dissipated energy which includes plastic dissipation and the surface energy (and any other dissipative forces that may be at work). The dissipated energy provides the thermodynamic resistance to fracture. Then the total energy dissipated is

$$G = 2\gamma + G_p$$

where γ is the surface energy and G_p is the plastic dissipation (and dissipation from other sources) per unit area of crack growth.

The modified version of Griffith's energy criterion can then be written as

$$\sigma_f \sqrt{a} = \sqrt{\frac{E\ G}{\pi}}.$$

For brittle materials such as glass, the surface energy term dominates and $G \approx 2\gamma = 2\ J/m^2$. For ductile materials such as steel, the plastic dissipation term dominates and $G \approx G_p = 1000\ J/m^2$. For polymers close to the glass transition temperature, we have intermediate values of $G \approx 2 - 1000\ J/m^2$.

Stress intensity factor

Another significant achievement of Irwin and his colleagues was to find a method of calculating the amount of energy available for fracture in terms of the asymptotic stress and displacement fields around a crack front in a linear elastic solid. This asymptotic expression for the stress field around a crack tip is

$$\sigma_{ij} \approx \left(\frac{K}{\sqrt{2\pi r}} \right) \ f_{ij}(\theta)$$

where σ_{ij} are the Cauchy stresses, r is the distance from the crack tip, θ is the angle with respect to the plane of the crack, and f_{ij} are functions that are independent of the crack geometry and loading conditions. Irwin called the quantity K the *stress intensity factor*.

Since the quantity f_{ij} is dimensionless, the stress intensity factor can be expressed in units of $\mathrm{MPa}\text{-}\sqrt{\mathrm{m}}$.

When a rigid line inclusion is considered, a similar asymptotic expression for the stress fields is obtained.

Strain energy release

Irwin was the first to observe that if the size of the plastic zone around a crack is small compared to the size of the crack, the energy required to grow the crack will not be critically dependent on the state of stress at the crack tip. In other words, a purely elastic solution may be used to calculate the amount of energy available for fracture.

The energy release rate for crack growth or *strain energy release rate* may then be calculated as the change in elastic strain energy per unit area of crack growth, i.e.,

$$G := -\left[\frac{\partial U}{\partial a}\right]_P = -\left[\frac{\partial U}{\partial a}\right]_u$$

where U is the elastic energy of the system and a is the crack length. Either the load P or the displacement u can be kept fixed while evaluating the above expressions.

Irwin showed that for a mode I crack (opening mode) the strain energy release rate and the stress intensity factor are related by:

$$G = G_I = \begin{cases} \dfrac{K_I^2}{E} & \text{plane stress} \\ \dfrac{(1-\nu^2)K_I^2}{E} & \text{plane strain} \end{cases}$$

where E is the Young's modulus, v is Poisson's ratio, and K_I is the stress intensity factor in mode I. Irwin also showed that the strain energy release rate of a planar crack in a linear elastic body can be expressed in terms of the mode I, mode II (sliding mode), and mode III (tearing mode) stress intensity factors for the most general loading conditions.

Next, Irwin adopted the additional assumption that the size and shape of the energy dissipation zone remains approximately constant during brittle fracture. This assumption suggests that the energy needed to create a unit fracture surface is a constant that depends only on the material. This new material property was given the name *fracture toughness* and designated G_{Ic}. Today, it is the critical stress intensity factor K_{Ic} which is accepted as the defining property in linear elastic fracture mechanics.

Limitations

The S.S. *Schenectady* split apart by brittle fracture while in harbor (1944)

But a problem arose for the NRL researchers because naval materials, e.g., ship-plate steel, are not perfectly elastic but undergo significant plastic deformation at the tip of a crack. One basic assumption in Irwin's linear elastic fracture mechanics is that the size of the plastic zone is small compared to the crack length. However, this assumption is quite restrictive for certain types of failure in structural steels though such steels can be prone to brittle fracture, which has led to a number of catastrophic failures.

Linear-elastic fracture mechanics is of limited practical use for structural steels for another more practical reason. Fracture toughness testing is very expensive and engineers believe that sufficient information for selection of steels can be obtained from the simpler and cheaper Charpy impact test.

Nonlinear elasticity and plasticity

Vertical stabilizer, which separated from American Airlines Flight 587, leading to a fatal crash

Most engineering materials show some nonlinear elastic and inelastic behavior under operating conditions that involve large loads. In such materials the assumptions of linear elastic fracture mechanics may not hold, that is,

- the plastic zone at a crack tip may have a size of the same order of magnitude as the crack size
- the size and shape of the plastic zone may change as the applied load is increased and also as the crack length increases.

Therefore a more general theory of crack growth is needed for elastic-plastic materials that can account for:

- the local conditions for initial crack growth which include the nucleation, growth, and coalescence of voids or decohesion at a crack tip.
- a global energy balance criterion for further crack growth and unstable fracture.

R-curve

An early attempt in the direction of elastic-plastic fracture mechanics was Irwin's **crack extension resistance curve** or **R-curve**. This curve acknowledges the fact that the resistance to fracture increases with growing crack size in elastic-plastic materials. The

R-curve is a plot of the total energy dissipation rate as a function of the crack size and can be used to examine the processes of slow stable crack growth and unstable fracture. However, the R-curve was not widely used in applications until the early 1970s. The main reasons appear to be that the R-curve depends on the geometry of the specimen and the crack driving force may be difficult to calculate.

J-integral

In the mid-1960s James R. Rice (then at Brown University) and G. P. Cherepanov independently developed a new toughness measure to describe the case where there is sufficient crack-tip deformation that the part no longer obeys the linear-elastic approximation. Rice's analysis, which assumes non-linear elastic (or monotonic deformation-theory plastic) deformation ahead of the crack tip, is designated the J integral. This analysis is limited to situations where plastic deformation at the crack tip does not extend to the furthest edge of the loaded part. It also demands that the assumed non-linear elastic behavior of the material is a reasonable approximation in shape and magnitude to the real material's load response.

Fully plastic failure

If the material is so tough that the yielded region ahead of the crack extends to the far edge of the specimen before fracture, the crack is no longer an effective stress concentrator. Instead, the presence of the crack merely serves to reduce the load-bearing area. In this regime the failure stress is conventionally assumed to be the average of the yield and ultimate strengths of the material.

Engineering applications

The following information is needed for a fracture mechanics prediction of failure:

- Applied load
- Residual stress
- Size and shape of the part
- Size, shape, location, and orientation of the crack

Usually not all of this information is available and conservative assumptions have to be made.

Occasionally post-mortem fracture-mechanics analyses are carried out. In the absence of an extreme overload, the causes are either insufficient toughness (K_{Ic}) or an excessively large crack that was not detected during routine inspection.

Short summary

Arising from the manufacturing process, interior and surface flaws are found in all metal structures. Not all such flaws are unstable under service conditions. Fracture mechanics is

the analysis of flaws to discover those that are safe (that is, do not grow) and those that are liable to propagate as cracks and so cause failure of the flawed structure. Ensuring safe operation of structure despite these inherent flaws is achieved through damage tolerance analysis. Fracture mechanics as a subject for critical study has barely been around for a century and thus is relatively new. There is a high demand for engineers with fracture mechanics expertise—particularly in this day and age where engineering failure is considered 'shocking' amongst the general public.

Appendix: mathematical relations

Griffith's criterion

For the simple case of a thin rectangular plate with a crack perpendicular to the load Griffith's theory becomes:

$$G = \frac{\pi \sigma^2 a}{E} \qquad (1.1)$$

where G is the strain energy release rate, σ is the applied stress, a is half the crack length, and E is the Young's modulus. The strain energy release rate can otherwise be understood as: *the rate at which energy is absorbed by growth of the crack*.

However, we also have that:

$$G_c = \frac{\pi \sigma_f^2 a}{E} \qquad (1.2)$$

If $G \geq G_c$, this is the criterion for which the crack will begin to propagate.

Irwin's modifications

Eventually a modification of Griffith's solids theory emerged from this work; a term called stress intensity replaced strain energy release rate and a term called fracture toughness replaced surface weakness energy. Both of these terms are simply related to the energy terms that Griffith used:

$$K_I = \sigma \sqrt{\pi a} \qquad (2.1)$$

and

$$K_c = \sqrt{E G_c} \text{ (for plane stress)} \qquad (2.2)$$

$$K_c = \sqrt{\frac{E G_c}{1 - \nu^2}} \text{ (for plane strain)} \qquad (2.3)$$

where K_I is the stress intensity, K_c the fracture toughness, and ν is Poisson's ratio. It is important to recognize the fact that fracture parameter K_c has different values when measured under plane stress and plane strain

Fracture occurs when $K_I \geq K_c$. For the special case of plane strain deformation, K_c becomes K_{Ic} and is considered a material property. The subscript I arises because of the different ways of loading a material to enable a crack to propagate. It refers to so-called "mode I" loading as opposed to mode II or III:

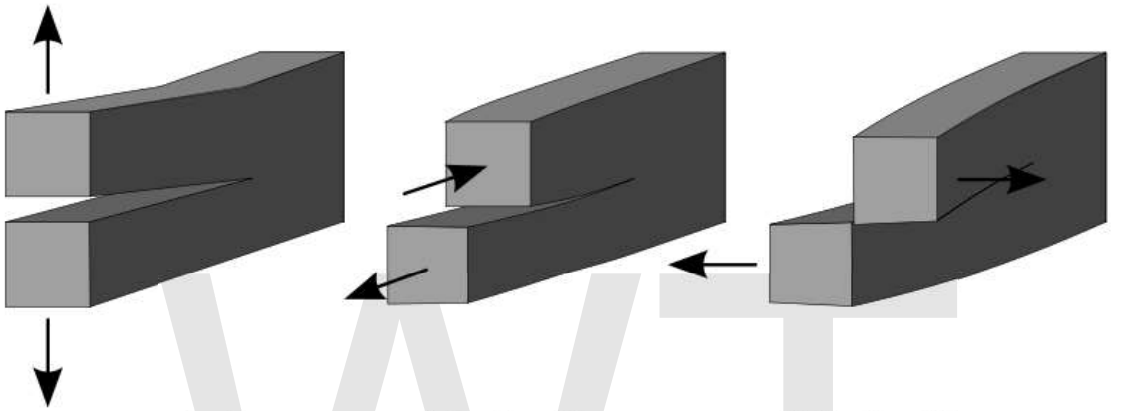

The three fracture modes.

There are three ways of applying a force to enable a crack to propagate:

- **Mode I crack** – Opening mode (a tensile stress normal to the plane of the crack)
- **Mode II crack** – Sliding mode (a shear stress acting parallel to the plane of the crack and perpendicular to the crack front)
- **Mode III crack** – Tearing mode (a shear stress acting parallel to the plane of the crack and parallel to the crack front)

We must note that the expression for K_I in equation 2.1 will be different for geometries other than the center-cracked infinite plate, as discussed in stress intensity. Consequently, it is necessary to introduce a dimensionless correction factor, Y, in order to characterize the geometry. We thus have:

$$K_I = Y\sigma\sqrt{\pi a} \qquad (2.4)$$

where Y is a function of the crack length and width of sheet given by:

$$Y\left(\frac{a}{W}\right) = \sqrt{\sec\left(\frac{\pi a}{W}\right)} \qquad (2.5)$$

for a sheet of finite width W containing a through-thickness crack of length $2a$, or

$$Y\left(\frac{a}{W}\right) = 1.12 - \frac{0.41}{\sqrt{\pi}}\frac{a}{W} + \frac{18.7}{\sqrt{\pi}}\left(\frac{a}{W}\right)^2 - \cdots \qquad (2.6)$$

for a sheet of finite width W containing a through-thickness edge crack of length a

Elasticity and plasticity

Since engineers became accustomed to using K_{Ic} to characterise fracture toughness, a relation has been used to reduce J_{Ic} to it:

$$K_{Ic} = \sqrt{E^* J_{Ic}}$$ where $E^* = E$ for plane stress and $E^* = \frac{E}{1-\nu^2}$ for plane strain (3.1)

The remainder of the mathematics employed in this approach is interesting, but is probably better summarised in external pages due to its complex nature.

Chapter 2

Fatigue (Material)

In materials science, **fatigue** is the progressive and localized structural damage that occurs when a material is subjected to cyclic loading. The nominal maximum stress values are less than the ultimate tensile stress limit, and may be below the yield stress limit of the material.

Fatigue occurs when a material is subjected to repeated loading and unloading. If the loads are above a certain threshold, microscopic cracks will begin to form at the surface. Eventually a crack will reach a critical size, and the structure will suddenly fracture. The shape of the structure will significantly affect the fatigue life; square holes or sharp corners will lead to elevated local stresses where fatigue cracks can initiate. Round holes and smooth transitions or fillets are therefore important to increase the fatigue strength of the structure.

Fatigue life

ASTM defines *fatigue life*, N_f, as the number of stress cycles of a specified character that a specimen sustains before failure of a specified nature occurs.

One method to predict fatigue life of materials is the Uniform Material Law (UML). UML was developed for fatigue life prediction of aluminum and titanium alloys by the end of 20th century and extended to high-strength steels.

Characteristics of fatigue

Fracture of an aluminium crank arm. Dark area of striations: slow crack growth. Bright granular area: sudden fracture.

- In metals and alloys, the process starts with dislocation movements, eventually forming persistent slip bands that nucleate short cracks.
- Fatigue is a stochastic process, often showing considerable scatter even in controlled environments.
- The greater the applied stress range, the shorter the life.
- Fatigue life scatter tends to increase for longer fatigue lives.
- Damage is cumulative. Materials do not recover when rested.
- Fatigue life is influenced by a variety of factors, such as temperature, surface finish, microstructure, presence of oxidizing or inert chemicals, residual stresses, contact (fretting), etc.
- Some materials (e.g., some steel and titanium alloys) exhibit a theoretical fatigue limit below which continued loading does not lead to structural failure.

- In recent years, researchers (see, for example, the work of Bathias, Murakami, and Stanzl-Tschegg) have found that failures occur below the theoretical fatigue limit at very high fatigue lives (10^9 to 10^{10} cycles). An ultrasonic resonance technique is used in these experiments with frequencies around 10–20 kHz.
- High cycle fatigue strength (about 10^3 to 10^8 cycles) can be described by stress-based parameters. A load-controlled servo-hydraulic test rig is commonly used in these tests, with frequencies of around 20–50 Hz. Other sorts of machines—like resonant magnetic machines—can also be used, achieving frequencies up to 250 Hz.
- Low cycle fatigue (typically less than 10^3 cycles) is associated with widespread plasticity in metals; thus, a strain-based parameter should be used for fatigue life prediction in metals and alloys. Testing is conducted with constant strain amplitudes typically at 0.01–5 Hz.

Timeline of early fatigue research history

- 1837: Wilhelm Albert publishes the first article on fatigue. He devised a test machine for conveyor chains used in the Clausthal mines.
- 1839: Jean-Victor Poncelet describes metals as being *tired* in his lectures at the military school at Metz.
- 1842: William John Macquorn Rankine recognises the importance of stress concentrations in his investigation of railroad axle failures. The Versailles train crash was caused by axle fatigue.
- 1843: Joseph Glynn reports on fatigue of axle on locomotive tender. He identifies the keyway as the crack origin.
- 1848: Railway Inspectorate report one of the first tyre failures, probably from a rivet hole in tread of railway carriage wheel. It was likely a fatigue failure.
- 1849: Eaton Hodgkinson is granted a *small sum of money* to report to the UK Parliament on his work in *ascertaining by direct experiment, the effects of continued changes of load upon iron structures and to what extent they could be loaded without danger to their ultimate security*.
- 1854: Braithwaite reports on common service fatigue failures and coins the term *fatigue*.
- 1860: Systematic fatigue testing undertaken by Sir William Fairbairn and August Wöhler.
- 1870: Wöhler summarises his work on railroad axles. He concludes that cyclic stress range is more important than peak stress and introduces the concept of *endurance limit*.

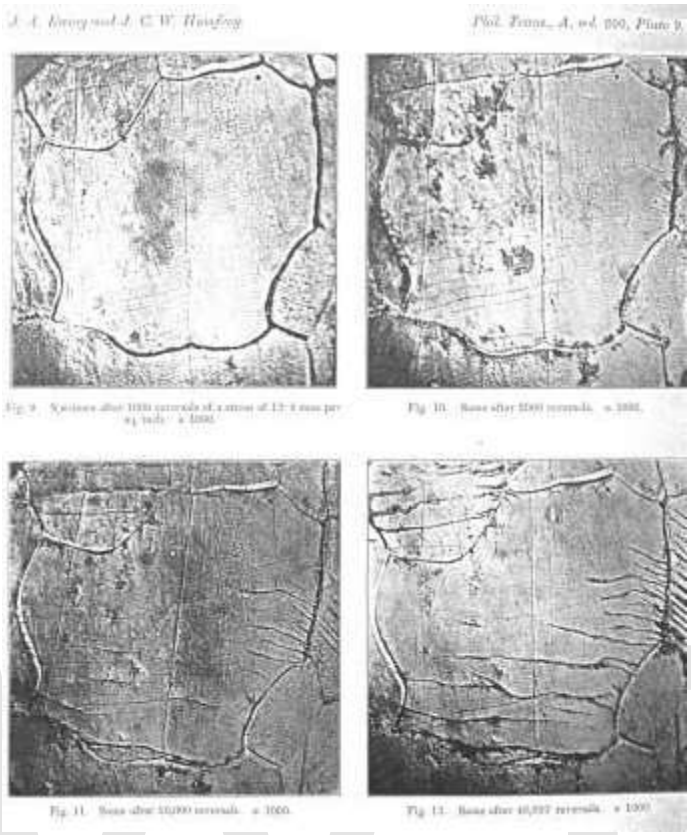

Micrographs showing how surface fatigue cracks grow as material is further cycled. From Ewing & Humfrey (1903)

- 1903: Sir James Alfred Ewing demonstrates the origin of fatigue failure in microscopic cracks.
- 1910: O. H. Basquin proposes a log-log relationship for SN curves, using Wöhler's test data.
- 1945: A. M. Miner popularises A. Palmgren's (1924) linear damage hypothesis as a practical design tool.
- 1954: L. F. Coffin and S. S. Manson explain fatigue crack-growth in terms of plastic strain in the tip of cracks.
- 1961: P. C. Paris proposes methods for predicting the rate of growth of individual fatigue cracks in the face of initial scepticism and popular defence of Miner's phenomenological approach.
- 1968: Tatsuo Endo and M. Matsuishi devise the rainflow-counting algorithm and enable the reliable application of Miner's rule to random loadings.
- 1970: W. Elber elucidates the mechanisms and importance of crack closure in slowing the growth of a fatigue crack due to the wedging effect of plastic deformation left behind the tip of the crack.

High-cycle fatigue

Historically, most attention has focused on situations that require more than 10^4 cycles to failure where stress is low and deformation primarily elastic.

The S-N curve

In high-cycle fatigue situations, materials performance is commonly characterised by an *S-N curve*, also known as a *Wöhler curve* . This is a graph of the magnitude of a cyclic stress (*S*) against the logarithmic scale of cycles to failure (*N*).

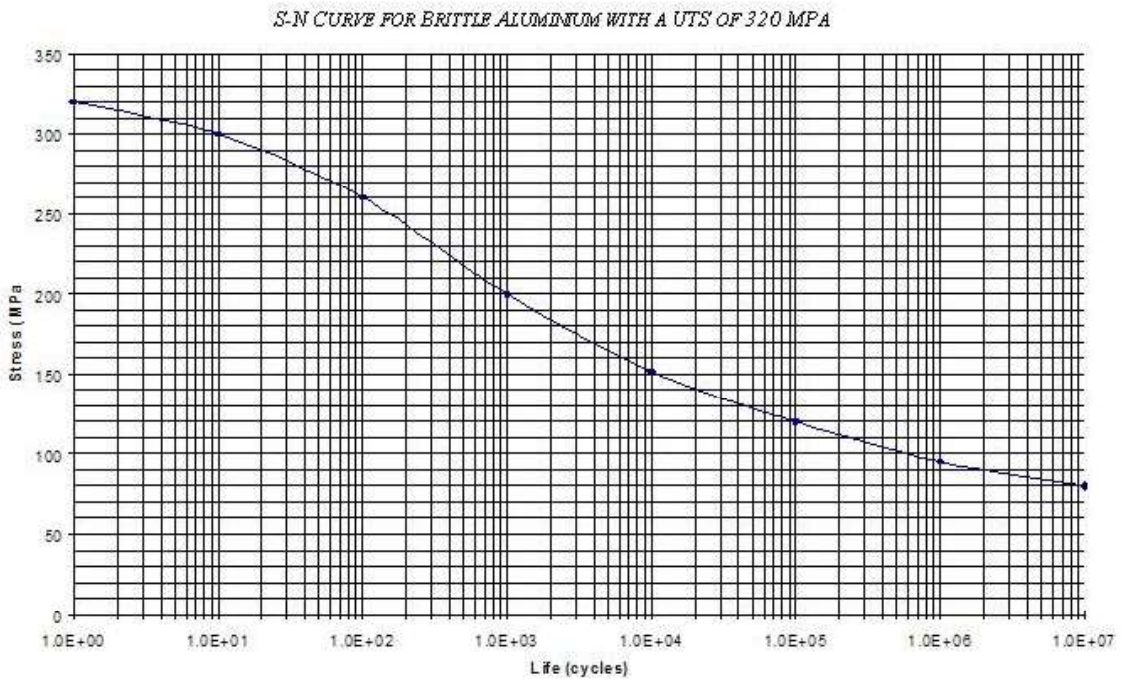

S-N curves are derived from tests on samples of the material to be characterised (often called *coupons*) where a regular sinusoidal stress is applied by a testing machine which also counts the number of cycles to failure. This process is sometimes known as *coupon testing*. Each coupon test generates a point on the plot though in some cases there is a *runout* where the time to failure exceeds that available for the test. Analysis of fatigue data requires techniques from statistics, especially survival analysis and linear regression.

Probabilistic nature of fatigue

As coupons sampled from a homogeneous frame will manifest variation in their number of cycles to failure, the S-N curve should more properly be an *S-N-P curve* capturing the probability of failure after a given number of cycles of a certain stress. Probability distributions that are common in data analysis and in design against fatigue include the

lognormal distribution, extreme value distribution, Birnbaum–Saunders distribution, and Weibull distribution.

Complex loadings

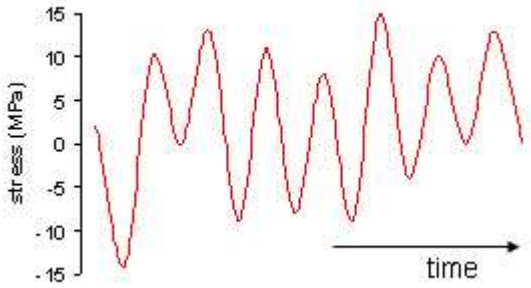

Spectrum loading

In practice, a mechanical part is exposed to a complex, often random, sequence of loads, large and small. In order to assess the safe life of such a part:

1. Reduce the complex loading to a series of simple cyclic loadings using a technique such as rainflow analysis;
2. Create a histogram of cyclic stress from the rainflow analysis to form a fatigue damage spectrum;
3. For each stress level, calculate the degree of cumulative damage incurred from the S-N curve; and
4. Combine the individual contributions using an algorithm such as *Miner's rule*.

Miner's rule

In 1945, M. A. Miner popularised a rule that had first been proposed by A. Palmgren in 1924. The rule, variously called *Miner's rule* or the *Palmgren-Miner linear damage hypothesis*, states that where there are k different stress magnitudes in a spectrum, S_i ($1 \leq i \leq k$), each contributing $n_i(S_i)$ cycles, then if $N_i(S_i)$ is the number of cycles to failure of a constant stress reversal S_i, failure occurs when:

$$\sum_{i=1}^{k} \frac{n_i}{N_i} = C$$

C is experimentally found to be between 0.7 and 2.2. Usually for design purposes, C is assumed to be 1.

This can be thought of as assessing what proportion of life is consumed by stress reversal at each magnitude then forming a linear combination of their aggregate.

Though Miner's rule is a useful approximation in many circumstances, it has several major limitations:

1. It fails to recognise the probabilistic nature of fatigue and there is no simple way to relate life predicted by the rule with the characteristics of a probability distribution. Industry analysts often use design curves, adjusted to account for scatter, to calculate $N_i(S_i)$.
2. There is sometimes an effect in the order in which the reversals occur. In some circumstances, cycles of low stress followed by high stress cause more damage than would be predicted by the rule. It does not consider the effect of overload or high stress which may result in a compressive residual stress. High stress followed by low stress may have less damage due to the presence of compressive residual stress.

Paris' Relationship

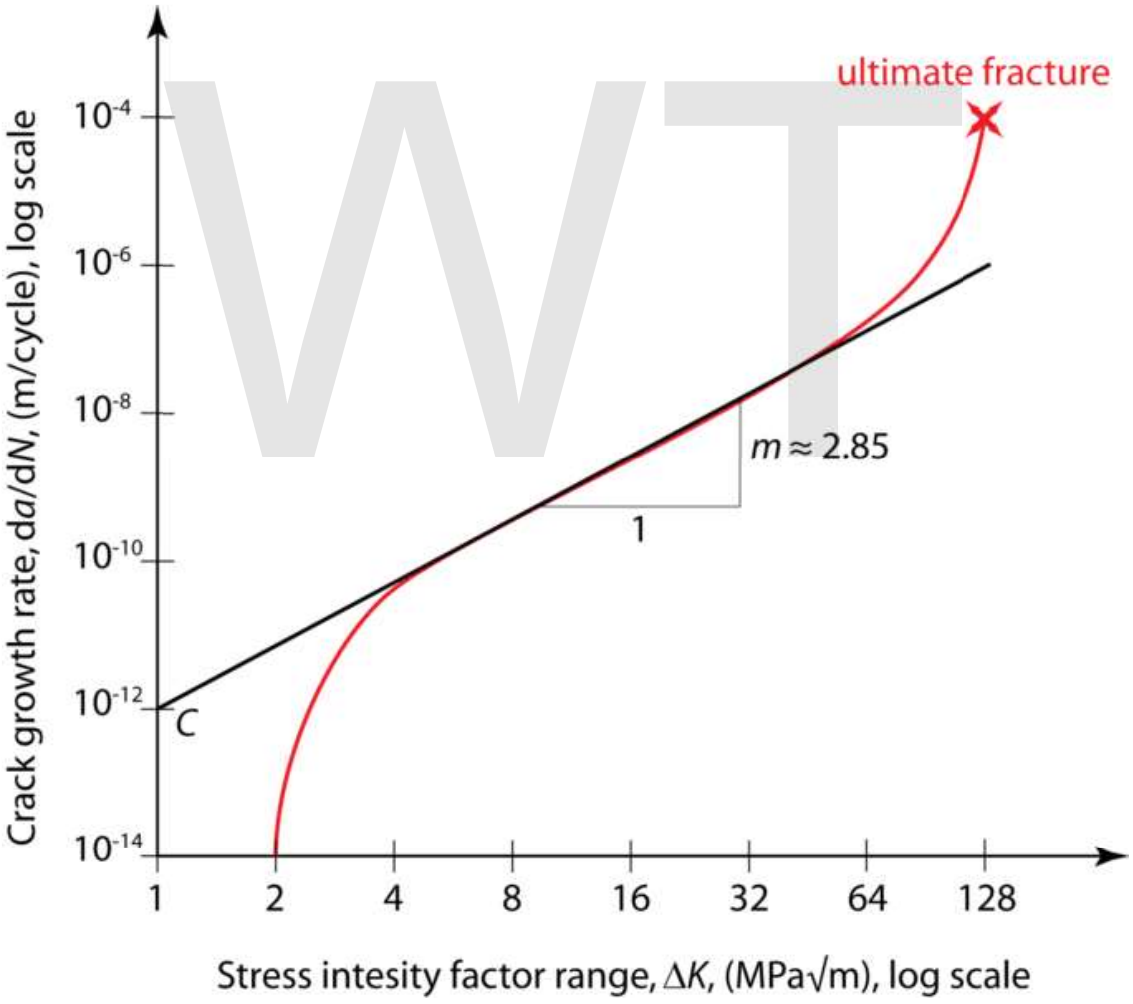

Typical fatigue crack growth rate graph.

In Fracture mechanics, Anderson, Gomez and Paris derived relationships for the stage II crack growth with cycles N, in terms of the cyclical component ΔK of the Stress Intensity Factor K

$$\frac{\mathrm{d}a}{\mathrm{d}N} = C(\Delta K)^m$$

where a is the crack length and m is typically in the range 3 to 5 (for metals).

This relationship was later modified (by Forman, 1967) to make better allowance for the mean stress, by introducing a factor depending on (1-R) where R = min stress/max stress, in the denominator.

Low-cycle fatigue

Where the stress is high enough for plastic deformation to occur, the account in terms of stress is less useful and the strain in the material offers a simpler description. Low-cycle fatigue is usually characterised by the *Coffin-Manson relation* (published independently by L. F. Coffin in 1954 and S. S. Manson 1953):

$$\frac{\Delta\epsilon_p}{2} = \epsilon'_f(2N)^c$$

-where:

- $\Delta\varepsilon_p$ /2 is the plastic strain amplitude;
- ε_f' is an empirical constant known as the *fatigue ductility coefficient*, the failure strain for a single reversal;
- 2*N* is the number of reversals to failure (*N* cycles);
- *c* is an empirical constant known as the *fatigue ductility exponent*, commonly ranging from -0.5 to -0.7 for metals in time independent fatigue. Slopes can be considerably steeper in the presence of creep or environmental interactions.

A similar relationship for materials such as Zirconium, used in the nuclear industry.

Fatigue and fracture mechanics

The account above is purely empirical and, though it allows life prediction and design assurance, life improvement or design optimisation can be enhanced using fracture mechanics. It can be developed in four stages.

1. Crack nucleation;
2. Stage I crack-growth;
3. Stage II crack-growth; and
4. Ultimate ductile failure.

Factors that affect fatigue-life

- **Cyclic stress state:** Depending on the complexity of the geometry and the loading, one or more properties of the stress state need to be considered, such as stress amplitude, mean stress, biaxiality, in-phase or out-of-phase shear stress, and load sequence,
- **Geometry:** Notches and variation in cross section throughout a part lead to stress concentrations where fatigue cracks initiate.
- **Surface quality.** Surface roughness cause microscopic stress concentrations that lower the fatigue strength. Compressive residual stresses can be introduced in the surface by e.g. shot peening to increase fatigue life. Such techniques for producing surface stress are often referred to as *peening*, whatever the mechanism used to produce the stress. Low Plasticity Burnishing, Laser peening, and ultrasonic impact treatment can also produce this surface compressive stress and can increase the fatigue life of the component. This improvement is normally observed only for high-cycle fatigue.

- **Material Type:** Fatigue life, as well as the behavior during cyclic loading, varies widely for different materials, e.g. composites and polymers differ markedly from metals.

- **Residual stresses:** Welding, cutting, casting, and other manufacturing processes involving heat or deformation can produce high levels of tensile residual stress, which decreases the fatigue strength.

- **Size and distribution of internal defects:** Casting defects such as gas porosity, non-metallic inclusions and shrinkage voids can significantly reduce fatigue strength.

- **Direction of loading:** For non-isotropic materials, fatigue strength depends on the **direction of the principal stress**.

- **Grain size:** For most metals, smaller grains yield longer fatigue lives, however, the presence of surface defects or scratches will have a greater influence than in a coarse grained alloy.

- **Environment:** Environmental conditions can cause erosion, corrosion, or gas-phase embrittlement, which all affect fatigue life. Corrosion fatigue is a problem encountered in many aggressive environments.

- **Temperature:** Extreme high or low temperatures can decrease fatigue strength.

Design against fatigue

Dependable design against fatigue-failure requires thorough education and supervised experience in structural engineering, mechanical engineering, or materials science. There

are three principal approaches to life assurance for mechanical parts that display increasing degrees of sophistication:

1. Design to keep stress below threshold of fatigue limit (infinite lifetime concept);
2. Design (conservatively) for a fixed life after which the user is instructed to replace the part with a new one (a so-called *lifed* part, finite lifetime concept, or "safe-life" design practice);
3. Instruct the user to inspect the part periodically for cracks and to replace the part once a crack exceeds a critical length. This approach usually uses the technologies of nondestructive testing and requires an accurate prediction of the rate of crack-growth between inspections. This is often referred to as damage tolerant design or "retirement-for-cause".

Stopping fatigue

Fatigue cracks that have begun to propagate can sometimes be stopped by drilling holes, called *drill stops*, in the path of the fatigue crack. This is not recommended as a general practice because the hole represents a stress concentration factor which depends on the size of the hole and geometry. There is thus the possibility of a new crack starting in the side of the hole. It is always far better to replace the cracked part entirely.

Material change

Changes in the materials used in parts can also improve fatigue life. For example, parts can be made from better fatigue rated metals. Complete replacement and redesign of parts can also reduce if not eliminate fatigue problems. Thus helicopter rotor blades and propellers in metal are being replaced by composite equivalents. They are not only lighter, but also much more resistant to fatigue. They are more expensive, but the extra cost is amply repaid by their greater integrity, since loss of a rotor blade usually leads to total loss of the aircraft. A similar argument has been made for replacement of metal fuselages, wings and tails of aircraft.

Infamous fatigue failures

Versailles train crash

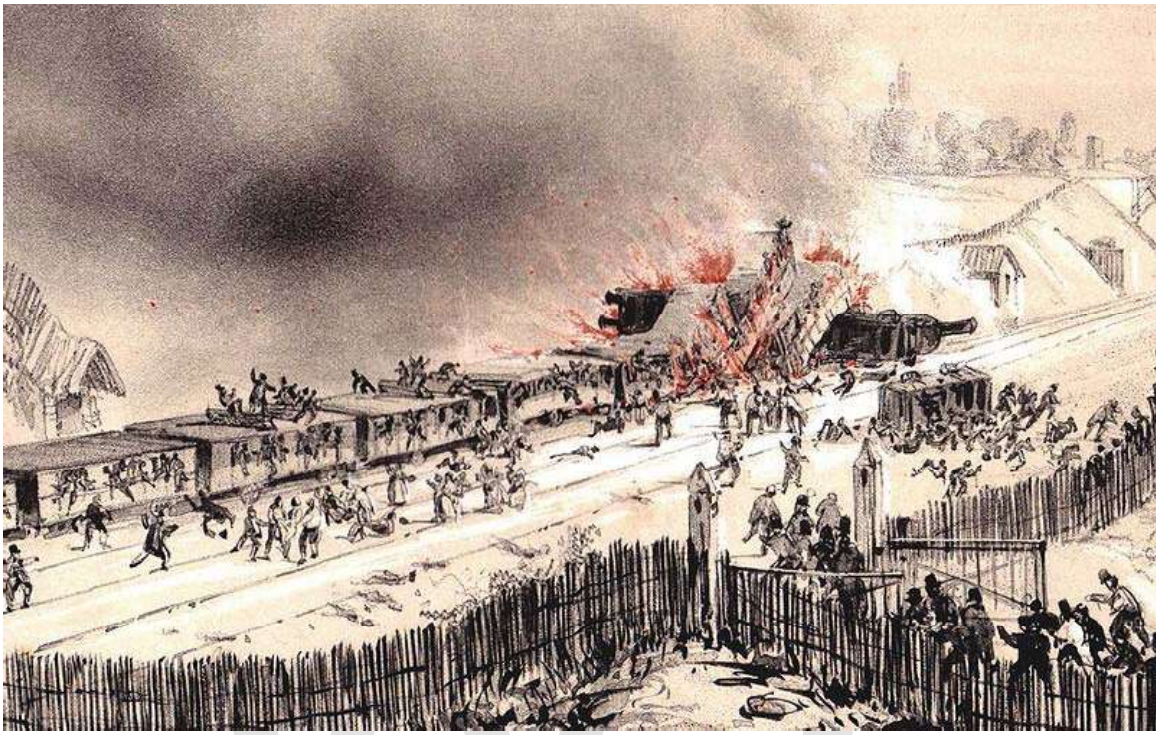

Versailles train disaster

Fig. 1.

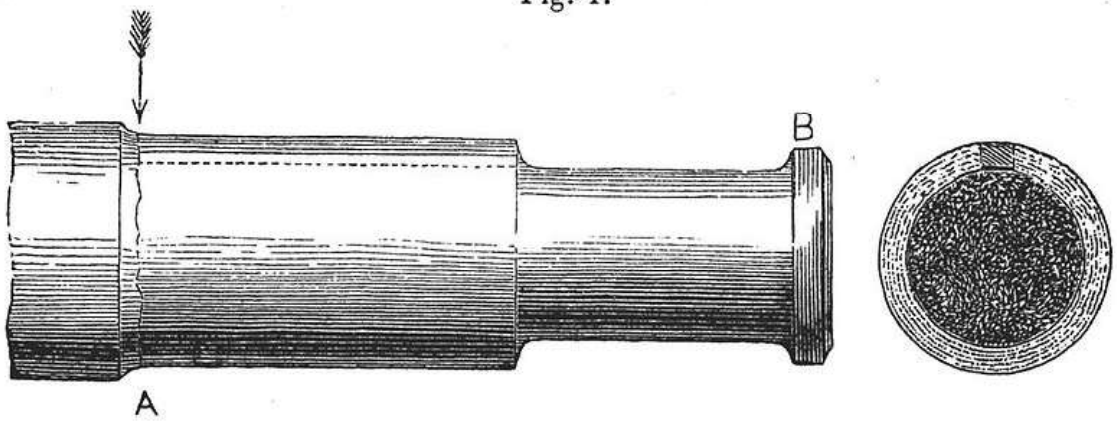

Drawing of a fatigue failure in an axle by Joseph Glynn, 1843.

Following the King's fete celebrations at the Palace of Versailles, a train returning to Paris crashed in May 1842 at Meudon after the leading locomotive broke an axle. The carriages behind piled into the wrecked engines and caught fire. At least 55 passengers were killed trapped in the carriages, including the explorer Jules Dumont d'Urville. This accident is known in France as the "Catastrophe ferroviaire de Meudon". The accident

was witnessed by the British locomotive engineer Joseph Locke and widely reported in Britain. It was discussed extensively by engineers, who sought an explanation.

The derailment had been the result of a broken locomotive axle. Rankine's investigation of broken axles in Britain highlighted the importance of stress concentration, and the mechanism of crack growth with repeated loading. His and other papers suggesting a crack growth mechanism through repeated stressing, however, were ignored, and fatigue failures occurred at an ever increasing rate on the expanding railway system. Other spurious theories seemed to be more acceptable, such as the idea that the metal had somehow "crystallized". The notion was based on the crystalline appearance of the fast fracture region of the crack surface, but ignored the fact that the metal was already highly crystalline.

de Havilland Comet

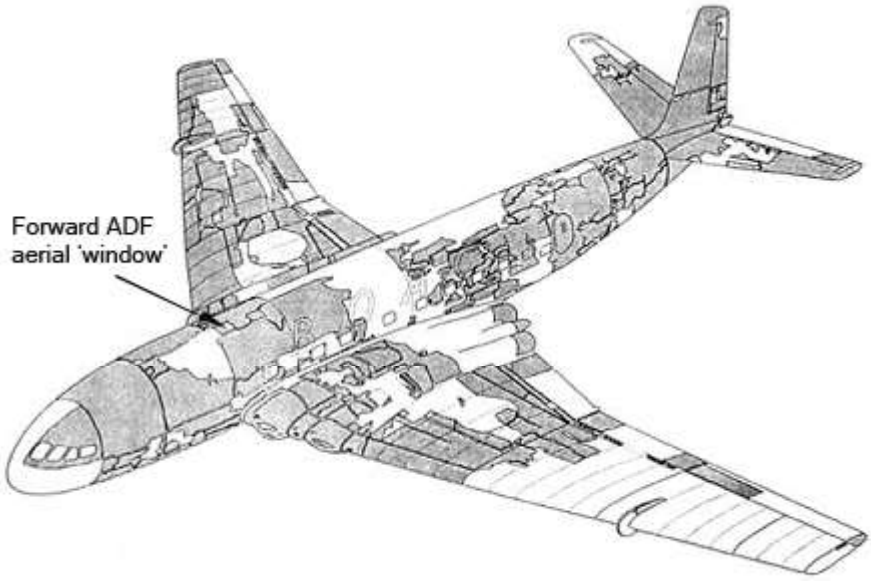

The recovered (shaded) parts of the wreckage of *G-ALYP* and the site (arrowed) of the failure

Two de Havilland Comet passenger jets broke up in mid-air and crashed within a few months of each other in 1954. As a result systematic tests were conducted on a fuselage immersed and pressurised in a water tank. After the equivalent of 3,000 flights investigators at the Royal Aircraft Establishment (RAE) were able to conclude that the crash had been due to failure of the pressure cabin at the forward Automatic Direction Finder window in the roof. This 'window' was in fact one of two apertures for the aerials of an electronic navigation system in which opaque fibreglass panels took the place of the window 'glass'. The failure was a result of metal fatigue caused by the repeated pressurisation and de-pressurisation of the aircraft cabin. Another fact was that the supports around the windows were riveted, not bonded, as the original specifications for the aircraft had called for. The problem was exacerbated by the punch rivet construction

technique employed. Unlike drill riveting, the imperfect nature of the hole created by punch riveting caused manufacturing defect cracks which may have caused the start of fatigue cracks around the rivet.

The fuselage fragment of *G-ALYP* on display in the Science Museum in London

The Comet's pressure cabin had been designed to a safety factor comfortably in excess of that required by British Civil Airworthiness Requirements (2.5 times the cabin proof pressure as opposed to the requirement of 1.33 times and an ultimate load of 2.0 times the cabin pressure) and the accident caused a revision in the estimates of the safe loading strength requirements of airliner pressure cabins.

In addition, it was discovered that the stresses around pressure cabin apertures were considerably higher than had been anticipated, especially around sharp-cornered cut-outs, such as windows. As a result, all future jet airliners would feature windows with rounded corners, the curve eliminating a stress concentration. This was a noticeable distinguishing feature of all later models of the Comet. Investigators from the RAE told a public inquiry that the sharp corners near the Comets' window openings acted as initiation sites for cracks. The skin of the aircraft was also too thin, and cracks from manufacturing stresses were present at the corners.

Alexander L. Kielland oil platform capsize

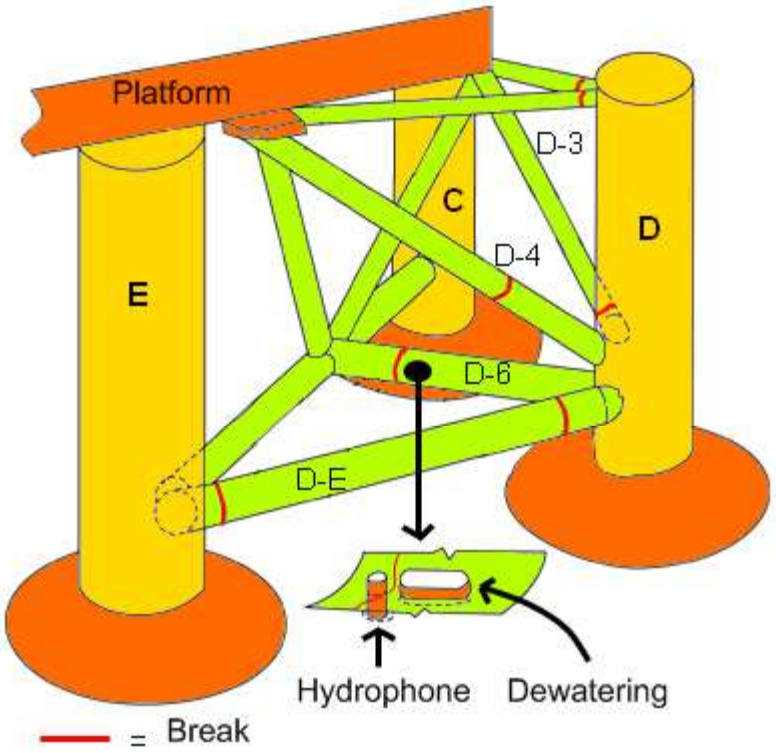

Fractures on the right side of the Alexander L. Kielland rig

The *Alexander L. Kielland* was a Norwegian semi-submersible drilling rig that capsized whilst working in the Ekofisk oil field in March 1980 killing 123 people. The capsize was the worst disaster in Norwegian waters since World War II. The rig, located approximately 320 km east from Dundee, Scotland, was owned by the Stavanger Drilling Company of Norway and was on hire to the U.S. company Phillips Petroleum at the time of the disaster. In driving rain and mist, early in the evening of 27 March 1980 more than 200 men were off duty in the accommodation on the *Alexander L. Kielland*. The wind was gusting to 40 knots with waves up to 12 m high. The rig had just been winched away from the *Edda* production platform. Minutes before 18:30 those on board felt a 'sharp crack' followed by 'some kind of trembling'. Suddenly the rig heeled over 30° and then stabilised. Five of the six anchor cables had broken, the one remaining cable preventing the rig from capsizing. The list continued to increase and at 18.53 the remaining anchor cable snapped and the rig turned upside down.

A year later in March 1981, the investigative report concluded that the rig collapsed owing to a fatigue crack in one of its six bracings (bracing D-6), which connected the collapsed D-leg to the rest of the rig. This was traced to a small 6 mm fillet weld which joined a non-load-bearing flange plate to this D-6 bracing. This flange plate held a sonar device used during drilling operations. The poor profile of the fillet weld contributed to a reduction in its fatigue strength. Further, the investigation found considerable amounts of lamellar tearing in the flange plate and cold cracks in the butt weld. Cold cracks in the

welds, increased stress concentrations due to the weakened flange plate, the poor weld profile, and cyclical stresses (which would be common in the North Sea), seemed to collectively play a role in the rig's collapse.

Others

- The 1919 Boston Molasses Disaster has been attributed to a fatigue failure.
- The 1957 "Mt. Pinatubo", presidential plane of Philippine President Ramon Magsaysay, crashed due to engine failure caused by metal fatigue.
- The 1968 Los Angeles Airways Flight 417 lost one of its main rotor blades due to fatigue failure.
- The 1985 Japan Airlines Flight 123 crashed after the aircraft lost its vertical stabilizer due to faulty repairs on the rear bulkhead.
- The 1988 Aloha Airlines Flight 243 suffered an explosive decompression due to fatigue failure.
- The 1989 United Airlines Flight 232 lost its tail engine due to fatigue failure.
- The 1992 El Al Flight 1862 lost both engines on its right-wing due to fatigue failure with the #3 Engine.
- The 1998 Eschede train disaster was caused by fatigue failure of a single composite wheel.
- The 2002 China Airlines Flight 611 had disintegrated in-flight due to fatigue failure.
- The 2005 Chalk's Ocean Airways Flight 101 lost its right wing due to fatigue failure brought about by inadequate maintenance practices.

Chapter 3

Fractography

Fractography is the study of fracture surfaces of materials. Fractographic methods are routinely used to determine the cause of failure in engineering structures, especially in product failure and the practice of forensic engineering or failure analysis. In material science research, fractography is used to develop and evaluate theoretical models of crack growth behavior.

One of the aims of fractographic examination is to determine the cause of failure by studying the characteristics of a fracture surface. Different types of crack growth (e.g. fatigue, stress corrosion cracking, hydrogen embrittlement) produce characteristic features on the surface, which can be used to help identify the failure mode. The overall pattern of cracking can be more important than a single crack, however, especially in the case of brittle materials like ceramics and glasses.

Methods

Crankshaft fatigue fracture

An important aim of fractography is to establish and examine the origin of cracking, as examination at the origin may reveal the cause of crack initiation. Initial fractographic examination is commonly carried out on a macro scale utilising low power optical microscopy and oblique lighting techniques to identify the extent of cracking, possible modes and likely origins. Optical microscopy or macrophotography are often enough to pinpoint the nature of the failure and the causes of crack initiation and growth if the loading pattern is known.

Common features that may be a cause for crack initiation are inclusions, voids or foreign material, points of stress concentration and "hachures", or the lines on fractures which show crack direction. The broken crankshaft shown at right failed from a surface defect near the bulb at lower centre, the single brittle crack growing up into the bulk material by small steps, a problem known as fatigue. The crankshaft also shows hachures which point back to the origin of the fracture. Some modes of crack growth can leave characteristic marks on the surface that identify the mode of crack growth and origin on a macro scale e.g. beachmarks or striations on fatigue cracks. The areas of the product can also be very revealing, especially if there are traces of sub-critical cracks, or cracks which have not grown to completion. They can indicate that the material was faulty when loaded, or alternatively, that the sample was overloaded at the time of failure.

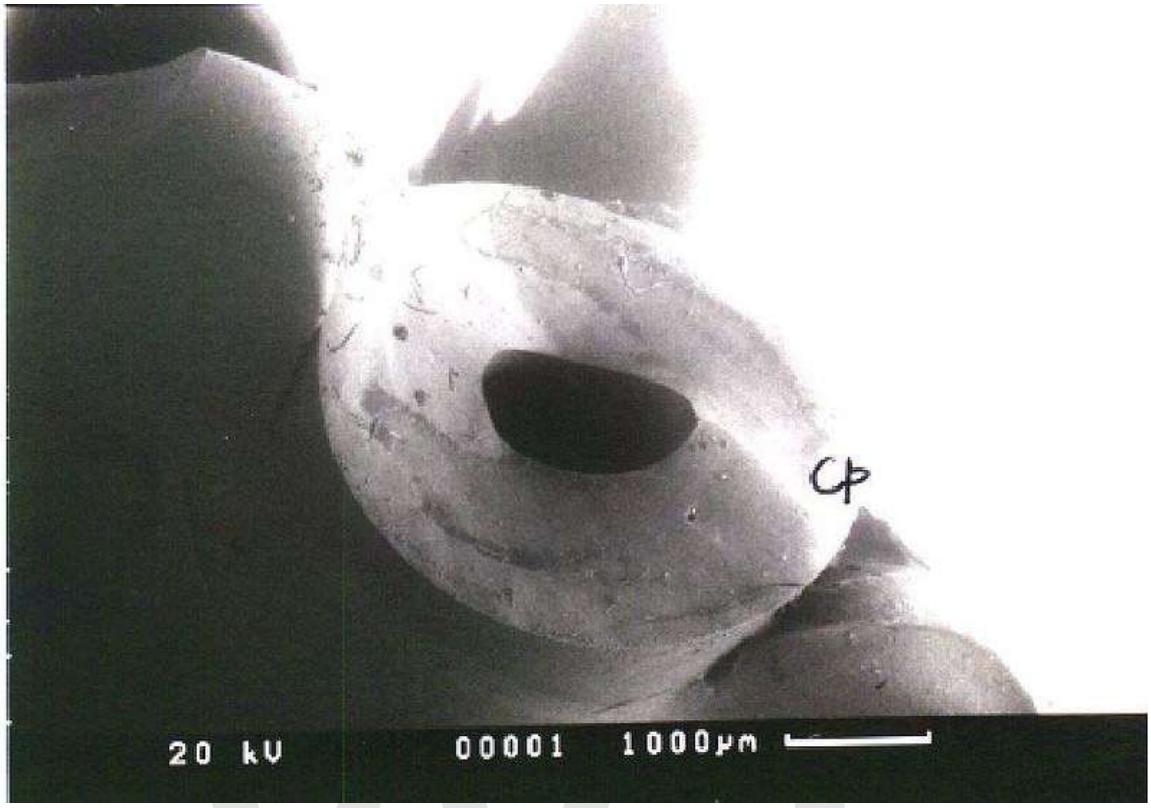

Fractured breast implant catheter in SEM

A Cusp (singularity) is formed where brittle cracks meet, as shown on the picture of a failed catheter (Cp). The cusp was formed by brittle failure of the catheter on a breast implant in silicone rubber. The origin of the cracks is at the shoulder at the left-hand side. Identifying such features will allow a fracture surface map to be made of the surface being studied. The implant failed because of overload, all the imposed loads being concentrated at the connection between the catheter and the bag holding salt solution. As a result, the patient reported loss of fluid from the implant, and it was extracted surgically and replaced.

Fracture surface map

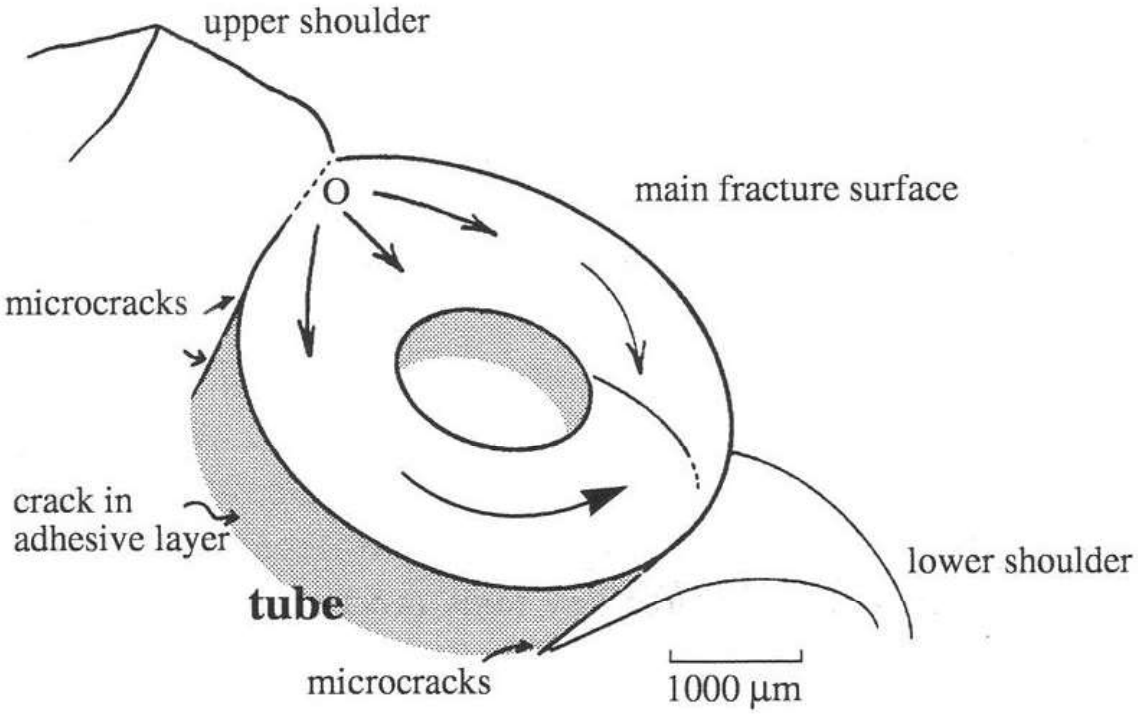

Fracture map of failed breast implant

A schematic fracture surface map is a valuable result of visual or microscopic examination. It seeks to isolate and identify the features on the surface which show how the product failed. Such a map can be a valuable way of presenting information which shows clearly how a crack was initiated and grew with time. In the case of the failed breast implant, the crack path was very simple, but the cause more subtle. Further scanning electron microscopy showed numerous microcracks between the bag and the catheter, indicating that the adhesive bond between the two components had failed prematurely, perhaps through faulty manufacture. The material of construction of both bag and catheter, silicone rubber is a physically weak elastomer, and product design must allow for the low tear or shear strength of the material.

Scanning electron microscopy

In many cases, fractography requires examination at a finer scale, which is usually carried out in a Scanning electron microscope or SEM. The resolution is much higher than the optical microscope, although samples are examined in a partial vacuum and colour is absent. Improved SEM's now allow examination at near atmospheric pressures, so allowing examination of sensitive materials such as those of biological origin. The atmosphere within the sample chamber can also be controlled using nitrogen or water vapour for example, a method known as environmental SEM or ESEM. The method is especially useful when combined with Energy dispersive X-ray spectroscopy or EDX,

which can be performed in the microscope, so very small areas of the sample can be analysed for their elemental distribution.

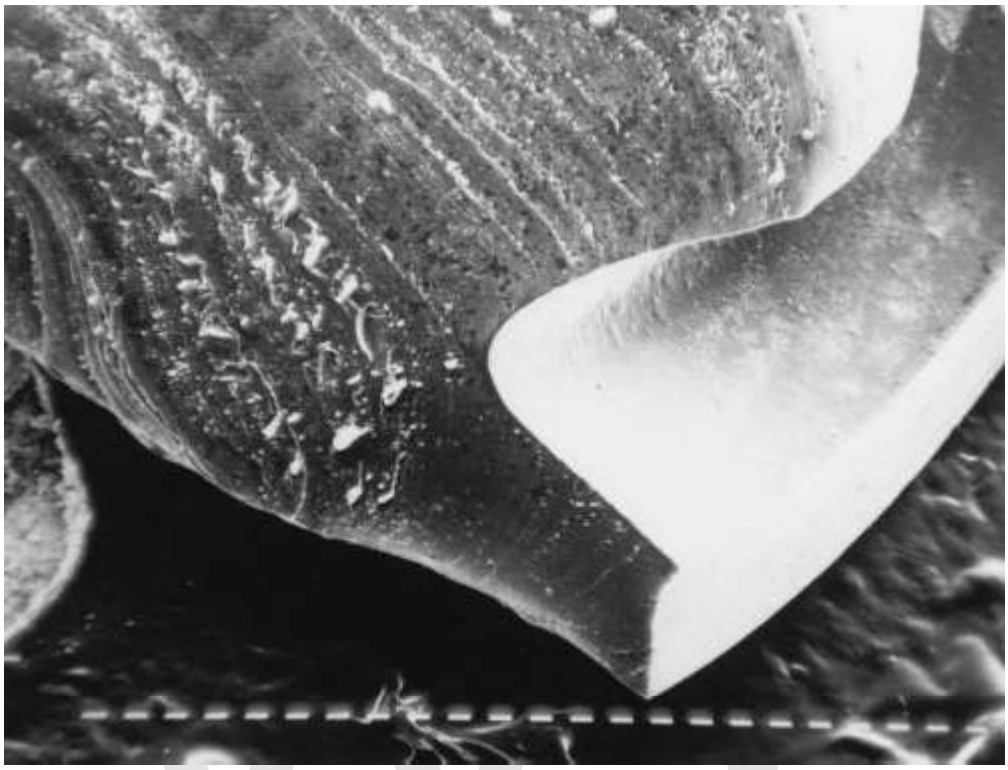

Fatigue fracture in rubber brake seal showing striations at left (SEM)

The fracture surface photograph shows a brittle fracture in a car brake seal. Crack growth can be seen from the fine lines or striations in the surface, indicative of fatigue. The problem led to an accident when the crack suddenly grew to completion, hydraulic fluid was lost, the driver lost braking power, and the vehicle crashed. The crack grew from cuts at the edge of the seal, probably caused by sharp particles trapped in the brake cylinder.

Applications

Fractography is a widely used technique in forensic engineering, forensic materials engineering and fracture mechanics to understand the causes of failures and also to verify theoretical failure predictions with real life failures. It is of use in forensic science for analysing broken products which have been used as weapons, such as broken bottles for example. Thus a defendant might claim that a bottle was faulty and broke accidentally when it impacted a victim of an assault. Fractography could show the allegation to be false, and that considerable force was needed to smash the bottle before using the broken end as a weapon to deliberately attack the victim. Bullet holes in glass windscreens or windows can also indicate the direction of impact and the energy of the projectile. In these cases, the overall pattern of cracking is vital to reconstructing the sequence of events, rather than the specific characteristics of a single crack.

Optical fractography and Electron fractography are two more types of fractography. Electron fractography is microscopic and needs an SEM (Scanning Electron Microscope) to be conducted. Optical fractography needs much less equipment.

Chapter 4

Focal Mechanism

The **focal mechanism** of an earthquake describes the inelastic deformation in the source region that generates the seismic waves. In the case of a fault-related event it refers to the orientation of the fault plane that slipped and the slip vector and is also known as a **fault-plane solution**. Focal mechanisms are derived from a solution of the moment tensor for the earthquake, which itself is estimated by an analysis of observed seismic waveforms. The focal mechanism can be derived from observing the pattern of "first motions", that is, whether the first arriving P waves break up or down. This method was used before waveforms were recorded and analysed digitally and this method is still used for earthquakes too small for easy moment tensor solution. Focal mechanisms are now mainly derived using semi-automatic analysis of the recorded waveforms.

Moment tensor solutions

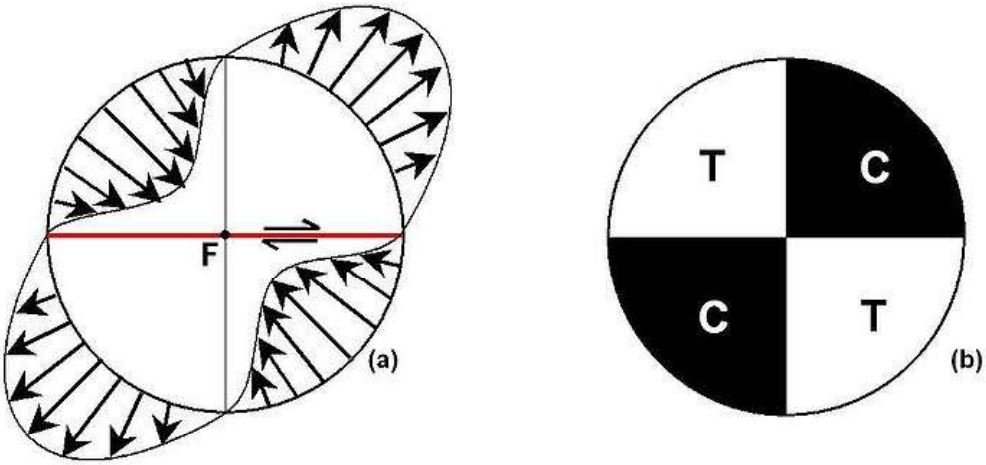

Schematic diagram showing the direction of initial movement of particles around the focus (F) of an earthquake on a W-E dextral strike-slip fault, viewed from above (a) and the equivalent zones of compressional (C) and tensional (T) sense first motion in the seismic waves radiating outward (b).

Note that due to the symmetry, an identical pattern would result from movement on an N-S sinistral strike-slip fault passing through the focus

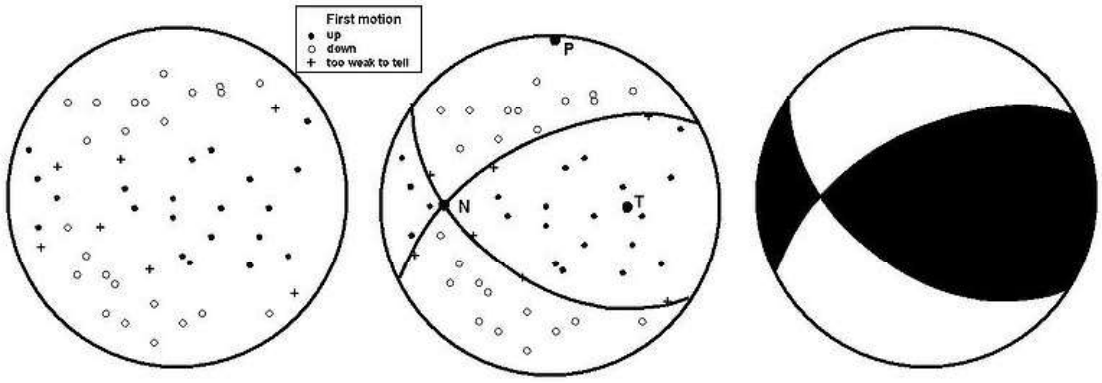

First motion data for a hypothetical earthquake from various seismograph stations

Nodal planes and N, P & T axes fitted to the data

Resultant 'beachball' plot showing that the earthquake resulted from reverse oblique movement on a fault of one of two possible orientations

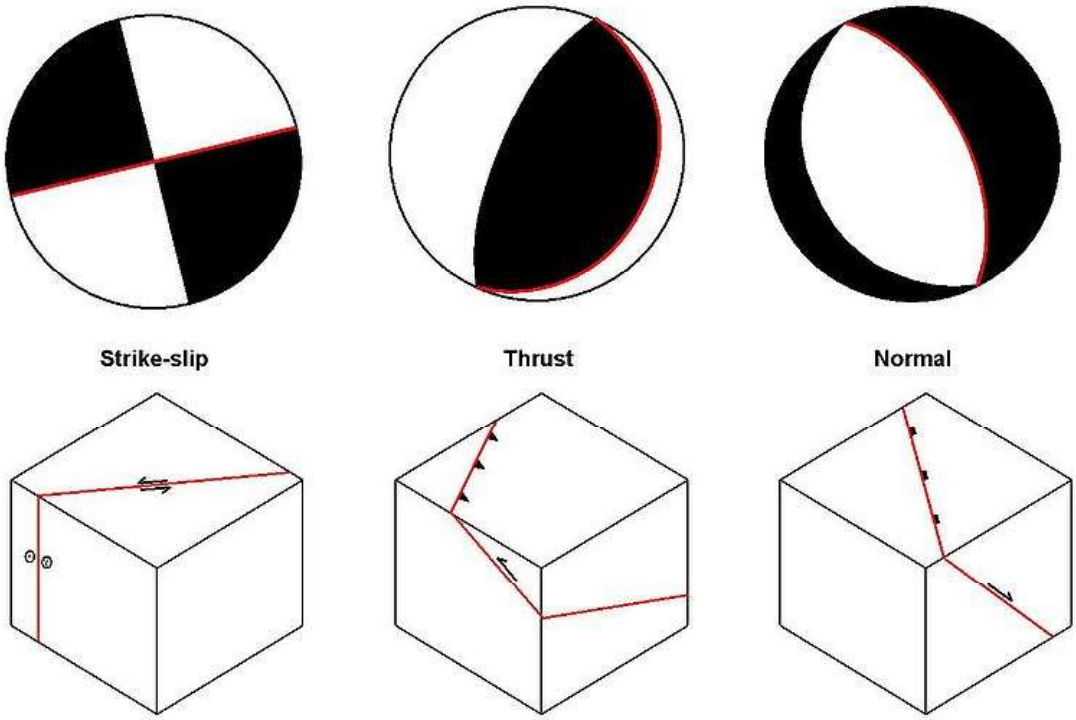

Types of 'beachball plot' associated with different fault end-members (nodal plane in red parallel to fault)

The moment tensor solution is typically displayed graphically using a so-called *beachball* diagram. The pattern of energy radiated during an earthquake with a single direction of motion on a single fault plane may be modelled as a *double couple*, which is described mathematically as a special case of a second order tensor (similar to those for stress and strain) known as the moment tensor.

Earthquakes not caused by fault movement have quite different patterns of energy radiation. In the case of an underground nuclear explosion, for instance, the seismic moment tensor is isotropic and this difference allows such explosions to be easily discriminated from their seismic response. This is an important part of monitoring to discriminate between earthquakes and explosions for the Comprehensive Test Ban Treaty.

Graphical representation ("beachball plot")

The data for an earthquake is plotted using a lower-hemisphere stereographic projection. The azimuth and take-off angle are used to plot the position of an individual seismic record. The take-off angle is the angle from the vertical of a seismic ray as it emerges from the earthquake focus. These angles are calculated from a standard set of tables that describe the relationship between the take-off angle and the distance between the focus and the observing station. By convention, filled symbols are used to plot data from

stations where the P-wave first motion recorded was up (a compressive wave), hollow symbols for down (a tensional wave), with dots for stations with arrivals too weak to get a sense of motion. If there are sufficient observations, one may draw two well-constrained orthogonal great circles that divide the compressive from the tensional observations and these are the nodal planes. Observations from stations with no clear first motion normally lie close to these planes. By convention the compressional quadrants are colour-filled and the tensional left white. The two nodal planes intersect at the N (neutral)-axis. The P and T axes are also often plotted; with the N axis these three directions respectively match the directions of the maximum, minimum and intermediate principle compressive stresses associated with the earthquake. The P-axis is plotted in the centre of the white segment, the T-axis in the centre of the colour-filled segment.

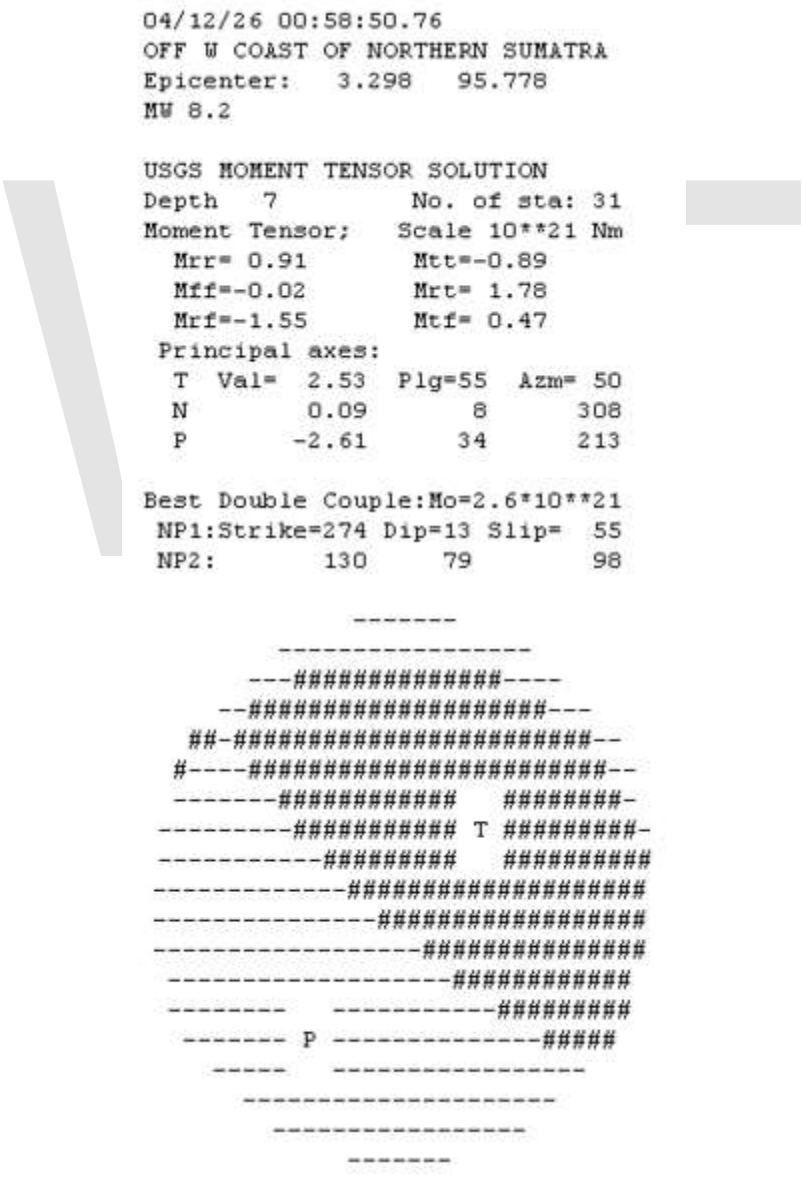

USGS moment tensor solution 2004 Indian Ocean earthquake

The fault plane responsible for the earthquake will be parallel to one of the nodal planes, the other being called the auxiliary plane. Unfortunately it is not possible to determine solely from a focal mechanism which of the nodal planes is in fact the fault plane. For this other geological or geophysical evidence is needed to remove the ambiguity. The slip vector, which is the direction of motion of one side of the fault relative to the other, lies within the fault plane, 90 deg from the N-axis.

To give an example, in the 2004 Indian Ocean earthquake, the moment tensor solution gives two nodal planes, one dipping northeast at 13 degrees and one dipping southwest at 79 degrees. In this case the earthquake can be confidently associated with the plane dipping shallowly to the northeast, as this is the orientation of the subducting slab as defined by historical earthquake locations and plate tectonic models.

Beach Ball Calculator

There are several programs available to prepare Focal Mechanism Solutions (FMS). BBC, a MATLAB based tool box, is available to prepare the beach ball diagrams. This software plots the first motion polarity data arrived at different stations. The compression and dilation are separated using mouse help. A final diagram is prepared automatically.

Chapter 5

Fracture Toughness

In materials science, **fracture toughness** is a property which describes the ability of a material containing a crack to resist fracture, and is one of the most important properties of any material for virtually all design applications. It is denoted K_{Ic} and has the units of $\mathrm{Pa}\sqrt{\mathrm{m}}$.

The subscript *Ic* denotes mode I crack opening under a normal tensile stress perpendicular to the crack, since the material can be made deep enough to stand shear (mode II) or tear (mode III).

Fracture toughness is a quantitative way of expressing a material's resistance to brittle fracture when a crack is present. If a material has much fracture toughness it will probably undergo ductile fracture. Brittle fracture is very characteristic of materials with less fracture toughness.

Fracture mechanics, which leads to the concept of fracture toughness, was broadly based on the work of A. A. Griffith who, among other things, studied the behavior of cracks in brittle materials.

A related concept is the *work of fracture* (γ_{wof}) which is directly proportional to K_{Ic}^2/E, where *E* is the Young's modulus of the material. Note that, in SI units, γ_{wof} is given in J/m^2.

Table of values

Here are some typical values of fracture toughness for various materials:

Material	K_{Ic} ($MPa\text{-}m^{1/2}$)
Metals	
Aluminum alloy (7075)	24

Steel alloy (4340)	50
Titanium alloy	44–66
Aluminum	14–28
Ceramics	
Aluminium oxide	3–5
Silicon carbide	3–5
Soda-lime-glass	0.7–0.8
Concrete	0.2–1.4
Polymers	
Polymethyl methacrylate	0.7–1.6
Polystyrene	0.7–1.1
Composites	
Mullite-fibre composite	1.8–3.3
Silica aerogels	0.0008–0.0048

Crack growth as a stability problem

Consider a body with flaws (cracks) that is subject to some loading; the stability of the crack can be assessed as follows. We can assume for simplicity that the loading is of constant displacement or displacement controlled type (such as loading with a screw jack); we can also simplify the discussion by characterizing the crack by its area, A. If we consider an adjacent state of the body as being one with a broader crack (area A+dA), we can then assess strain energy in the two states and evaluate strain energy release rate.

The rate is reckoned with respect to the change in crack area, so if we use U for strain energy, the strain energy release rate is numerically dU/dA. It may be noted that for a body loaded in constant displacement mode, the displacement is applied and the force level is dictated by stiffness (or compliance) of the body. If the crack grows in size, the stiffness decreases, so the force level will decrease. This decrease in force level under the same displacement (strain) level indicates that the elastic strain energy stored in the body is decreasing—is being released. Hence the term strain energy release rate which is usually denoted with symbol *G*.

The strain energy release rate is higher for higher loads and broader cracks. If the strain energy so released exceeds a critical value G_c, then the crack will grow spontaneously. For brittle materials, G_c can be equated to the surface energy of the (two) new crack surfaces; in other words, in brittle materials, a crack will grow spontaneously if the strain energy released is equal to or more than the energy required to grow the crack surface(s). The stability condition can be written as

elastic energy released = surface energy created.

If the elastic energy releases is less than the critical value, then the crack will not grow; equality signifies neutral stability and if the strain energy release rate exceeds the critical value, the crack will start growing in an unstable manner. For ductile materials, energy associated with plastic deformation has to be taken into account. When there is plastic deformation at the crack tip (as occurs most often in metals) the energy to propagate the crack may increase by several orders of magnitude as the work related to plastic deformation may be much larger than the surface energy. In such cases, the stability criterion has to restated as

elastic energy released = surface energy + plastic deformation energy.

Practically, this means a higher value for the critical value G_c. From the definition of G, we can deduce that it has dimensions of work (or energy) /area or force/length. For ductile metals G_{Ic} is around 50–200 kJ/m^2, for brittle metals it is usually 1–5 and for glasses and brittle polymers it is almost always less than 0.5.

The problem can also be formulated in terms of stress instead of energy, leading to the terms stress intensity factor K (or K_I for mode I) and critical stress intensity factor K_c (and K_{Ic}). These K_c and K_{Ic} (etc.) quantities are commonly referred to as fracture toughness, though it is equivalent to use G_c. Typical values for $K_{Ic}$are 150 MN/m$^{3/2}$ for ductile (very tough) metals, 25 for brittle ones and 1–10 for glasses and brittle polymers. Notice the different units used by G_{Ic} and K_{Ic}. Engineers tend to use the latter as an indication of toughness.

Transformation toughening

Composites exhibiting the highest level of fracture toughness are typically made of a pure alumina or some silica-alumina (SiO2 /Al2O3) matrix with tiny inclusions of zirconia (ZrO2) dispersed as uniformly as possible within the solid matrix. (*Note: a wet chemical approach is typically necessary in order to establish the compositional uniformity of the ceramic body before firing).

The process of "transformation toughening" is based on the assumption that zirconia undergoes several martensitic (displacive, diffusionless) phase transformations (cubic → tetragonal → monoclinic) between room temperature and practical sintering (or firing) temperatures. Thus, due to the volume restrictions induced by the solid matrix, metastable crystalline structures can become frozen in which impart an internal strain field surrounding each zirconia inclusion upon cooling. This enables a zirconia particle (or inclusion) to absorb the energy of an approaching crack tip front in its nearby vicinity.

Thus, the application of large shear stresses during fracture nucleates the transformation of a zirconia inclusion from the metastable phase. The subsequent volume expansion from the inclusion (via an increase in the height of the unit cell) introduces compressive stresses which therefore strengthen the matrix near the approaching crack tip front. Zirconia "whiskers" may be used expressly for this purpose.

Appropriately referred to by its first discoverers as "ceramic steel", the stress intensity factor values for window glass (silica), transformation toughened alumina, and a typical iron/carbon steel range from 1 to 20 to 50 respectively.

Conjoint action

There are number of instances where this picture of a critical crack is modified by corrosion. Thus, fretting corrosion occurs when a corrosive medium is present at the interface between two rubbing surfaces. Fretting (in the absence of corrosion) results from the disruption of very small areas that bond and break as the surfaces undergo friction, often under vibrating conditions. The bonding contact areas deform under the localised pressure and the two surfaces gradually wear away. Fracture mechanics dictates that each minute localised fracture has to satisfy the general rule that the elastic energy released as the bond fractures has to exceed the work done in plastically deforming it and in creating the (very tiny) fracture surfaces. This process is enhanced when corrosion is present, not least because the corrosion products act as an abrasive between the rubbing surfaces.

Fatigue is another instance where cyclical stressing, this time of a bulk lump of metal, causes small flaws to develop. Ultimately one such flaw exceeds the critical condition and fracture propagates across the whole structure. The fatigue life of a component is the time it takes for criticality to be reached, for a given regime of cyclical stress. **Corrosion fatigue** is what happens when a cyclically stressed structure is subjected to a corrosive environment at the same time. This not only serves to initiate surface cracks but actually modifies the crack growth process. As a result the fatigue life is shortened, often considerably.

Stress-corrosion cracking (SCC)

This phenomenon is the unexpected sudden failure of normally ductile metals subjected to a constant tensile stress in a corrosive environment. Certain austenitic stainless steels and aluminium alloys crack in the presence of chlorides, mild steel cracks in the presence of alkali (**boiler cracking**) and copper alloys crack in ammoniacal solutions (**season cracking**). Worse still, high-tensile structural steels crack in an unexpectedly brittle manner in a whole variety of aqueous environments, especially chloride. With the possible exception of the latter, which is a special example of *hydrogen cracking*, all the others display the phenomenon of subcritical crack growth; i.e. small surface flaws propagate (usually smoothly) under conditions where fracture mechanics predicts that failure should not occur. That is, in the presence of a corrodent, cracks develop and propagate well below K_{Ic}. In fact, the subcritical value of the stress intensity, designated as K_{Iscc}, may be less than 1% of K_{Ic}, as the following table shows:

Alloy	K_{Ic} ($MN/m^{3/2}$)	SCC environment	K_{Iscc} ($MN/m^{3/2}$)
13Cr steel	60	3% NaCl	12

18Cr-8Ni	200	42% $MgCl_2$	10
Cu-30Zn	200	NH_4OH, pH7	1
Al-3Mg-7Zn	25	aqueous halides	5
Ti-6Al-1V	60	0.6M KCl	20

The subcritical nature of propagation may be attributed to the chemical energy released as the crack propagates. That is,

> *elastic energy released* + *chemical energy* = *surface energy* + *deformation energy*.

The crack initiates at K_{Iscc} and thereafter propagates at a rate governed by the slowest process, which most of the time is the rate at which corrosive ions can diffuse to the crack tip. As the crack advances so K rises (because crack size appears in the calculation of stress intensity). Finally it reaches K_{Ic} , whereupon swift fracture ensues and the component fails. One of the practical difficulties with SCC is its unexpected nature. Stainless steels, for example, are employed because under most conditions they are passive; i.e. effectively inert. Very often one finds a single crack has propagated whiles the left metal surface stays apparently unaffected.

Chapter 6

Fracture

A **fracture** is the (local) separation of an object or material into two, or more, pieces under the action of stress.

The word *fracture* is often applied to bones of living creatures (that is, a bone fracture), or to crystals or crystalline materials, such as gemstones or metal. Sometimes, in crystalline materials, individual crystals fracture without the body actually separating into two or more pieces. Depending on the substance which is fractured, a fracture reduces strength (most substances) or inhibits transmission of light (optical crystals).

A detailed understanding of how fracture occurs in materials may be assisted by the study of fracture mechanics.

Fracture strength

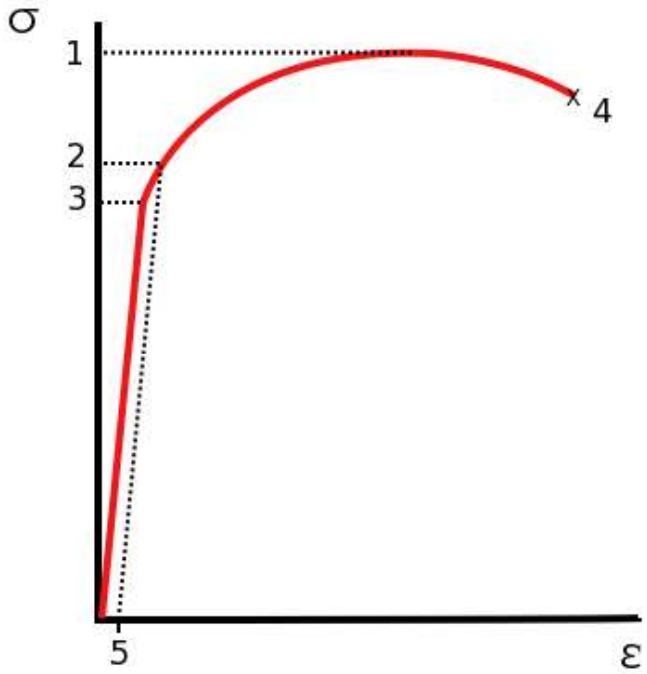

Stress vs. strain curve typical of aluminum
1. Ultimate tensile strength
2. Yield strength
3. Proportional limit stress
4. Fracture
5. Offset strain (typically 0.2%)

Fracture strength, also known as **breaking strength**, is the stress at which a specimen fails via fracture. This is usually determined for a given specimen by a tensile test, which charts the stress-strain curve. The final recorded point is the fracture strength.

Ductile materials have a fracture strength lower than the ultimate tensile strength (UTS), whereas in brittle materials the fracture strength is equivalent to the UTS. If a ductile material reaches its ultimate tensile strength in a load-controlled situation, it will continue to deform, with no additional load application, until it ruptures. However, if the loading is displacement-controlled, the deformation of the material may relieve the load, preventing rupture.

If the stress-strain curve is plotted in terms of *true stress* and *true strain* the curve will always slope upwards and never reverse, as true stress is corrected for the decrease in cross-sectional area. The true stress on the material at the time of rupture is known as the breaking strength. This is the maximum stress on the true stress-strain curve, given by point 3 on curve B.

Types

Brittle fracture

Brittle fracture in glass.

Fracture of an Aluminum Crank Arm. Bright: Brittle fracture. Dark: Fatigue fracture.

In *brittle fracture*, no apparent plastic deformation takes place before fracture. In brittle crystalline materials, fracture can occur by *cleavage* as the result of tensile stress acting normal to crystallographic planes with low bonding (cleavage planes). In amorphous solids, by contrast, the lack of a crystalline structure results in a conchoidal fracture, with cracks proceeding normal to the applied tension.

The theoretical strength of a crystalline material is (roughly)

$$\sigma_{\text{theoretical}} = \sqrt{\frac{E\gamma}{r_o}}$$

where: -

E is the Young's modulus of the material,

γ is the surface energy, and
r_o is the equilibrium distance between atomic centers.

On the other hand, a crack introduces a stress concentration modeled by

$$\sigma_{\text{elliptical crack}} = \sigma_{\text{applied}}(1 + 2\sqrt{\frac{a}{\rho}}) = 2\sigma_{\text{applied}}\sqrt{\frac{a}{\rho}} \text{ (For sharp cracks)}$$

where: -

σ_{applied} is the loading stress,
a is half the length of the crack, and
ρ is the radius of curvature at the crack tip.

Putting these two equations together, we get

$$\sigma_{\text{fracture}} = \sqrt{\frac{E\gamma\rho}{4ar_o}}.$$

Looking closely, we can see that sharp cracks (small ρ) and large defects (large a) both lower the fracture strength of the material.

Recently, scientists have discovered supersonic fracture, the phenomenon of crack motion faster than the speed of sound in a material. This phenomenon was recently also verified by experiment of fracture in rubber-like materials.

Ductile fracture

Ductile failure of a specimen strained axially.

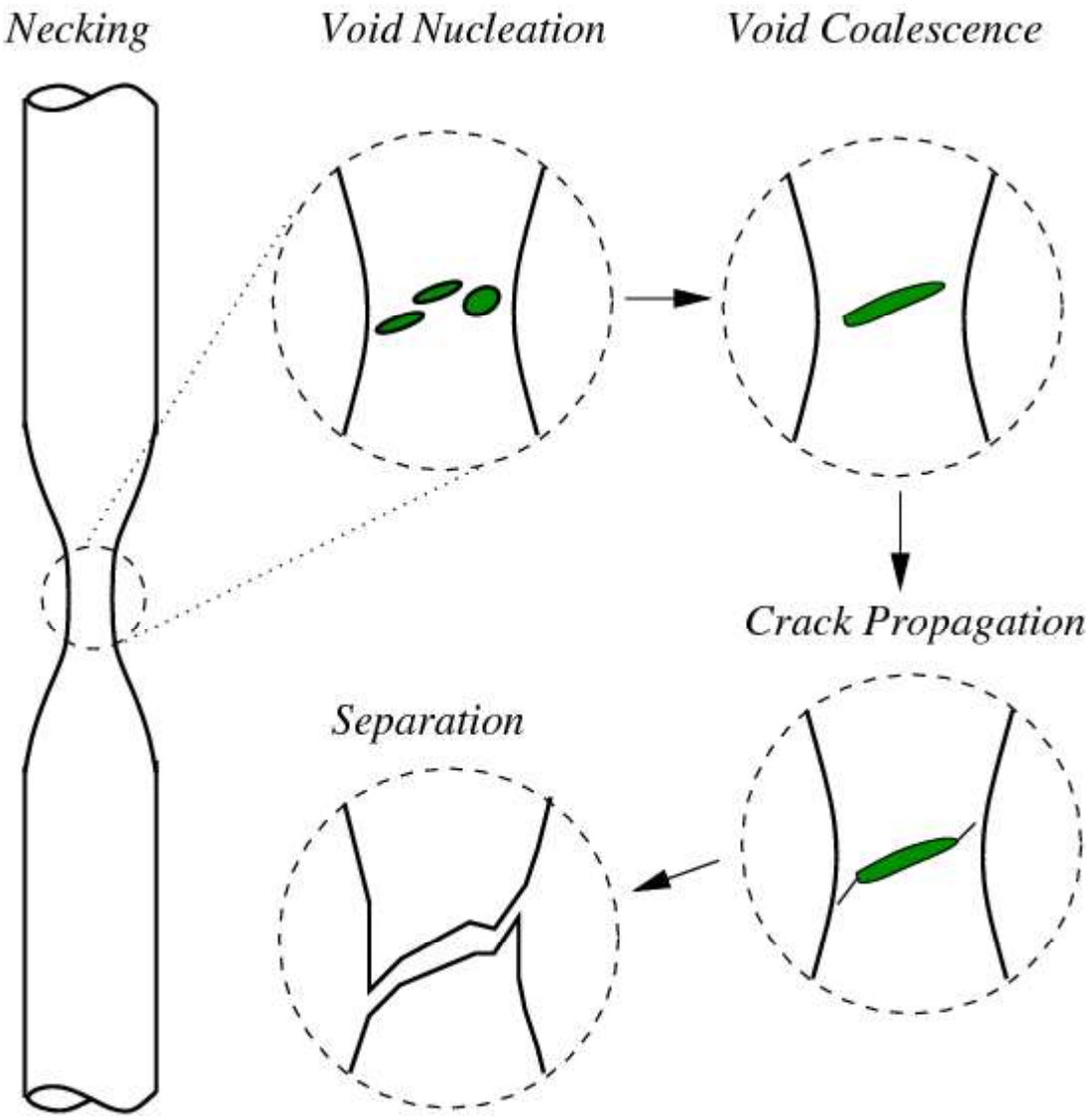

Schematic representation of the steps in ductile fracture (in pure tension).

In *ductile fracture*, extensive plastic deformation takes place before fracture. The terms *rupture* or *ductile rupture* describe the ultimate failure of tough ductile materials loaded in tension. Rather than cracking, the material "pulls apart," generally leaving a rough surface. In this case there is slow propagation and an absorption of a large amount energy before fracture.

Many ductile metals, especially materials with high purity, can sustain very large deformation of 50–100% or more strain before fracture under favorable loading condition and environmental condition. The strain at which the fracture happens is controlled by the purity of the materials. At room temperature, pure iron can undergo deformation up to 100% strain before breaking, while cast iron or high-carbon steels can barely sustain 3% of strain.

Because ductile rupture involves a high degree of plastic deformation, the fracture behavior of a propagating crack as modeled above changes fundamentally. Some of the energy from stress concentrations at the crack tips is dissipated by plastic deformation before the crack actually propagates.

The basic steps are: void formation, void coalescence (also known as crack formation), crack propagation, and failure, often resulting in a cup-and-cone shaped failure surface.

Crack separation modes

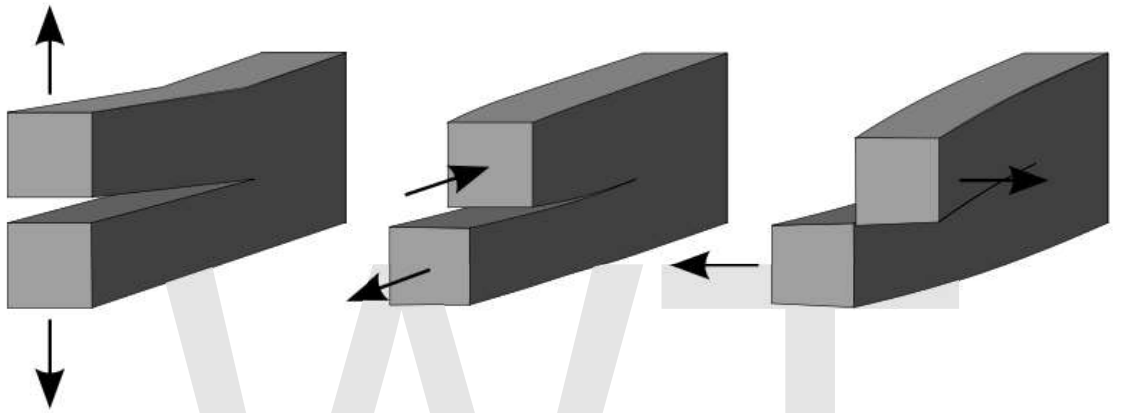

The three fracture modes.

There are three ways of applying a force to enable a crack to propagate:

- **Mode I crack** – Opening mode (a tensile stress normal to the plane of the crack)
- **Mode II crack** – Sliding mode (a shear stress acting parallel to the plane of the crack and perpendicular to the crack front)
- **Mode III crack** – Tearing mode (a shear stress acting parallel to the plane of the crack and parallel to the crack front)

Chapter 7

Structural Fracture Mechanics

Structural Fracture Mechanics is the field of structural engineering concerned with the study of load-carrying structures that includes one or several failed or damaged components. It uses methods of analytical solid mechanics, structural engineering, safety engineering, probability theory, and catastrophe theory to calculate the load and stress in the structural components and analyze the safety of a damaged structure.

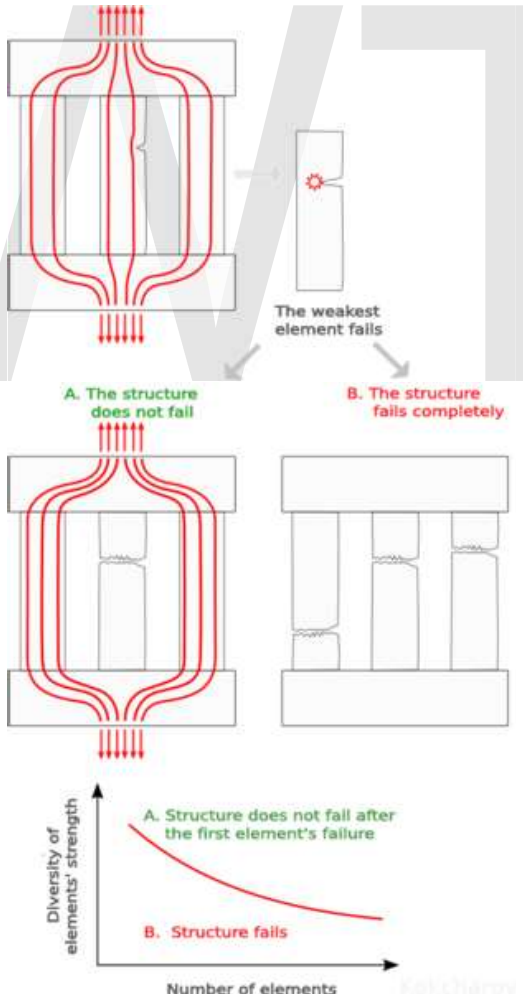

Model of Structural Fracture Mechanics.

There is a direct analogy between Fracture Mechanics of solid and Structural Fracture Mechanics:

Analogy between Fracture Mechanics of solid and Structural Fracture Mechanics		
	Fracture Mechanics	**Structural Fracture Mechanics**
Model	Solid with a crack	Multi-component structure with a failed component
Defect driving force	Stress intensity factor	Overload stress
System property	Fracture toughness	Reserve ability / Structural robustness

There are different causes of the first component failure: 1) mechanical overload, fatigue (material), unpredicted scenario, etc. 2) “human intervention” like unprofessional behavior or a terrorist attack.

The are two typical scenarios:

A. A localized failure does NOT cause immediate collapse of the entire structure.

B. The entire structure fails immediately after one of its components fails.

If the structure does not collapse immediately there is a limited period of time until the catastrophic structural failure of the entire structure. There is a critical number of structural elements that defines whether the system has reserve ability or not.

Safety engineers use the failure of the first component as an indicator and try to intervene during the given period of time to avoid the catastrophe of the entire structure. For example, “Leak-Before-Break” methodology means that a leak will be discovered prior to a catastrophic failure of the entire piping system occurring in service. It has been applied to pressure vessels, nuclear piping, gas and oil pipelines, etc.

The methods of Structural Fracture Mechanics are used as checking calculations to estimate sensitivity of a structure to its component failure.

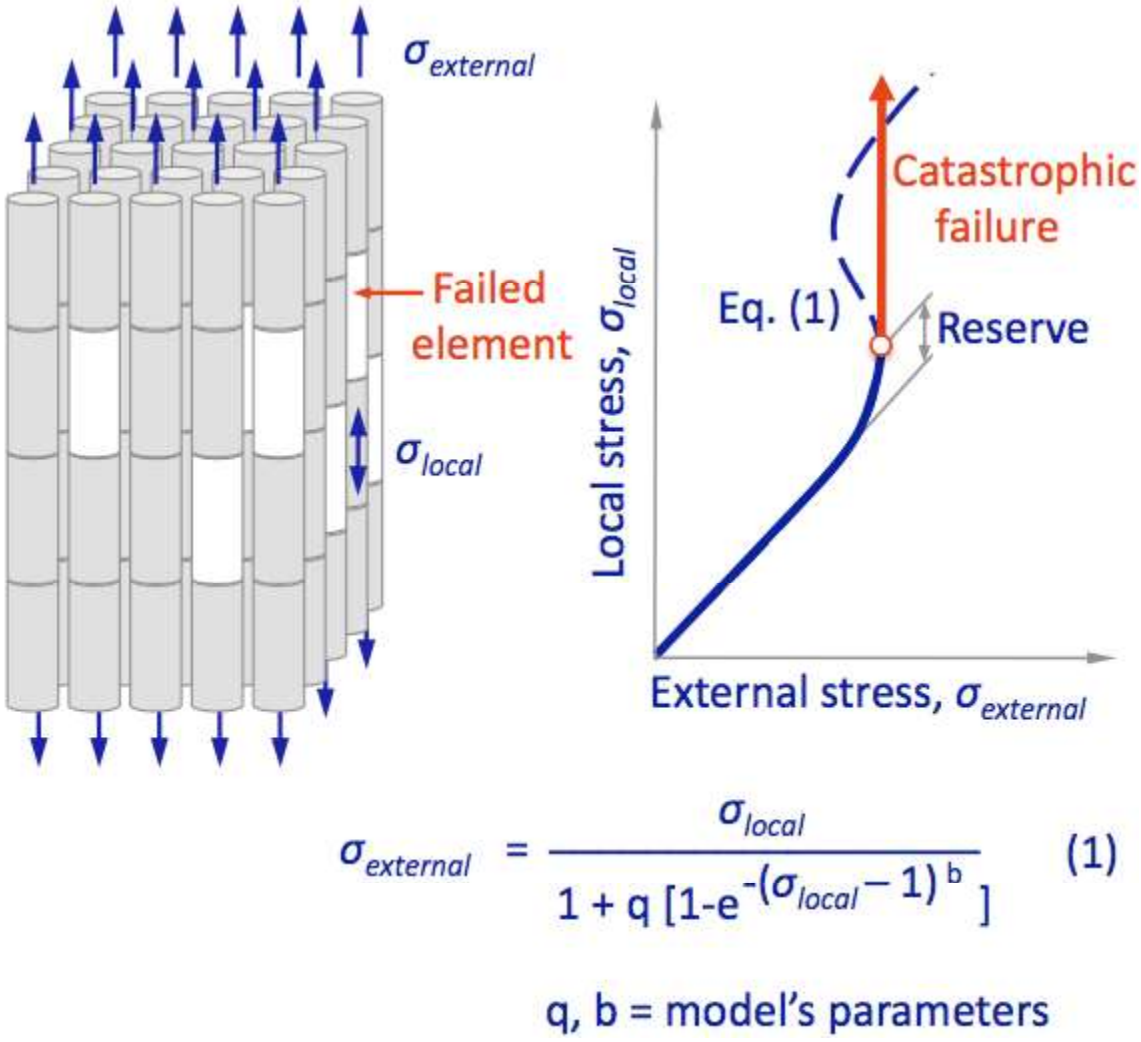

Catastrophe failure model and reserve ability of a complex system.

The failure of a complex system with parallel redundancy can be estimated based on probabilistic properties of the system elements. The model supposes that failure of several elements causes neighboring elements overloading. The model equation (1) shows the relationship between local and external stresses. The equation (1) is similar to the cusp catastrophe behavior. The theory predicts reserve ability of the complex system and the critical external stress.

Chapter 8

Peridynamics

A ductile fracture of an Al-Mg-Si alloy. A fracture is a mathematical singularity to which the classical equations of continuum mechanics cannot be applied directly - **Peridynamics** offers a numerical method.

Peridynamics is a formulation of continuum mechanics that is oriented toward deformations with discontinuities, especially fractures.

Purpose of peridynamics

The peridynamic theory is based on integral equations, in contrast with the classical theory of continuum mechanics, which is based on partial differential equations. Since partial derivatives do not exist on crack surfaces and other singularities, the classical equations of continuum mechanics cannot be applied directly when such features are present in a deformation. The integral equations of the peridynamic theory can be applied directly, because they do not require partial derivatives.

The ability to apply the same equations directly at all points in a mathematical model of a deforming structure helps the peridynamic approach avoid the need for the special techniques of fracture mechanics. For example, in peridynamics, there is no need for a separate crack growth law based on a stress intensity factor.

Definition and basic terminology

The basic equation of peridynamics is the following equation of motion:

$$\rho(x)\ddot{u}(x,t) = \int_R f(u(x',t) - u(x,t), x' - x, x)dV_{x'} + b(x,t)$$

where x is a point in a body R, t is time, u is the displacement vector field, and ρ is the mass density in the undeformed body. x' is a dummy variable of integration.

The vector valued function f is the force density that x' exerts on x. This force density depends on the relative displacement and relative position vectors between x' and x. The dimensions of f are force per volume squared. The function f is called the "pairwise force function" and contains all the constitutive (material-dependent) properties. It describes how the internal forces depend on the deformation.

The interaction between any x and x' is called a "bond." The physical mechanism in this interaction need not be specified. It is usually assumed that f vanishes whenever x' is outside a neighborhood of x (in the undeformed configuration) called the *horizon.*

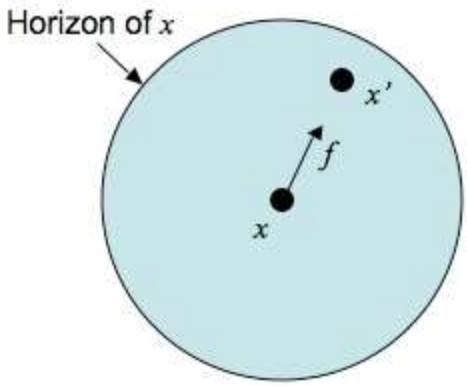

The term "peridynamic," an adjective, was proposed in the year 2000 and comes from the prefix *peri,* which means *all around*, *near*, or *surrounding*; and the root *dyna*, which means *force* or *power.* The term "peridynamics," a noun, is a shortened form of the phrase *peridynamic model of solid mechanics*.

Pairwise force functions

Using the abbreviated notation $u = u(x,t)$ and $u' = u(x',t)$ Newton's third law places the following restriction on f:

$$f(u-u', x-x', x') = -f(u'-u, x'-x, x)$$

for any x,x',u,u'. This equation states that the force density vector that x exerts on x' equals minus the force density vector that x' exerts on x. Balance of angular momentum requires that f be parallel to the vector connecting the deformed position of x to the deformed position of x':

$$((x'+u')-(x+u)) \times f(u'-u, x'-x, x) = 0.$$

A pairwise force function is specified by a graph of $|f|$ versus bond elongation e, defined by

$$e = |(x'+u')-(x+u)| - |x'-x|.$$

A schematic of a pairwise force function for the bond connecting two typical points is shown in the following figure:

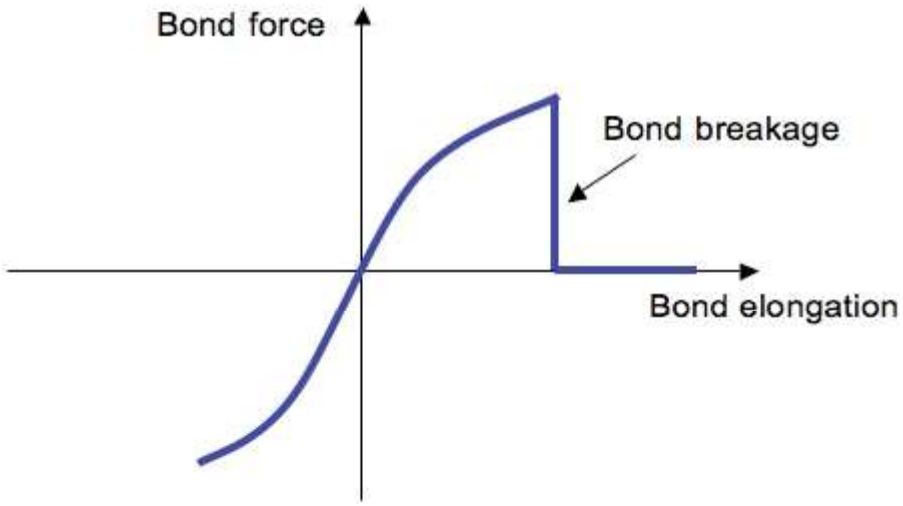

Damage

Damage is incorporated in the pairwise force function by allowing bonds to break when their elongation exceeds some prescribed value. After a bond breaks, it no longer sustains any force, and the endpoints are effectively disconnected from each other. When a bond breaks, the force it was carrying is redistributed to other bonds that have not yet broken. This increased load makes it more likely that these other bonds will break. The process of bond breakage and load redistribution, leading to further breakage, is how cracks grow in the peridynamic model.

Peridynamic states

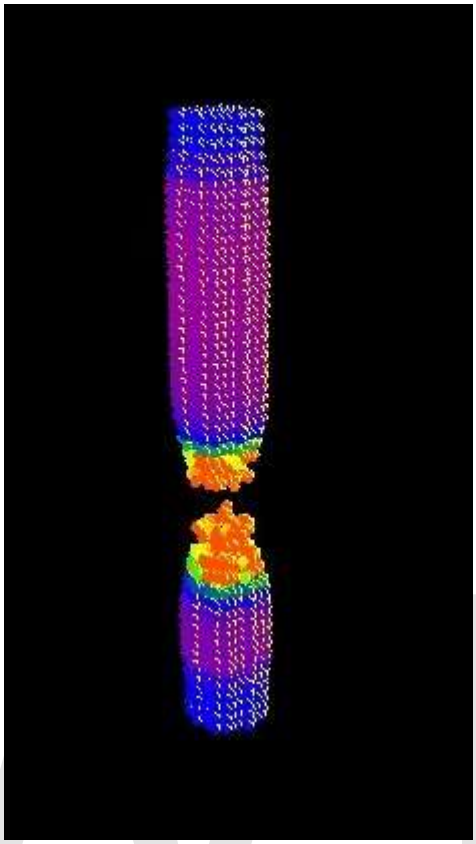

Computer model of the necking of an aluminum rod under tension. Colors indicate temperature increase due to plastic heating. Calculation performed with the Emu computer code using peridynamic states.

The theory described above assumes that each peridynamic bond responds independently of all the others. This is an oversimplification for most materials and leads to restrictions on the types of materials that can be modeled. In particular, this assumption implies that any isotropic linear elastic solid is restricted to a Poisson ratio of 1/4.

To address this lack of generality, the idea of "peridynamic states" was introduced. This allows the force density in each bond to depend on the stretches in all the bonds connected to its endpoints, in addition to its own stretch. For example, the force in a bond could depend on the net volume changes at the endpoints. The effect of this volume change, relative to the effect of the bond stretch, determines the Poisson ratio. With peridynamic states, any material that can be modeled within the standard theory of continuum mechanics can be modeled as a peridynamic material, while retaining the advantages of the peridynamic theory for fracture.

Chapter 9

Bending

Bending of an I-beam

In engineering mechanics, **bending** (also known as **flexure**) characterizes the behavior of a slender structural element subjected to an external load applied perpendicularly to a longitudinal axis of the element. The structural element is assumed to be such that at least one of its dimensions is a small fraction, typically 1/10 or less, of the other two. When the length is considerably longer than the width and the thickness, the element is called a beam. A closet rod sagging under the weight of clothes on clothes hangers is an example of a beam experiencing bending. On the other hand, a shell is a structure of any geometric form where the length and the width are of the same order of magnitude but the thickness of the structure (known as the 'wall') is considerably smaller. A large diameter, but thin-walled, short tube supported at its ends and loaded laterally is an example of a shell experiencing bending.

In the absence of a qualifier, the term *bending* is ambiguous because bending can occur locally in all objects. To make the usage of the term more precise, engineers refer to the *bending of rods*, the *bending of beams*, the *bending of plates*, the *bending of shells* and so on.

Quasistatic bending of beams

A beam deforms and stresses develop inside it when a transverse load is applied on it. In the quasistatic case, the amount of bending deflection and the stresses that develop are assumed not to change over time. In a horizontal beam supported at the ends and loaded downwards in the middle, the material at the over-side of the beam is compressed while the material at the underside is stretched. There are two forms of internal stresses caused by lateral loads:

- Shear stress parallel to the lateral loading plus complementary shear stress on planes perpendicular to the load direction;
- Direct compressive stress in the upper region of the beam, and direct tensile stress in the lower region of the beam.

These last two forces form a couple or moment as they are equal in magnitude and opposite in direction. This bending moment resists the sagging deformation characteristic of a beam experiencing bending. The stress distribution in a beam can be predicted quite accurately even when some simplifying assumptions are used.

Euler-Bernoulli bending theory

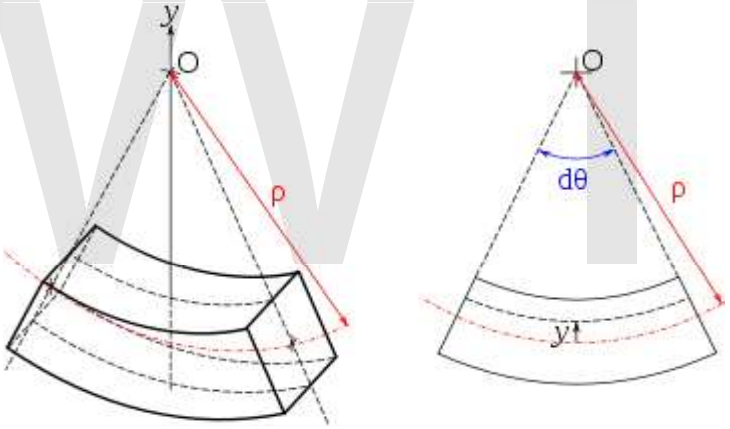

Element of a bent beam: the fibers form concentric arcs, the top fibers are compressed and bottom fibers stretched.

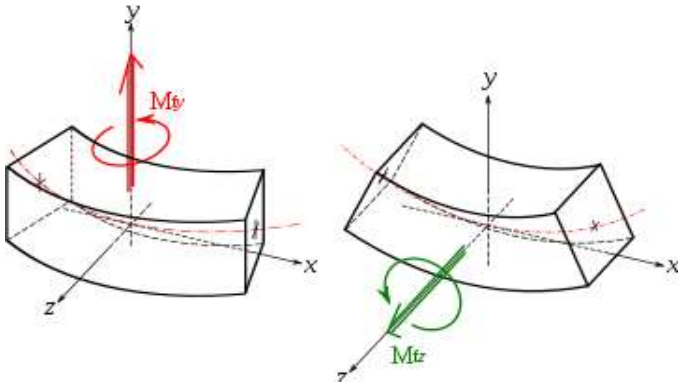

Bending moments in a beam

In the Euler-Bernoulli theory of slender beams, a major assumption is that 'plane sections remain plane'. In other words, any deformation due to shear across the section is not accounted for (no shear deformation). Also, this linear distribution is only applicable if the maximum stress is less than the yield stress of the material. For stresses that exceed yield, refer to article plastic bending. At yield, the maximum stress experienced in the section (at the furthest points from the neutral axis of the beam) is defined as the flexural strength.

The Euler-Bernoulli equation for the quasistatic bending of slender, isotropic, homogeneous beams of constant cross-section under an applied transverse load $q(x)$ is

$$EI \frac{\mathrm{d}^4 w(x)}{\mathrm{d}x^4} = q(x)$$

where E is the Young's modulus, I is the area moment of inertia of the cross-section, and $w(x)$ is the deflection of the neutral axis of the beam.

After a solution for the displacement of the beam has been obtained, the bending moment (M) and shear force (Q) in the beam can be calculated using the relations

$$M(x) = -EI \frac{\mathrm{d}^2 w}{\mathrm{d}x^2}; \quad Q(x) = \frac{\mathrm{d}M}{\mathrm{d}x}$$

Simple beam bending is often analyzed with the Euler-Bernoulli beam equation. The conditions for using simple bending theory are :

1. The beam is subject to pure bending. This means that the shear force is zero, and that no torsional or axial loads are present.
2. The material is isotropic and homogeneous.
3. The material obeys Hooke's law (it is linearly elastic and will not deform plastically).
4. The beam is initially straight with a cross section that is constant throughout the beam length.
5. The beam has an axis of symmetry in the plane of bending.
6. The proportions of the beam are such that it would fail by bending rather than by crushing, wrinkling or sideways buckling.
7. Cross-sections of the beam remain plane during bending.

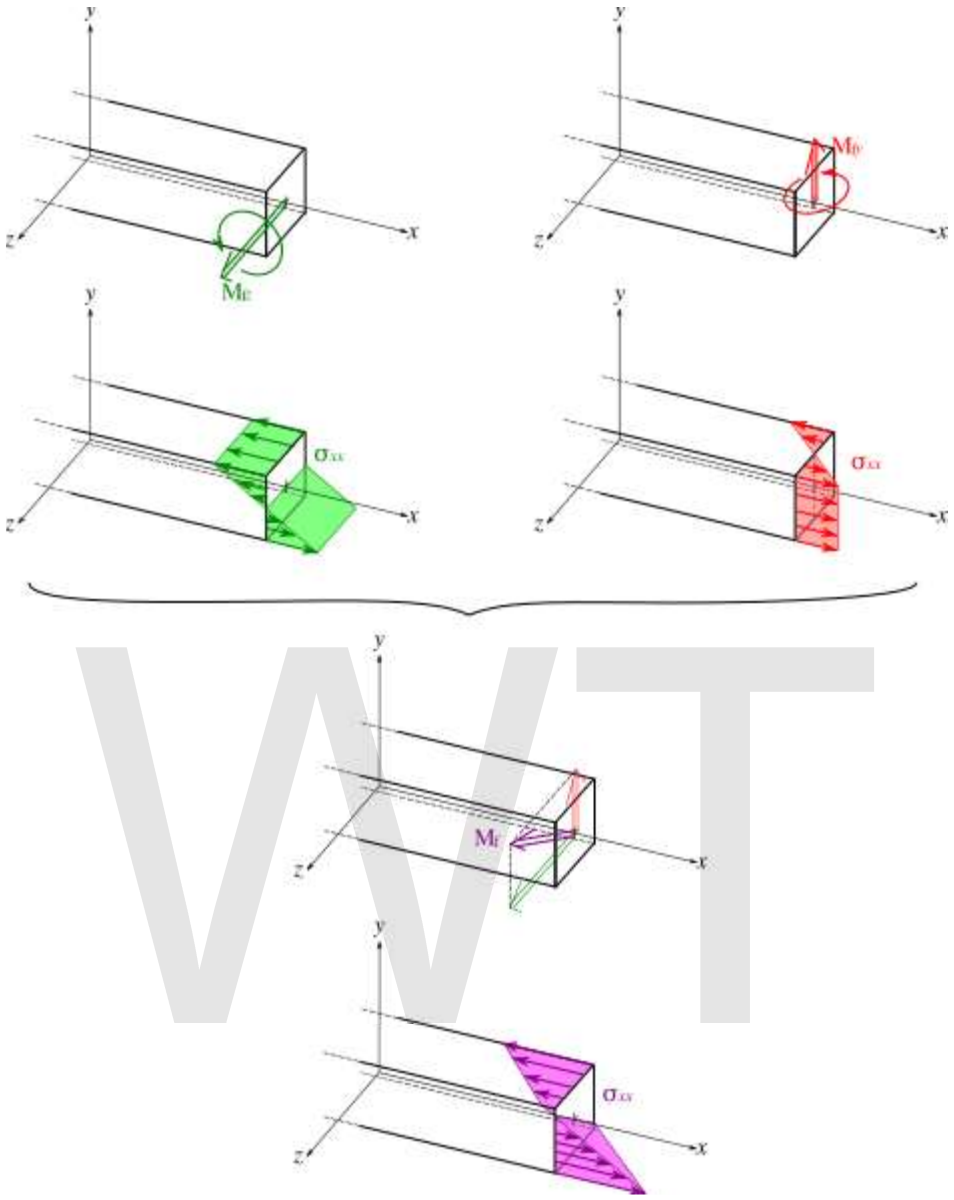

Deflection of a beam deflected symmetrically and principle of superposition

Compressive and tensile forces develop in the direction of the beam axis under bending loads. These forces induce stresses on the beam. The maximum compressive stress is found at the uppermost edge of the beam while the maximum tensile stress is located at the lower edge of the beam. Since the stresses between these two opposing maxima vary linearly, there therefore exists a point on the linear path between them where there is no bending stress. The locus of these points is the neutral axis. Because of this area with no stress and the adjacent areas with low stress, using uniform cross section beams in bending is not a particularly efficient means of supporting a load as it does not use the full capacity of the beam until it is on the brink of collapse. Wide-flange beams (I-beams) and truss girders effectively address this inefficiency as they minimize the amount of material in this under-stressed region.

The classic formula for determining the bending stress in a beam under simple bending is:

$$\sigma = \frac{My}{I_x}$$

where

- σ is the bending stress
- M - the moment about the neutral axis
- y - the perpendicular distance to the neutral axis
- I_x - the second moment of area about the neutral axis x

Extensions of Euler-Bernoulli beam bending theory

Plastic bending

The equation $\sigma = \frac{My}{I_x}$ is valid only when the stress at the extreme fiber (i.e. the portion of the beam farthest from the neutral axis) is below the yield stress of the material from which it is constructed. At higher loadings the stress distribution becomes non-linear, and ductile materials will eventually enter a *plastic hinge* state where the magnitude of the stress is equal to the yield stress everywhere in the beam, with a discontinuity at the neutral axis where the stress changes from tensile to compressive. This plastic hinge state is typically used as a limit state in the design of steel structures.

Complex or asymmetrical bending

The equation above is only valid if the cross-section is symmetrical. For homogeneous beams with asymmetrical sections, the axial stress in the beam is given by

$$\sigma_x(y,z) = -\frac{(M_z\ I_y + M_y\ I_{yz})}{I_y\ I_z - I_{yz}^2}y + \frac{(M_y\ I_z + M_z\ I_{yz})}{I_y\ I_z - I_{yz}^2}z$$

where y,z are the coordinates of a point on the cross section at which the stress is to be determined as shown to the right, M_y and M_z are the bending moments about the y and z centroid axes, I_y and I_z are the second moments of area (distinct from moments of inertia) about the y and z axes, and I_{yz} is the product of moments of area. Using this equation it is possible to calculate the bending stress at any point on the beam cross section regardless of moment orientation or cross-sectional shape. Note that M_y,M_z,I_y,I_z,I_{yz} do not change from one point to another on the cross section.

Large bending deformation

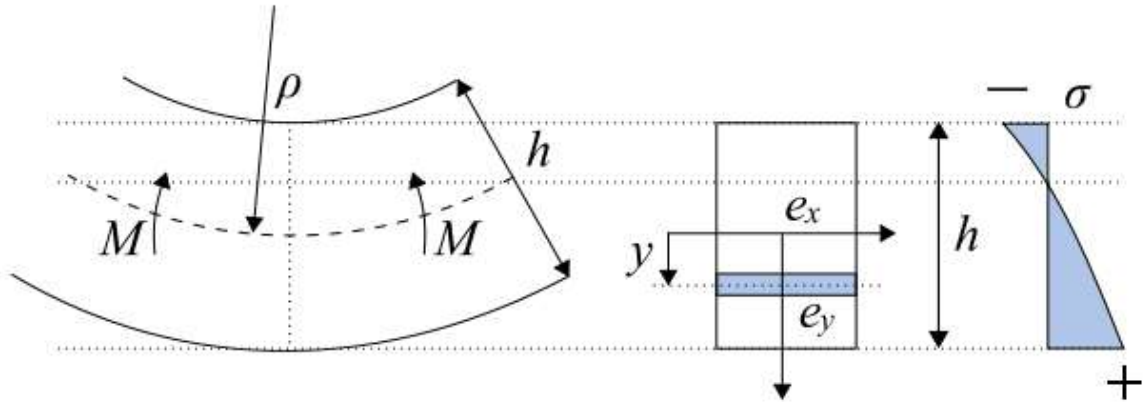

For large deformations of the body, the stress in the cross-section is calculated using an extended version of this formula. First the following assumptions must be made:

1. Assumption of flat sections - before and after deformation the considered section of body remains flat (i.e. is not swirled).
2. Shear and normal stresses in this section that are perpendicular to the normal vector of cross section have no influence on normal stresses that are parallel to this section.

Large bending considerations should be implemented when the bending radius ρ is smaller than ten section heights h:

$$\rho < 10h$$

With those assumptions the stress in large bending is calculated as:

$$\sigma = \frac{F}{A} + \frac{M}{\rho A} + \frac{M}{I_x'} y \frac{\rho}{\rho + y}$$

where

F is the normal force
A is the section area
M is the bending moment
ρ is the local bending radius (the radius of bending at the current section)
I_x' is the area moment of inertia along the **x** axis, at the *y* place
y is the position along **y** axis on the section area in which the stress σ is calculated

When bending radius ρ approaches infinity and *y* is near zero, the original formula is back:

$$\sigma = \frac{F}{A} \pm \frac{My}{I}.$$

Timoshenko bending theory

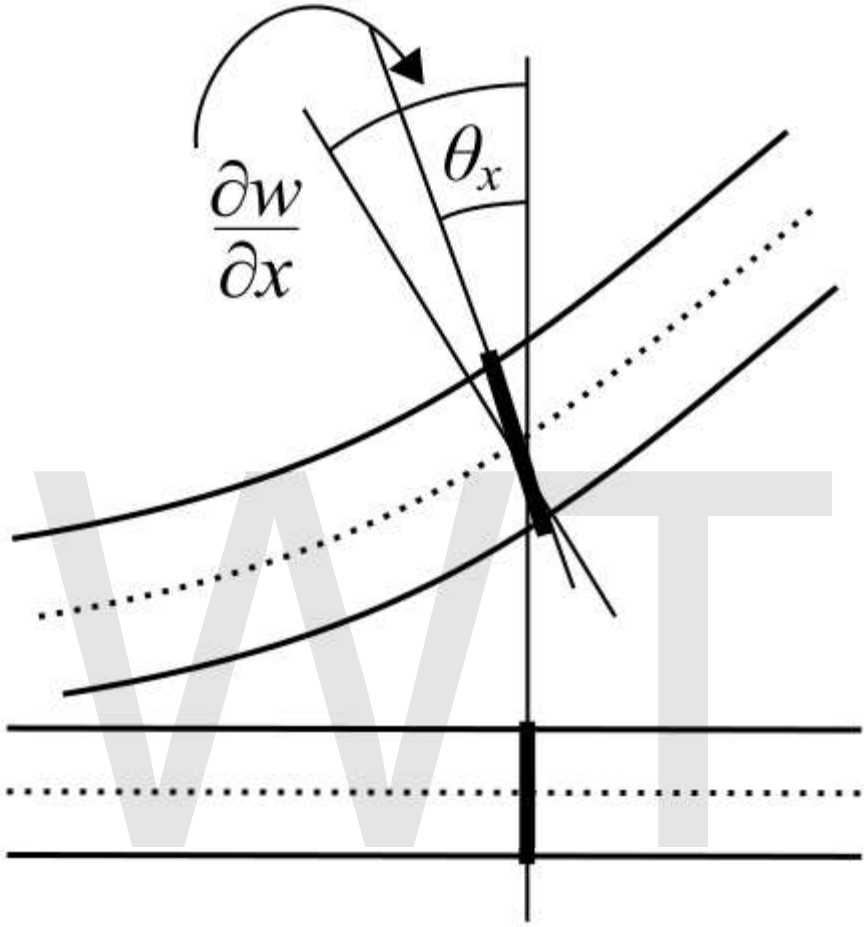

Deformation of a Timoshenko beam. The normal rotates by an amount θ which is not equal to *dw* / *dx*.

In 1921, Timoshenko improved upon the Euler-Bernoulli theory of beams by adding the effect of shear into the beam equation. The kinematic assumptions of the Timoshenko theory are

- normals to the axis of the beam remain straight after deformation
- there is no change in beam thickness after deformation

However, normals to the axis are not required to remain perpendicular to the axis after deformation.

The equation for the quasistatic bending of a linear elastic, isotropic, homogeneous beam of constant cross-section beam under these assumptions is

$$EI\,\frac{\mathrm{d}^4 w}{\mathrm{d}x^4} = q(x) - \frac{EI}{kAG}\,\frac{\mathrm{d}^2 q}{\mathrm{d}x^2}$$

where I is the area moment of inertia of the cross-section, A is the cross-sectional area, G is the shear modulus, and k is a **shear correction factor**. For materials with Poisson's ratios (ν) close to 0.3, the shear correction factor for a rectangular cross-section is approximately

$$k = \frac{5 + 5\nu}{6 + 5\nu}$$

The rotation ($\varphi(x)$) of the normal is described by the equation

$$\frac{\mathrm{d}\varphi}{\mathrm{d}x} = -\frac{\mathrm{d}^2 w}{\mathrm{d}x^2} - \frac{q(x)}{kAG}$$

The bending moment (M) and the shear force (Q) are given by

$$M(x) = -EI\,\frac{\mathrm{d}\varphi}{\mathrm{d}x}\,;\quad Q(x) = kAG\left(\frac{\mathrm{d}w}{\mathrm{d}x} - \varphi\right) = -EI\,\frac{\mathrm{d}^2\varphi}{\mathrm{d}x^2} = \frac{\mathrm{d}M}{\mathrm{d}x}$$

Dynamic bending of beams

The dynamic bending of beams, also known as flexural vibrations of beams, was first investigated by Daniel Bernoulli in the late 18th century. Bernoulli's equation of motion of a vibrating beam tended to overestimate the natural frequencies of beams and was improved marginally by Rayleigh in 1877 by the addition of a mid-plane rotation. In 1921 Stephen Timoshenko improved the theory further by incorporating the effect of shear on the dynamic response of bending beams. This allowed the theory to be used for problems involving high frequencies of vibration where the dynamic Euler-Bernoulli theory is inadequate. The Euler-Bernoulli and Timoshenko theories for the dynamic bending of beams continue to be used widely by engineers.

Euler-Bernoulli theory

The Euler-Bernoulli equation for the dynamic bending of slender, isotropic, homogeneous beams of constant cross-section under an applied transverse load $q(x,t)$ is

$$EI\,\frac{\partial^4 w}{\partial x^4} + m\,\frac{\partial^2 w}{\partial t^2} = q(x,t)$$

where E is the Young's modulus, I is the area moment of inertia of the cross-section, $w(x,t)$ is the deflection of the neutral axis of the beam, and m is mass per unit length of the beam.

Free vibrations

For the situation where there is no transverse load on the beam, the bending equation takes the form

$$EI\,\frac{\partial^4 w}{\partial x^4} + m\,\frac{\partial^2 w}{\partial t^2} = 0$$

Free, harmonic vibrations of the beam can then be expressed as

$$w(x,t) = \mathrm{Re}[\hat{w}(x)\; e^{-i\omega t}] \quad \Longrightarrow \quad \frac{\partial^2 w}{\partial t^2} = -\omega^2\; w(x,t)$$

and the bending equation can be written as

$$EI\,\frac{\mathrm{d}^4 \hat{w}}{\mathrm{d}x^4} - m\omega^2 \hat{w} = 0$$

The general solution of the above equation is

$$\hat{w} = A_1 \cosh(\beta x) + A_2 \sinh(\beta x) + A_3 \cos(\beta x) + A_4 \sin(\beta x)$$

$$\beta := \left(\frac{m}{EI}\,\omega^2\right)^{1/4}$$

where A_1,A_2,A_3,A_4 are constants and

The mode shapes of a cantilevered I-beam

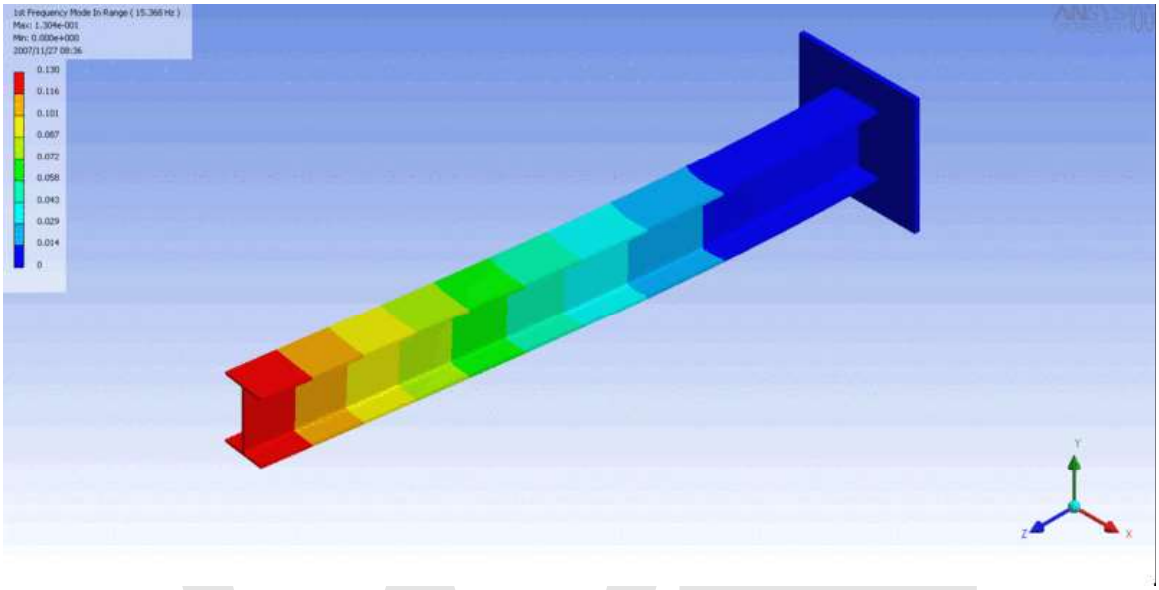

1st lateral bending

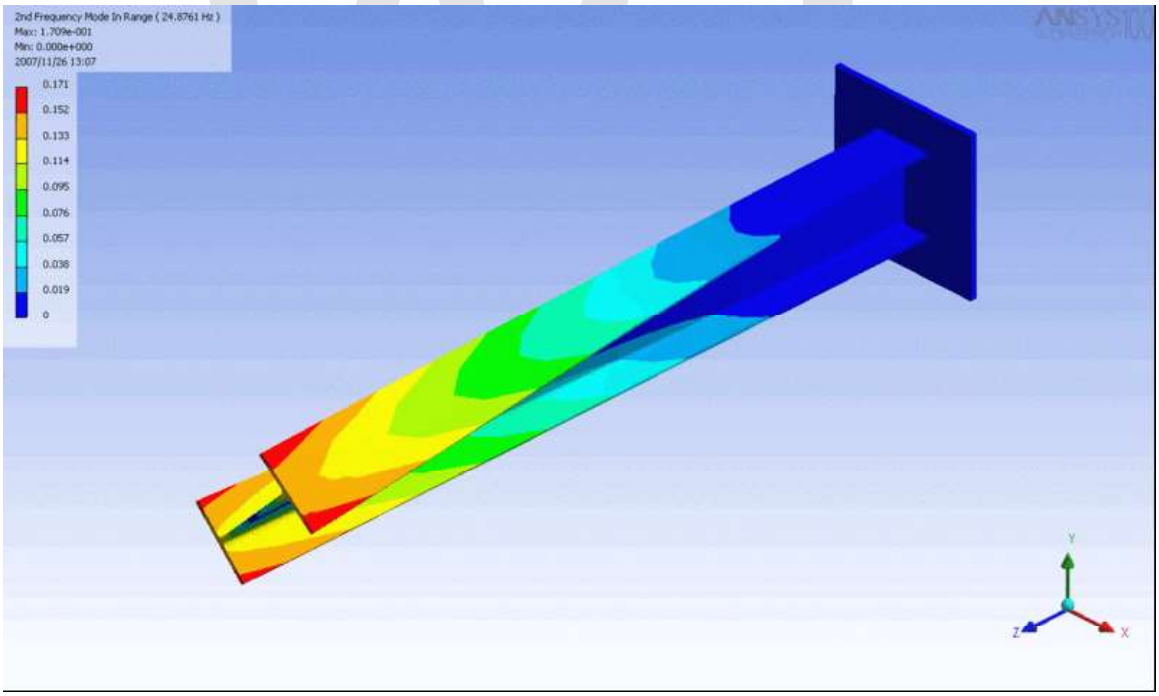

1st torsional

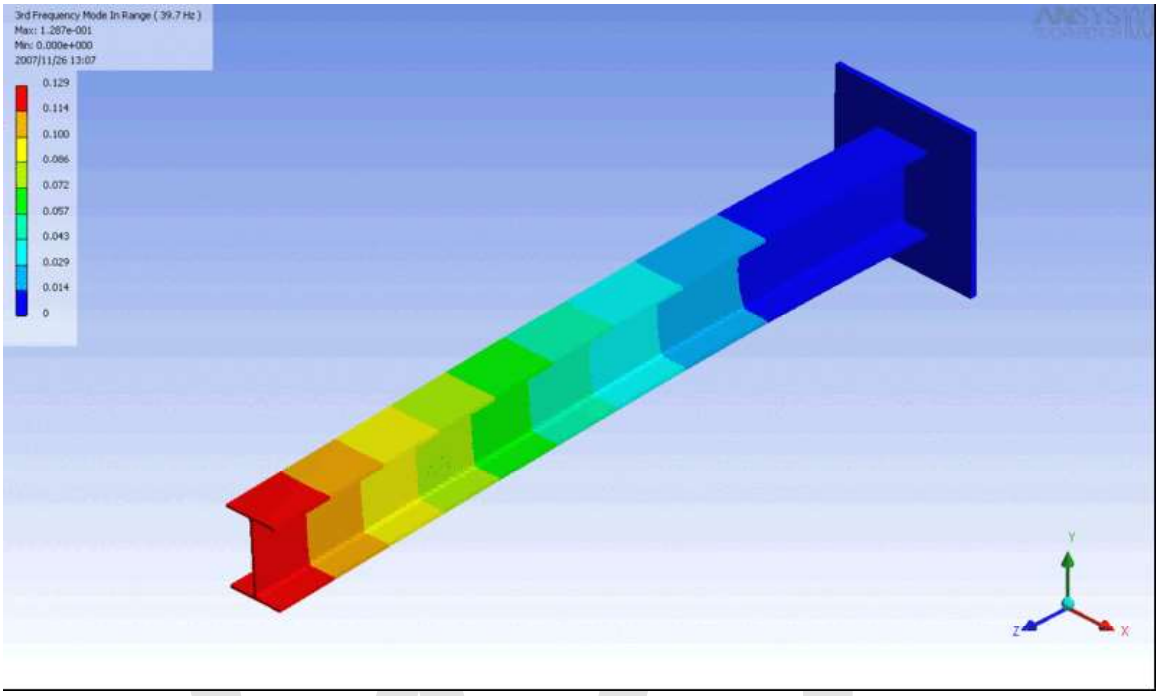

1st vertical bending

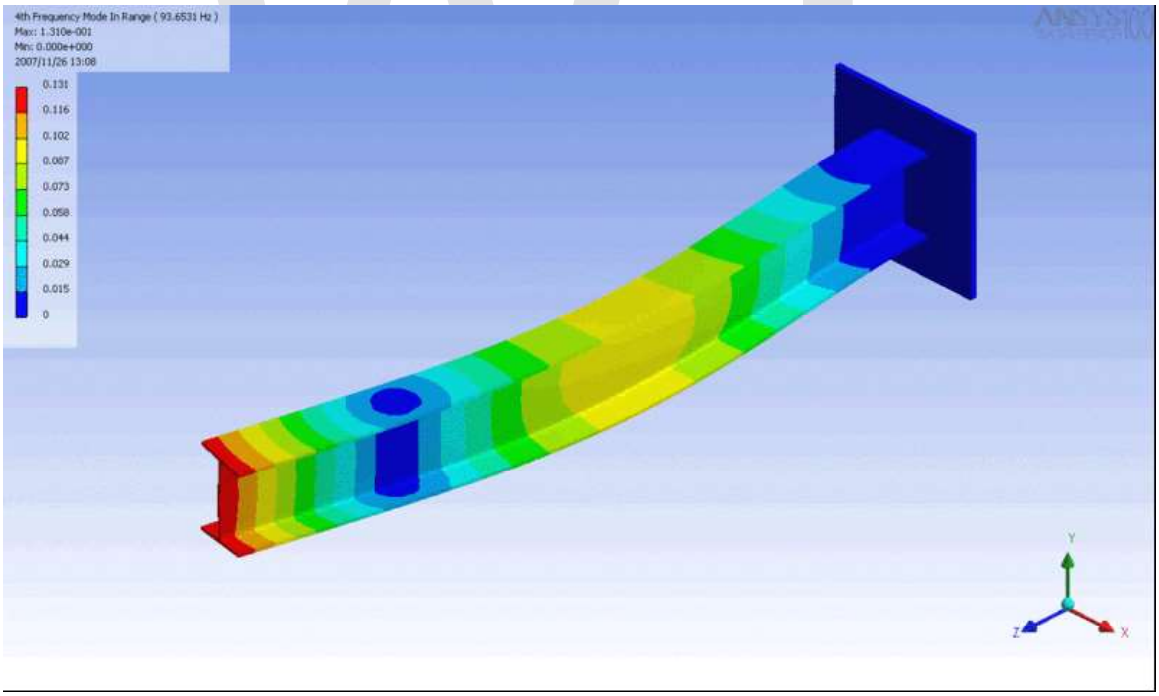

2nd lateral bending

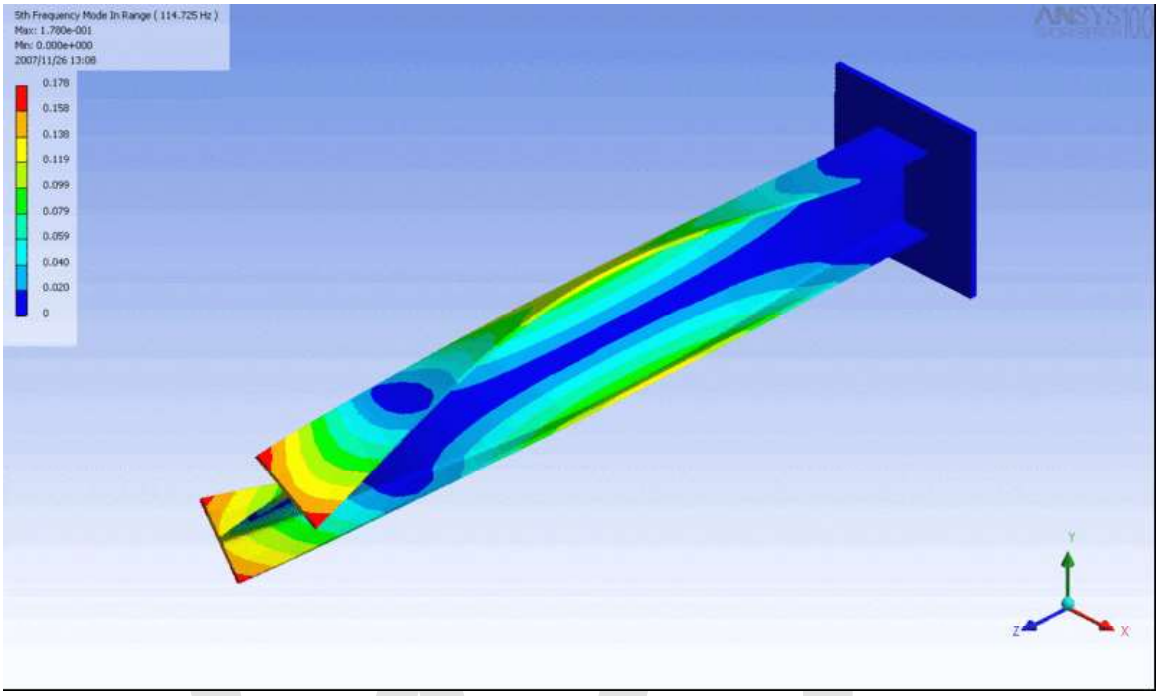

2nd torsional

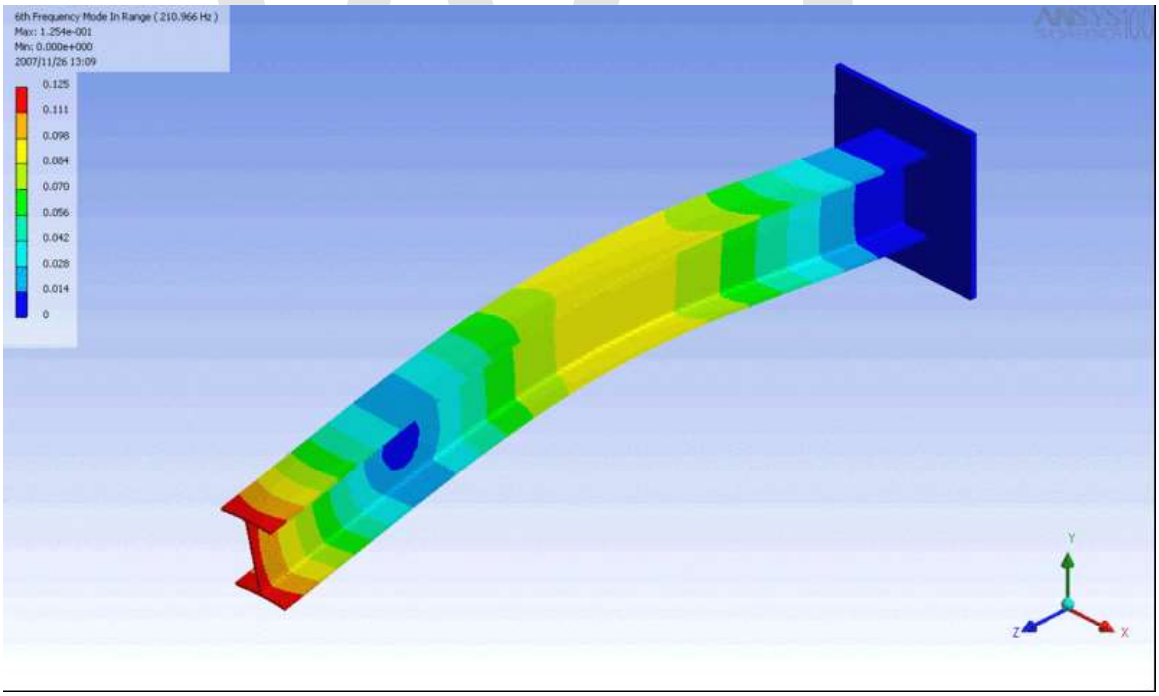

2nd vertical bending

Timoshenko-Rayleigh theory

In 1877, Rayleigh proposed an improvement to the dynamic Euler-Bernoulli beam theory by including the effect of rotational inertia of the cross-section of the beam. Timoshenko improved upon that theory in 1922 by adding the effect of shear into the beam equation. Shear deformations of the normal to the mid-surface of the beam are allowed in the Timoshenko-Rayleigh theory.

The equation for the bending of a linear elastic, isotropic, homogeneous beam of constant cross-section beam under these assumptions is

$$EI\,\frac{\partial^4 w}{\partial x^4}+m\,\frac{\partial^2 w}{\partial t^2}-\left(J+\frac{EIm}{kAG}\right)\frac{\partial^4 w}{\partial x^2\,\partial t^2}+\frac{Jm}{kAG}\frac{\partial^4 w}{\partial t^4}=q(x,t)+\frac{J}{kAG}\frac{\partial^2 q}{\partial t^2}-\frac{EI}{kAG}\frac{\partial^2 q}{\partial x^2}$$

where $J=\frac{mI}{A}$ is the polar moment of inertia of the cross-section, $m = \rho A$ is the mass per unit length of the beam, ρ is the density of the beam, A is the cross-sectional area, G is the shear modulus, and k is a **shear correction factor**. For materials with Poisson's ratios (ν) close to 0.3, the shear correction factor are approximately

$$\begin{aligned} k &= \tfrac{5+5\nu}{6+5\nu} \quad \text{rectangular cross-section} \\ &= \tfrac{6+12\nu+6\nu^2}{7+12\nu+4\nu^2} \quad \text{circular cross-section} \end{aligned}$$

Free vibrations

For free, harmonic vibrations the Timoshenko-Rayleigh equations take the form

$$EI\,\frac{\mathrm{d}^4\hat{w}}{\mathrm{d}x^4}+m\omega^2\left(\frac{J}{m}+\frac{EI}{kAG}\right)\frac{\mathrm{d}^2\hat{w}}{\mathrm{d}x^2}+m\omega^2\left(\frac{\omega^2 J}{kAG}-1\right)\hat{w}=0$$

This equation can be solved by noting that all the derivatives of w must have the same form to cancel out and hence as solution of the form e^{kx} may be expected. This observation leads to the characteristic equation

$$\alpha\,k^4+\beta\,k^2+\gamma=0\,;\;\;\alpha:=EI\,,\;\;\beta:=m\omega^2\left(\frac{J}{m}+\frac{EI}{kAG}\right)\,,\;\;\gamma:=m\omega^2\left(\frac{\omega^2 J}{kAG}-1\right)$$

The solutions of this quartic equation are

$$k_1=+\sqrt{z_+}\,,\quad k_2=-\sqrt{z_+}\,,\quad k_3=+\sqrt{z_-}\,,\quad k_4=-\sqrt{z_-}$$

where

$$z_+ := \frac{-\beta + \sqrt{\beta^2 - 4\alpha\gamma}}{2\alpha}, \quad z_- := \frac{-\beta - \sqrt{\beta^2 - 4\alpha\gamma}}{2\alpha}$$

The general solution of the Timoshenko-Rayleigh beam equation for free vibrations can then be written as

$$\hat{w} = A_1\, e^{k_1 x} + A_2\, e^{-k_1 x} + A_3\, e^{k_3 x} + A_4\, e^{-k_3 x}$$

Quasistatic bending of plates

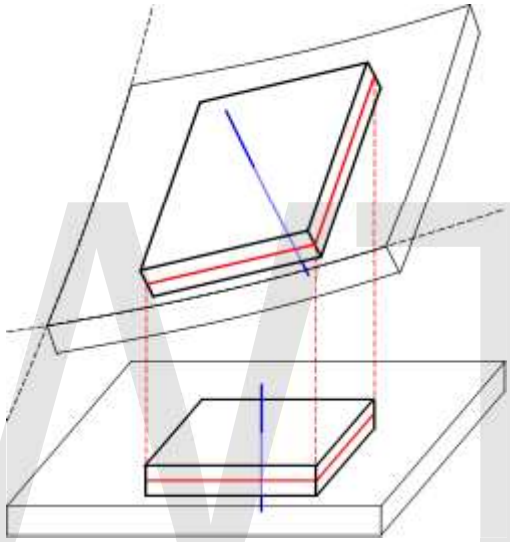

Deformation of a thin plate highlighting the displacement, the mid-surface (red) and the normal to the mid-surface (blue)

The defining feature of beams is that one of the dimensions is much *larger* than the other two. A structure is called a plate when it is flat and one of its dimensions is much *smaller* than the other two. There several theories that attempt to describe the deformation and stress in a plate under applied loads two of which have been used widely. These are

- the Kirchhoff-Love theory of plates (also called classical plate theory)
- the Mindlin-Reissner plate theory (also called the first-order shear theory of plates)

Kirchhoff-Love theory of plates

The assumptions of Kirchhoff-Love theory are

- straight lines normal to the mid-surface remain straight after deformation
- straight lines normal to the mid-surface remain normal to the mid-surface after deformation

- the thickness of the plate does not change during a deformation.

These assumptions imply that

$$u_\alpha(\mathbf{x}) = -x_3 \ \frac{\partial w^0}{\partial x_\alpha} = -x_3 \ w^0_{,\alpha} \ ; \quad \alpha = 1,2$$
$$u_3(\mathbf{x}) = w^0(x_1, x_2)$$

where $\mathbf{u}$ is the displacement of a point in the plate and w^0 is the displacement of the mid-surface.

The strain-displacement relations are

$$\varepsilon_{\alpha\beta} = -x_3 \ w^0_{,\alpha\beta}$$
$$\varepsilon_{\alpha 3} = 0$$
$$\varepsilon_{33} = 0$$

The equilibrium equations are

$$M_{\alpha\beta,\alpha\beta} + q(x) = 0 \ ; \quad M_{\alpha\beta} := \int_{-h}^{h} x_3 \ \sigma_{\alpha\beta} \ dx_3$$

where $q(x)$ is an applied load normal to the surface of the plate.

In terms of displacements, the equilibrium equations for an isotropic, linear elastic plate in the absence of external load can be written as

$$w^0_{,1111} + 2 \ w^0_{,1212} + w^0_{,2222} = 0$$

In direct tensor notation,

$$\nabla^2 \nabla^2 w = 0$$

Mindlin-Reissner theory of plates

The special assumption of this theory is that normals to the mid-surface remain straight and inextensible but not necessarily normal to the mid-surface after deformation. The displacements of the plate are given by

$$u_\alpha(\mathbf{x}) = -x_3 \ \varphi_\alpha \ ; \quad \alpha = 1,2$$
$$u_3(\mathbf{x}) = w^0(x_1, x_2)$$

where φ_α are the rotations of the normal.

The strain-displacement relations that result from these assumptions are

$$\varepsilon_{\alpha\beta} = -x_3 \ \varphi_{\alpha,\beta}$$
$$\varepsilon_{\alpha 3} = \frac{1}{2}\,\kappa\,\left(w^0_{,\alpha} - \varphi_\alpha\right)$$
$$\varepsilon_{33} = 0$$

where κ is a shear correction factor.

The equilibrium equations are

$$M_{\alpha\beta,\beta} - Q_\alpha = 0$$
$$Q_{\alpha,\alpha} + q = 0$$

where

$$Q_\alpha := \kappa \int_{-h}^{h} \sigma_{\alpha 3}\ dx_3$$

Dynamic bending of plates

Dynamics of thin Kirchhoff plates

The dynamic theory of plates determines the propagation of waves in the plates, and the study of standing waves and vibration modes. The equations that govern the dynamic bending of Kirchhoff plates are

$$M_{\alpha\beta,\alpha\beta} - q(x,t) = J_1\ \ddot{w}^0 - J_3\ \ddot{w}^0_{,\alpha\alpha}$$

where, for a plate with density $\rho = \rho(x)$,

$$J_1 := \int_{-h}^{h} \rho\ dx_3\ ; \quad J_3 := \int_{-h}^{h} x_3^2\ \rho\ dx_3$$

and

$$\ddot{w}^0 = \frac{\partial^2 w^0}{\partial t^2}\ ; \quad \ddot{w}^0_{,\alpha\beta} = \frac{\partial^2 \ddot{w}^0}{\partial x_\alpha \partial x_\beta}$$

The figures below show some vibrational modes of a circular plate.

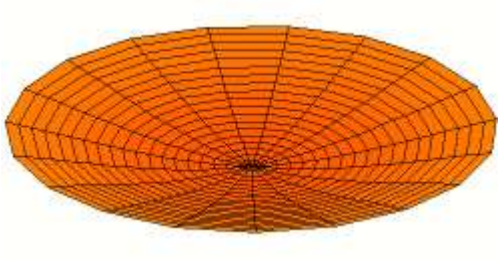

mode $k = 0$, $p = 1$

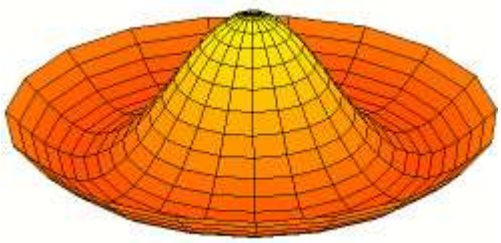

mode $k = 0$, $p = 2$

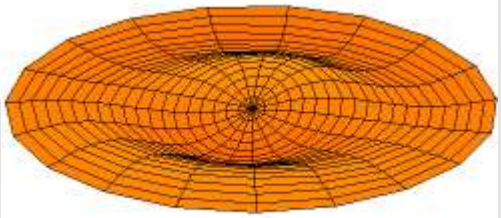

mode $k = 1$, $p = 2$

Chapter 10

Euler–Bernoulli Beam Equation

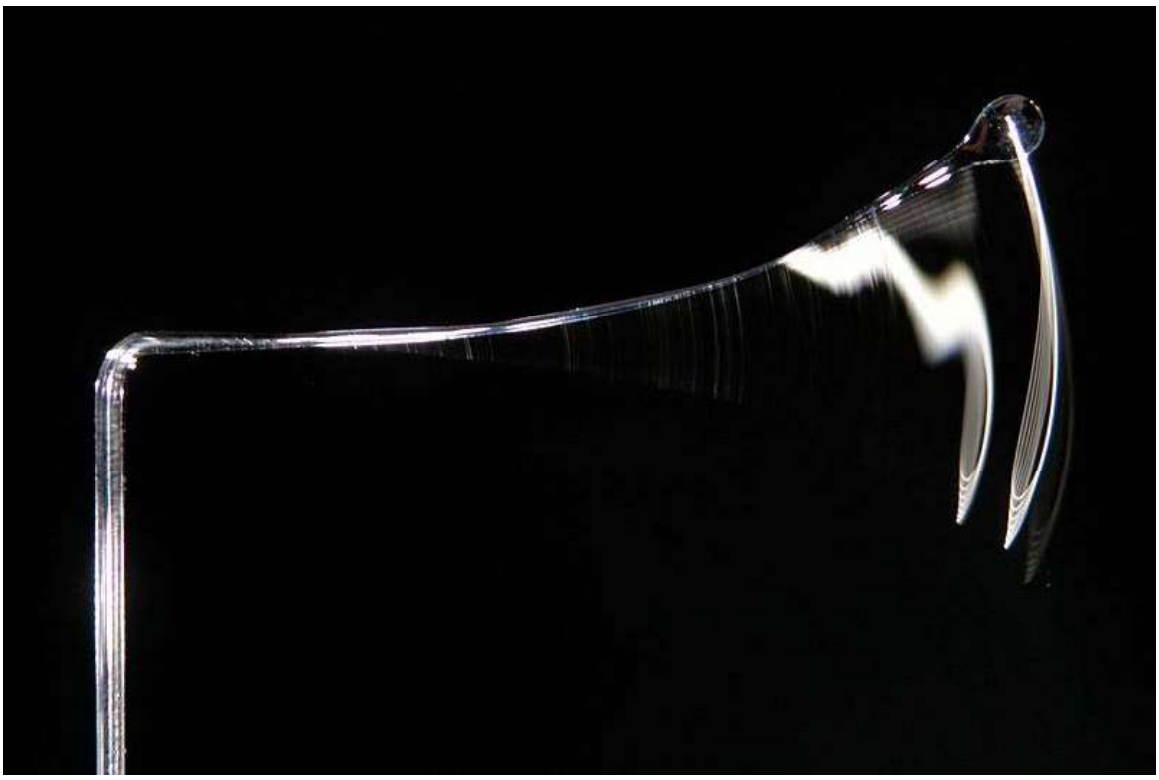

This vibrating glass beam may be modeled as a cantilever beam with acceleration, variable linear density, variable section modulus, some kind of dissipation, springy end loading, and possibly a point mass at the free end.

Euler–Bernoulli beam theory (also known as **engineer's beam theory**, **classical beam theory** or just **beam theory**) is a simplification of the linear theory of elasticity which provides a means of calculating the load-carrying and deflection characteristics of beams. It covers the case for small deflections of a beam which is subjected to lateral loads only. It is thus a special case of Timoshenko beam theory which accounts for shear deformation and is applicable for thick beams. It was first enunciated circa 1750 , but was not applied on a large scale until the development of the Eiffel Tower and the Ferris

wheel in the late 19th century. Following these successful demonstrations, it quickly became a cornerstone of engineering and an enabler of the Second Industrial Revolution.

Additional analysis tools have been developed such as plate theory and finite element analysis, but the simplicity of beam theory makes it an important tool in the sciences, especially structural and mechanical engineering.

History

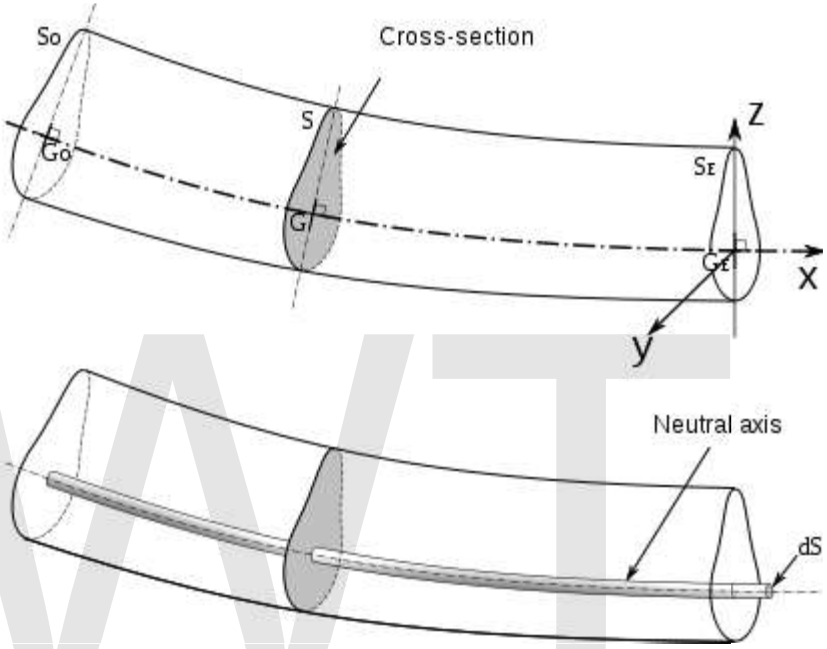

Schematic of cross-section of a bent beam showing the neutral axis.

Prevailing consensus is that Galileo Galilei made the first attempts at developing a theory of beams, but recent studies argue that Leonardo da Vinci was the first to make the crucial observations. Da Vinci lacked Hooke's law and calculus to complete the theory, whereas Galileo was held back by an incorrect assumption he made.

The Bernoulli beam is named after Jacob Bernoulli, who made the significant discoveries. Leonhard Euler and Daniel Bernoulli were the first to put together a useful theory circa 1750. At the time, science and engineering were generally seen as very distinct fields, and there was considerable doubt that a mathematical product of academia could be trusted for practical safety applications. Bridges and buildings continued to be designed by precedent until the late 19th century, when the Eiffel Tower and Ferris wheel demonstrated the validity of the theory on large scales.

Static beam equation

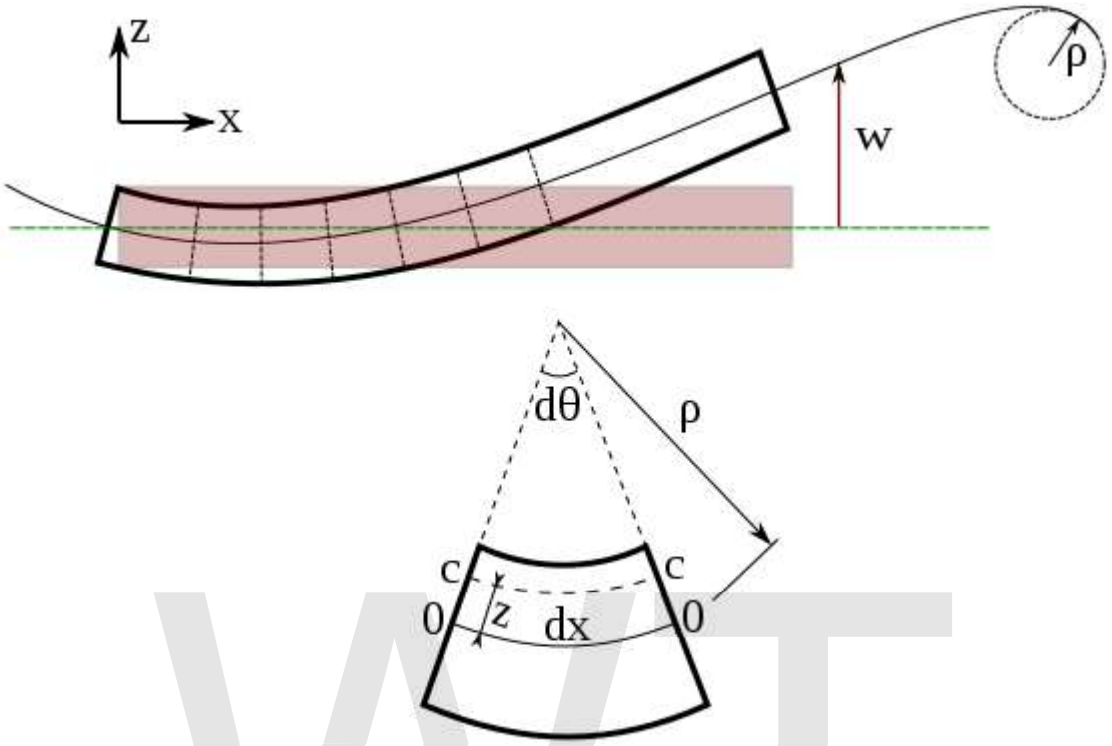

Bending of an Euler-Bernoulli beam. Each cross-section of the beam is at 90 degrees to the neutral axis.

The Euler-Bernoulli equation describes the relationship between the beam's deflection and the applied load:

$$\frac{\mathrm{d}^2}{\mathrm{d}x^2}\left(EI\frac{\mathrm{d}^2 w}{\mathrm{d}x^2}\right) = q.$$

The curve $w(x)$ describes the deflection w of the beam at some position x (recall that the beam is modeled as a one-dimensional object). q is a distributed load, in other words a force per unit length (analogous to pressure being a force per area); it may be a function of x, w, or other variables.

Note that E is the elastic modulus and that I is the second moment of area. I must be calculated with respect to the centroidal axis perpendicular to the applied loading. For an Euler-Bernoulli beam not under any axial loading this axis is called the neutral axis.

Often, $w = w(x)$, $q = q(x)$, and EI is a constant, so that:

$$EI\frac{\mathrm{d}^4 w}{\mathrm{d}x^4} = q(x).$$

This equation, describing the deflection of a uniform, static beam, is used widely in engineering practice. Tabulated expressions for the deflection *w* for common beam configurations can be found in engineering handbooks. For more complicated situations the deflection can be determined by solving the Euler-Bernoulli equation using techniques such as the "slope deflection method", "moment distribution method", "moment area method, "conjugate beam method", "the principle of virtual work", "direct integration", "Castigliano's method", "Macaulay's method" or the "direct stiffness method".

Successive derivatives of *w* have important meanings:

- w is the deflection.
- $\frac{\mathrm{d}w}{\mathrm{d}x} = \varphi$ is the slope of the beam.
- $-EI\frac{\mathrm{d}^2w}{\mathrm{d}x^2} = M$ is the bending moment in the beam.
- $-\frac{\mathrm{d}}{\mathrm{d}x}\left(EI\frac{\mathrm{d}^2w}{\mathrm{d}x^2}\right) = Q$ is the shear force in the beam.

The stresses in a beam can be calculated from the above expressions after the deflection due to a given load has been determined.

A number of different sign conventions can be found in the literature on the bending of beams and care should be take to maintain consistency. In this chapter, the sign convention has been chosen so the coordinate system is right handed. Forces acting in the positive *x* and *z* directions are assumed positive. The sign of the bending moment is chosen so that a positive value leads to a tensile stress at the bottom cords. The sign of the shear force has been chosen such that it matches the sign of the bending moment.

Dynamic beam equation

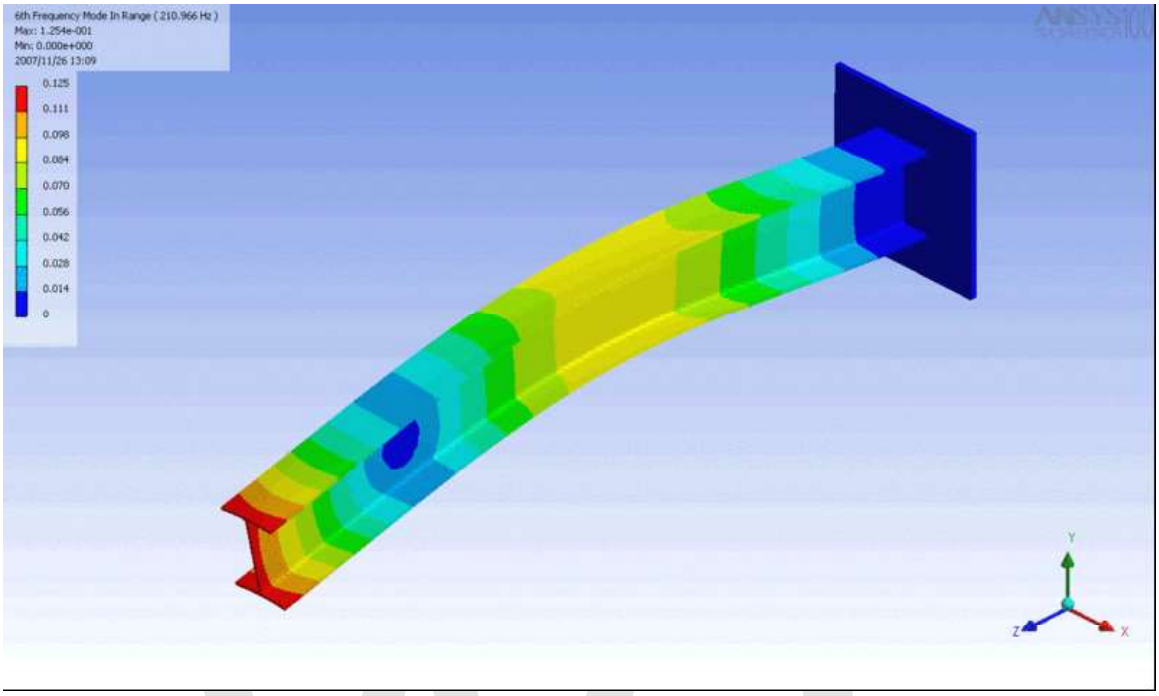

Vibration of a wide-flange beam (I-beam).

The dynamic beam equation is the Euler-Lagrange equation for the following action

$$S = \int_0^L \left[\frac{1}{2}\mu \left(\frac{\partial w}{\partial t} \right)^2 - \frac{1}{2} EI \left(\frac{\partial^2 w}{\partial x^2} \right)^2 + q(x)w(x,t) \right] dx$$

The first term represents the kinetic energy where μ is the mass per unit length; the second one represents the potential energy due to internal forces (when considered with a negative sign) and the third term represents the potential energy due to the external load $q(x)$. The Euler-Lagrange equation is used to determine the function that minimizes the functional S. For a dynamic Euler-Bernoulli beam, the Euler-Lagrange equation is

$$\frac{\partial^2}{\partial x^2} \left(EI \frac{\partial^2 w}{\partial x^2} \right) = -\mu \frac{\partial^2 w}{\partial t^2} + q(x)$$

Stress

Besides deflection, the beam equation describes forces and moments and can thus be used to describe stresses. For this reason, the Euler–Bernoulli beam equation is widely used in engineering, especially civil and mechanical, to determine the strength (as well as deflection) of beams under bending.

Both the bending moment and the shear force cause stresses in the beam. The stress due to shear force is maximum along the neutral axis of the beam (when the width of the beam, t, is constant along the cross section of the beam; otherwise an integral involving the first moment and the beam's width needs to be evaluated for the particular cross section), and the maximum tensile stress is at either the top or bottom surfaces. Thus the maximum principal stress in the beam may be neither at the surface nor at the center but in some general area. However, shear force stresses are negligible in comparison to bending moment stresses in all but the stockiest of beams as well as the fact that stress concentrations commonly occur at surfaces, meaning that the maximum stress in a beam is likely to be at the surface.

Simple or symmetrical bending

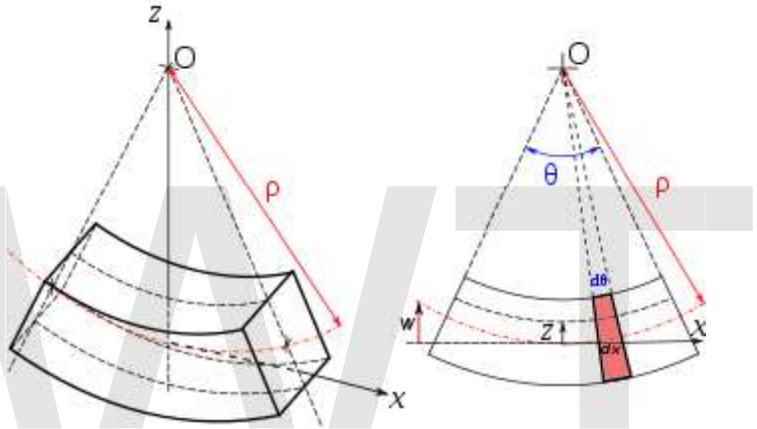

Element of a bent beam: the fibers form concentric arcs, the top fibers are compressed and bottom fibers stretched.

For beam cross-sections that are symmetrical about a plane perpendicular to the neutral plane, it can be shown that the tensile stress experienced by the beam may be expressed as:

$$\sigma = \frac{Mz}{I} = -zE\,\frac{\mathrm{d}^2 w}{\mathrm{d}x^2}.$$

Here, z is the distance from the neutral axis to a point of interest; and M is the bending moment. Note that this equation implies that pure bending (of positive sign) will cause zero stress at the neutral axis, positive (tensile) stress at the "top" of the beam, and negative (compressive) stress at the bottom of the beam; and also implies that the maximum stress will be at the top surface and the minimum at the bottom. This bending stress may be superimposed with axially applied stresses, which will cause a shift in the neutral (zero stress) axis.

Maximum stresses at a cross-section

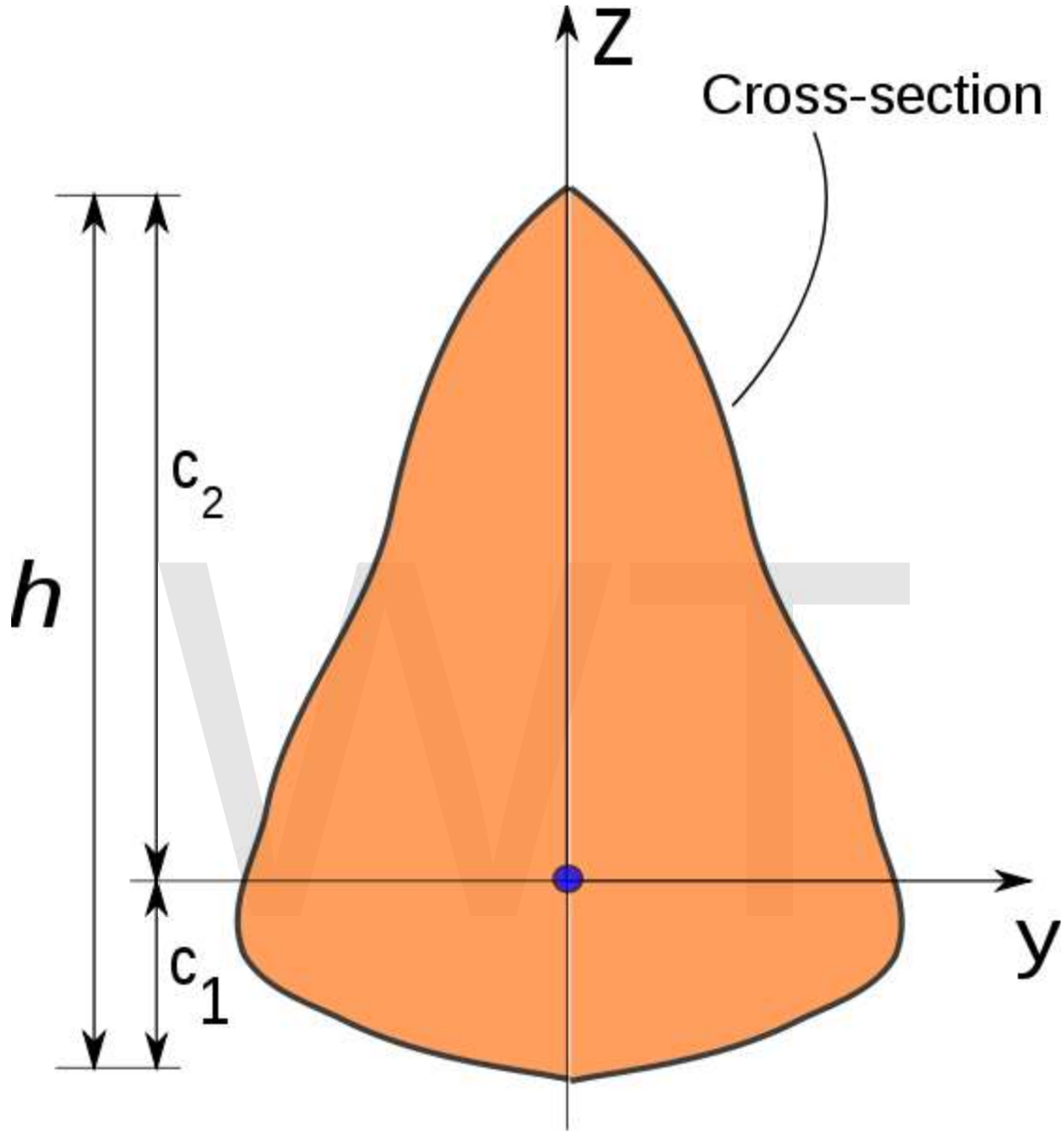

Quantities used in the definition of the section modulus of a beam.

The maximum tensile stress at a cross-section is at the location $z = c_1$ and the maximum compressive stress is at the location $z = -c_2$ where the height of the cross-section is $h = c_1 + c_2$. These stresses are

$$\sigma_1 = \frac{Mc_1}{I} = \frac{M}{S_1}; \quad \sigma_2 = -\frac{Mc_2}{I} = -\frac{M}{S_2}$$

The quantities S_1,S_2 are the section moduli and are defined as

$$S_1 = \frac{I}{c_1}\,; \quad S_2 = \frac{I}{c_2}$$

The section modulus combines all the important geometric information about a beam's section into one quantity. For the case where a beam is doubly-symmetric, $c_1 = c_2$ and we have one section modulus $S = I / c$.

Strain in an Euler–Bernoulli beam

We need an expression for the strain in terms of the deflection of the neutral surface to relate the stresses in an Euler-Bernoulli beam to the deflection. To obtain that expression we use the assumption that normals to the neutral surface remain normal during the deformation and that deflections are small. These assumptions imply that the beam bends into an arc of a circle of radius ρ and that the neutral surface does not change in length during the deformation.

Let dx be the length of an element of the neutral surface in the undeformed state. For small deflections, the element does not change its length after bending but deforms into an arc of a circle of radius ρ. If dθ is the angle subtended by this arc, then $\mathrm{d}x = \rho\ \mathrm{d}\theta$.

Let us now consider another segment of the element at a distance z above the neutral surface. The initial length of this element is dx. However, after bending, the length of the element becomes $\mathrm{d}x' = (\rho - z)\ \mathrm{d}\theta = \mathrm{d}x - z\ \mathrm{d}\theta$. The strain in that segment of the beam is given by

$$\varepsilon_x = \frac{\mathrm{d}x' - \mathrm{d}x}{\mathrm{d}x} = -\frac{z}{\rho} = -\kappa\ z$$

where κ is the curvature of the beam. This gives us the axial strain in the beam as a function of distance from the neutral surface. However, we still need to find a relation between the radius of curvature and the beam deflection w.

Relation between curvature and beam deflection

Let P be a point on the neutral surface of the beam at a distance x from the origin of the (x,z) coordinate system. The slope of the beam, i.e., the angle made by the neutral surface with the x-axis, at this point is

$$\theta(x) = \frac{\mathrm{d}w}{\mathrm{d}x}$$

Therefore, for an infinitesimal element dx, the relation $\mathrm{d}x = \rho\ \mathrm{d}\theta$can be written as

$$\frac{1}{\rho} = \frac{\mathrm{d}\theta}{\mathrm{d}x} = \frac{\mathrm{d}^2 w}{\mathrm{d}x^2} = \kappa$$

Hence the strain in the beam may be expressed as

$$\varepsilon_x = -z\frac{\mathrm{d}^2 w}{\mathrm{d}x^2}$$

Stress-strain relations

For a one-dimensional linear elastic material, the stress is related to be strain by $\sigma = E\varepsilon$ where E is the Young's modulus. Hence the stress in an Euler-Bernoulli beam is given by

$$\sigma_x = -zE\frac{\mathrm{d}^2 w}{\mathrm{d}x^2}$$

Note that the above relation, when compared with the relation between the axial stress and the bending moment, leads to

$$M = -EI\frac{\mathrm{d}^2 w}{\mathrm{d}x^2}$$

Since the shear force is given by $Q = \mathrm{d}M / \mathrm{d}x$, we also have

$$Q = -EI\frac{\mathrm{d}^3 w}{\mathrm{d}x^3}$$

Boundary considerations

The beam equation contains a fourth-order derivative in x. To find a unique solution $w(x,t)$ we need four boundary conditions. The boundary conditions usually model *supports*, but they can also model point loads, distributed loads and moments. The *support* or displacement boundary conditions are used to fix values of displacement (w) and rotations ($\mathrm{d}w / \mathrm{d}x$) on the boundary. Such boundary conditions are also called Dirichlet boundary conditions. Load and moment boundary conditions involve higher derivatives of w and represent momentum flux. Flux boundary conditions are also called Neumann boundary conditions.

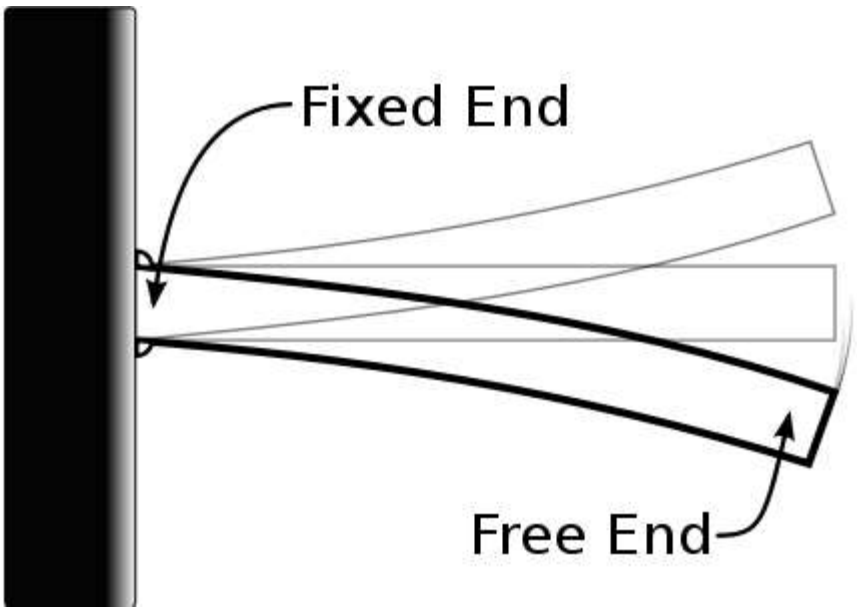

A cantilever beam.

As an example consider a cantilever beam that is built-in at one end and free at the other as shown in the adjacent figure. At the built-in end of the beam there cannot be any displacement or rotation of the beam. This means that at the left end both deflection and slope are zero. Since no external bending moment is applied at the free end of the beam, the bending moment at that location is zero. In addition, if there is no external force applied to the beam, the shear force at the free end is also zero.

Taking the x coordinate of the left end as 0 and the right end as L (the length of the beam), these statements translate to the following set of boundary conditions (assume EI is a constant):

$$w|_{x=0} = 0 \quad ; \quad \left.\frac{\partial w}{\partial x}\right|_{x=0} = 0 \qquad \text{(fixed end)}$$

$$\left.\frac{\partial^2 w}{\partial x^2}\right|_{x=L} = 0 \quad ; \quad \left.\frac{\partial^3 w}{\partial x^3}\right|_{x=L} = 0 \qquad \text{(free end)}$$

A simple support (pin or roller) is equivalent to a point force on the beam which is adjusted in such a way as to fix the position of the beam at that point. A fixed support or clamp, is equivalent to the combination of a point force and a point torque which is adjusted in such a way as to fix both the position and slope of the beam at that point. Point forces and torques, whether from supports or directly applied, will divide a beam into a set of segments, between which the beam equation will yield a continuous solution, given four boundary conditions, two at each end of the segment. Assuming that the product EI is a constant, and defining $\lambda = F / EI$ where F is the magnitude of a point force, and $\tau = M / EI$ where M is the magnitude of a point torque, the boundary conditions appropriate for some common cases is given in the table below. The change in a

particular derivative of w across the boundary as x increases is denoted by Δ followed by that derivative. For example, $\Delta w'' = w''(x+) - w''(x-)$ where $w''(x+)$ is the value of w'' at the lower boundary of the upper segment, while $w''(x-)$ is the value of w'' at the upper boundary of the lower segment. When the values of the particular derivative are not only continuous across the boundary, but fixed as well, the boundary condition is written e.g. $\Delta w'' = 0$ * which actually constitutes two separate equations (e.g. $w''(x-) = w''(x+) =$ fixed).

Boundary	w'''	w''	w'	w
Clamp			$\Delta w' = 0$ *	$\Delta w = 0$ *
Simple support		$\Delta w'' = 0$	$\Delta w' = 0$	$\Delta w = 0$ *
Point force	$\Delta w''' = \lambda$	$\Delta w'' = 0$	$\Delta w' = 0$	$\Delta w = 0$
Point torque	$\Delta w''' = 0$	$\Delta w'' = \tau$	$\Delta w' = 0$	$\Delta w = 0$
Free end	$w''' = 0$	$w'' = 0$		
Clamp at end			w' fixed	w fixed
Simply supported end		$w'' = 0$		w fixed
Point force at end	$w''' = \lambda$	$w'' = 0$		
Point torque at end	$w''' = 0$	$w'' = \tau$		

Note that in the first cases, in which the point forces and torques are located between two segments, there are four boundary conditions, two for the lower segment, and two for the upper. When forces and torques are applied to an end of the beam, there are two boundary conditions given which apply at that end.

Loading considerations

Applied loads may be represented either through boundary conditions or through the function $q(x,t)$ which represents an external distributed load. Using distributed loading is often favorable for simplicity. Boundary conditions are, however, often used to model loads depending on context; this practice being especially common in vibration analysis.

By nature, the distributed load is very often represented in a piecewise manner, since in practice a load isn't typically a continuous function. Point loads can be modeled with help of the Dirac delta function. For example, consider a static uniform cantilever beam of length L with an upward point load F applied at the free end. Using boundary conditions, this may be modeled in two ways. In the first approach, the applied point load is approximated by a shear force applied at the free end. In that case the governing equation and boundary conditions are:

$$EI\frac{\mathrm{d}^4 w}{\mathrm{d}x^4} = 0$$

$$w|_{x=0} = 0 \quad ; \quad \left.\frac{\mathrm{d}w}{\mathrm{d}x}\right|_{x=0} = 0 \quad ; \quad \left.\frac{\mathrm{d}^2 w}{\mathrm{d}x^2}\right|_{x=L} = 0 \quad ; \quad -EI\left.\frac{\mathrm{d}^3 w}{\mathrm{d}x^3}\right|_{x=L} = F$$

Alternatively we can represent the point load as a distribution using the Dirac function. In that case the equation and boundary conditions are

$$EI\frac{\mathrm{d}^4 w}{\mathrm{d}x^4} = F\delta(x-L)$$

$$w|_{x=0} = 0 \quad ; \quad \left.\frac{\mathrm{d}w}{\mathrm{d}x}\right|_{x=0} = 0 \quad ; \quad \left.\frac{\mathrm{d}^2 w}{\mathrm{d}x^2}\right|_{x=L} = 0$$

Note that shear force boundary condition (third derivative) is removed, otherwise there would be a contradiction. These are equivalent boundary value problems, and both yield the solution

$$w = \frac{F}{6EI}(3Lx^2 - x^3) \ .$$

The application of several point loads at different locations will lead to $w(x)$ being a piecewise function. Use of the Dirac function greatly simplifies such situations; otherwise the beam would have to be divided into sections, each with four boundary conditions solved separately. A well organized family of functions called Singularity functions are often used as a shorthand for the Dirac function, its derivative, and its antiderivatives.

Dynamic phenomena can also be modeled using the static beam equation by choosing appropriate forms of the load distribution. As an example, the free vibration of a beam can be accounted for by using the load function:

$$q(x,t) = \mu\frac{\partial^2 w}{\partial t^2}$$

where μ is the linear mass density of the beam, not necessarily a constant. With this time-dependent loading, the beam equation will be a partial differential equation:

$$\frac{\partial^2}{\partial x^2}\left(EI\frac{\partial^2 w}{\partial x^2}\right) = \mu\frac{\partial^2 w}{\partial t^2}.$$

Another interesting example describes the deflection of a beam rotating with a constant angular frequency of ω:

$$q(x) = \mu\omega^2 w(x)$$

This is a centripetal force distribution. Note that in this case, q is a function of the displacement (the dependent variable), and the beam equation will be an autonomous ordinary differential equation.

Examples

Three-point bending

The three point bending test is a classical experiment in mechanics. It represents the case of a beam resting on two roller supports and subjected to a concentrated load applied in the middle of the beam. The shear is constant in absolute value: it is half the central load, P / 2. It changes sign in the middle of the beam. The bending moment varies linearly from one end, where it is 0, and the center where its absolute value is PL / 4, is where the risk of rupture is the most important. The deformation of the beam is described by a polynomial of third degree over a half beam (the other half being symmetrical). The bending moments (M) , shear forces (Q), and deflections (w) for a beam subjected to a central point load and an asymmetric point load are given in the table below.

Distribution	Max. value

Simply supported beam with central load

$$M(x) = \begin{cases} \frac{Px}{2}, & \text{for } 0 \le x \le \frac{L}{2} \\ \frac{P(L-x)}{2}, & \text{for } \frac{L}{2} < x \le L \end{cases} \qquad M_{L/2} = \frac{PL}{4}$$

$$Q(x) = \begin{cases} \frac{P}{2}, & \text{for } 0 \le x \le \frac{L}{2} \\ \frac{P}{2}, & \text{for } \frac{L}{2} < x \le L \end{cases} \qquad |Q_0| = |Q_L| = \frac{P}{2}$$

$$w(x) = \begin{cases} \frac{Px(4x^2-3L^2)}{48EI}, & \text{for } 0 \le x \le \frac{L}{2} \\ \frac{P(x-L)(L^2-8Lx+4x^2)}{48EI}, & \text{for } \frac{L}{2} < x \le L \end{cases} \qquad w_{L/2} = \frac{PL^3}{48EI}$$

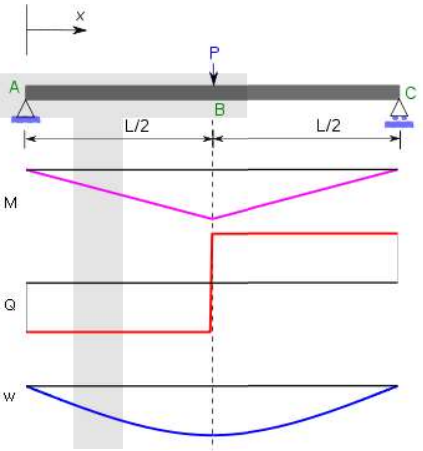

Simply supported beam with asymmetric load

$$M(x) = \begin{cases} \frac{Pbx}{L}, & \text{for } 0 \le x \le a \\ \frac{Pbx}{L} - P(x-a), & \text{for } a < x \le L \end{cases} \qquad M_B = \frac{Pab}{L}$$

$$Q(x) = \begin{cases} \frac{Pb}{L}, & \text{for } 0 \le x \le a \\ -\frac{Pb}{L} - P, & \text{for } a < x \le L \end{cases} \qquad Q_A = \frac{Pb}{L}$$

$$Q_C = \frac{P(b-L)}{L}$$

$$w(x) = \begin{cases} \frac{Pbx(L^2-b^2-x^2)}{6LEI}, & 0 \le x \le a \\ \frac{Pbx(L^2-b^2-x^2)}{6LEI} + \frac{P(x-a)^3}{6EI}, & a < x \le L \end{cases} \qquad w_{\max} = \frac{\sqrt{3}Pb(L^2-b^2)^{\frac{3}{2}}}{27LEI}$$

at $x = \sqrt{\frac{L^2-b^2}{3}}$

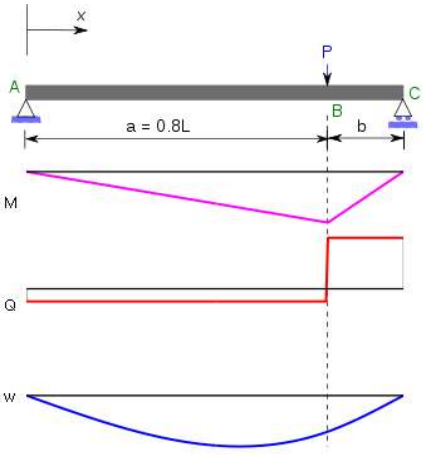

Cantilever beams

Another important class of problems involves cantilever beams. The bending moments (M) , shear forces (Q), and deflections (w) for a cantilever beam subjected to a point load at the free end and a uniformly distributed load are given in the table below.

Distribution	Max. value	
Cantilever beam with end load		
$M(x) = P(x - L)$	$M_A = PL$	
$Q(x) = P$	$Q_{\max} = P$	
$w(x) = \frac{Px^2(3L-x)}{6EI}$	$w_C = \frac{PL^3}{3EI}$	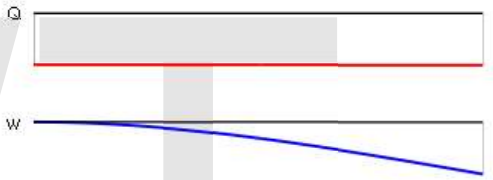
Cantilever beam with uniformly distributed load		
$M(x) = -\frac{q(L^2-2Lx+x^2)}{2}$	$M_A = \frac{qL^2}{2}$	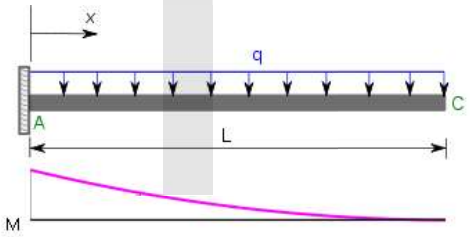
$Q(x) = q(L - x),$	$Q_A = qL$	
$w(x) = \frac{qx^2(6L^2-4Lx+x^2)}{24EI}$	$w_C = \frac{qL^4}{8EI}$	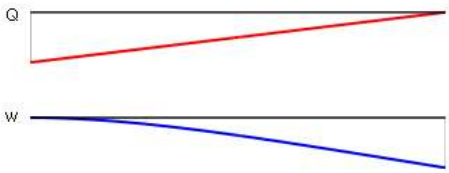

Solutions for several other commonly encountered configurations are readily available in textbooks on mechanics of materials and engineering handbooks.

Statically indeterminate beams

The bending moments and shear forces in Euler-Bernoulli beams can often be determined directly using static balance of forces and moments. However, for certain boundary conditions, the number of reactions can exceed the number of independent equilibrium equations. Such beams are called **statically indeterminate**.

The built-in beams shown in the figure below are statically indeterminate. To determine the stresses and deflections of such beams, the most direct method is to solve the Euler-Bernoulli beam equation with appropriate boundary conditions. But direct analytical solutions of the beam equation are possible only for the simplest cases. Therefore, additional techniques such as linear superposition are often used to solve statically indeterminate beam problems.

The superposition method involves adding the solutions of a number of statically determinate problems which are chosen such that the boundary conditions for the sum of the individual problems add up to those of the original problem.

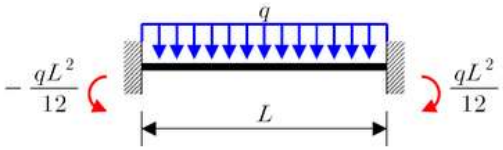

(a) Uniformly distributed load q.

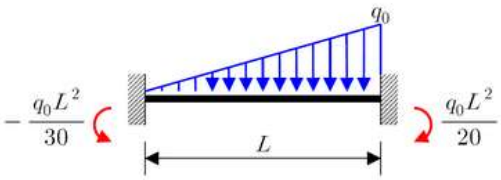

(b) Linearly distributed load with maximum q_0

$$M_{\max} = \frac{qL^2}{12}\ ;\quad w_{\max} = \frac{qL^4}{384EI}$$

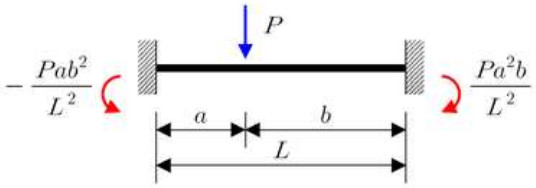

(c) Concentrated load P

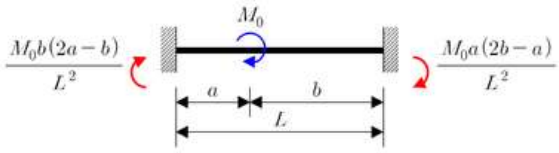

(d) Moment M_0

Another commonly encountered statically indeterminate beam problem is the cantilevered beam with the free end supported on a roller. The bending moments, shear forces, and deflections of such a beam are listed below.

Distribution	Max. value
$M(x) = -\frac{q}{8}(L^2 - 5Lx + 4x^2)$	$M_B = -\frac{9qL^2}{128}$ at $x = \frac{5L}{8}$
	$M_A = \frac{qL^2}{8}$
$Q(x) = -\frac{q}{8}(8x - 5L)$	$Q_A = -\frac{5qL}{8}$

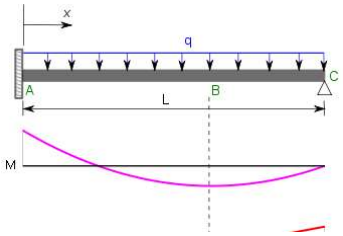

$$w(x) = \frac{qx^2}{48EI}(3L^2 - 5Lx + 2x^2)\, w_{\max} = \frac{qL^4}{185EI} \text{ at } x = 0.5785L$$

Extensions

The kinematic assumptions upon which the Euler-Bernoulli beam theory is founded allow it to be extended to more advanced analysis. Simple superposition allows for three-dimensional transverse loading. Using alternative constitutive equations can allow for viscoelastic or plastic beam deformation. Euler-Bernoulli beam theory can also be extended to the analysis of curved beams, beam buckling, composite beams, and geometrically nonlinear beam deflection.

Euler-Bernoulli beam theory does not account for the effects of transverse shear strain. As a result it underpredicts deflections and overpredicts natural frequencies. For thin beams (beam length to thickness ratios of the order 20 or more) these effects are of minor importance. For thick beams, however, these effects can be significant. More advanced beam theories such as the Timoshenko beam theory (developed by the Russian-born scientist Stephen Timoshenko) have been developed to account for these effects.

Large deflections

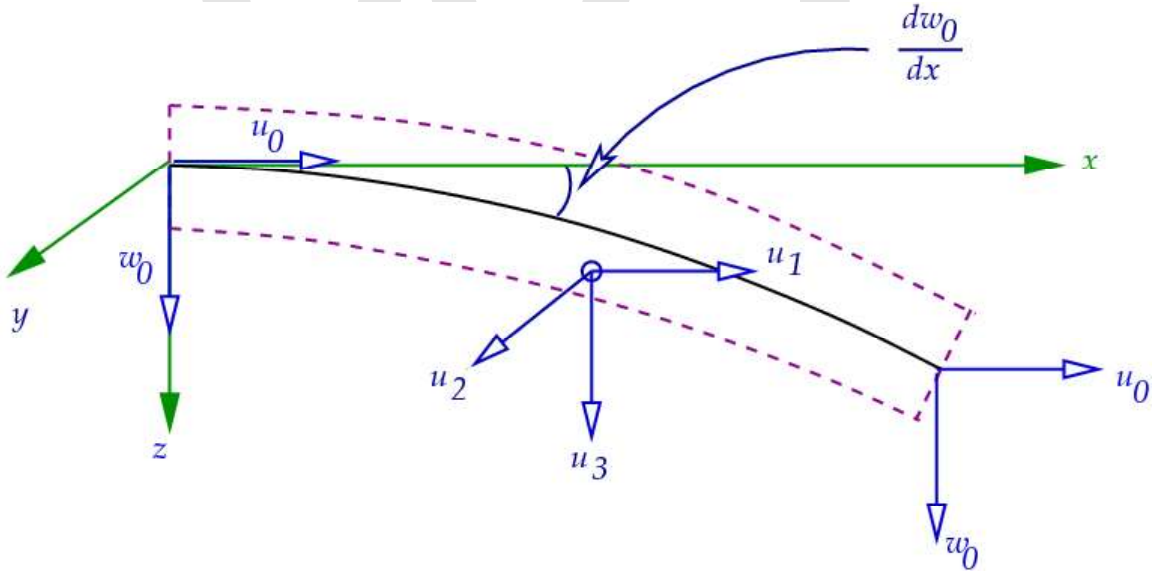

Euler-Bernoulli beam

The original Euler-Bernoulli theory is valid only for infinitesimal strains and small rotations. The theory can be extended in a straightforward manner to problems involving moderately large rotations provided that the strain remains small by using the von Karman strains.

The Euler-Bernoulli hypotheses that plane sections remain plane and normal to the axis of the beam lead to displacements of the form

$$u_1 = u_0(x) - z\frac{dw_0}{dx}\ ;\quad u_2 = 0\ ;\quad u_3 = w_0(x)$$

Using the definition of the Lagrangian Green strain from finite strain theory, we can find the **von Karman strains** for the beam that are valid for large rotations but small strains. These strains have the form

$$\varepsilon_{11} = \frac{du_0}{dx_1} - x_3\frac{d^2w_0}{dx_1^2} + \frac{1}{2}\left[\left(\frac{du_0}{dx_1} - x_3\frac{d^2w_0}{dx_1^2}\right)^2 + \left(\frac{dw_0}{dx_1}\right)^2\right]$$

$$\varepsilon_{22} = 0$$

$$\varepsilon_{33} = \frac{1}{2}\left(\frac{dw_0}{dx_1}\right)^2$$

$$\varepsilon_{23} = 0$$

$$\varepsilon_{31} = \frac{1}{2}\left(\frac{dw_0}{dx_1} - \frac{dw_0}{dx_1}\right) - \frac{1}{2}\left[\left(\frac{du_0}{dx_1} - x_3\frac{d^2w_0}{dx_1^2}\right)\left(\frac{dw_0}{dx_1}\right)\right]$$

$$\varepsilon_{12} = 0$$

From the principle of virtual work, the balance of forces and moments in the beams gives us the equilibrium equations

$$\frac{dN_{xx}}{dx} + f(x) = 0$$

$$\frac{d^2M_{xx}}{dx^2} + q(x) + \frac{d}{dx}\left(N_{xx}\frac{dw_0}{dx}\right) = 0$$

where $f(x)$ is the axial load, $q(x)$ is the transverse load, and

$$N_{xx} = \int_A \sigma_{xx}\, dA\ ;\quad M_{xx} = \int_A z\sigma_{xx}\, dA$$

To close the system of equations we need the constitutive equations that relate stresses to strains (and hence stresses to displacements). For large rotations and small strains these relations are

$$N_{xx} = A_{xx}\left[\frac{du_0}{dx} + \frac{1}{2}\left(\frac{dw_0}{dx}\right)^2\right] - B_{xx}\frac{d^2w_0}{dx^2}$$

$$M_{xx} = B_{xx}\left[\frac{du_0}{dx} + \frac{1}{2}\left(\frac{dw_0}{dx}\right)^2\right] - D_{xx}\frac{d^2w_0}{dx^2}$$

where

$$A_{xx} = \int_A E\ dA\ ;\quad B_{xx} = \int_A zE\ dA\ ;\quad D_{xx} = \int_A z^2 E\ dA\ .$$

The quantity A_{xx} is the **extensional stiffness**, B_{xx} is the coupled **extensional-bending stiffness**, and D_{xx} is the **bending stiffness**.

For the situation where the beam has a uniform cross-section and no axial load, the governing equation for a large-rotation Euler-Bernoulli beam is

$$EI\ \frac{\mathrm{d}^4 w}{\mathrm{d}x^4} - \frac{3}{2}\ EA\ \left(\frac{\mathrm{d}w}{\mathrm{d}x}\right)^2\left(\frac{\mathrm{d}^2 w}{\mathrm{d}x^2}\right) = q(x)$$

Chapter 11

Stress (Mechanics)

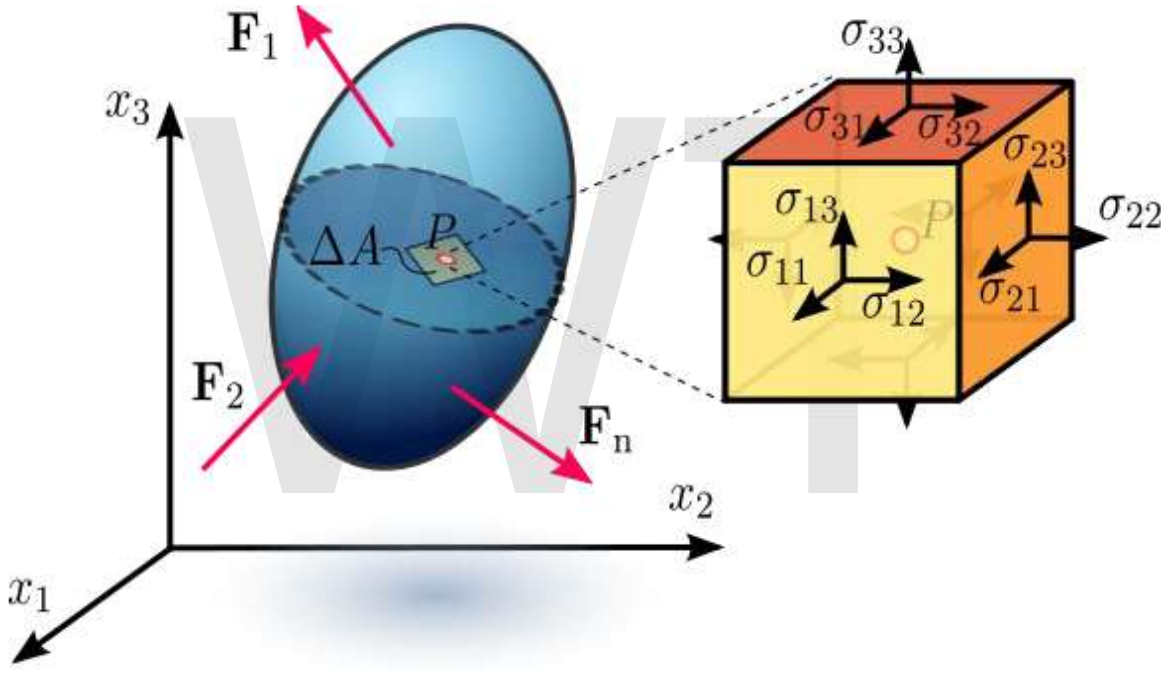

Figure 1.1 Stress in a loaded deformable material body assumed as a continuum.

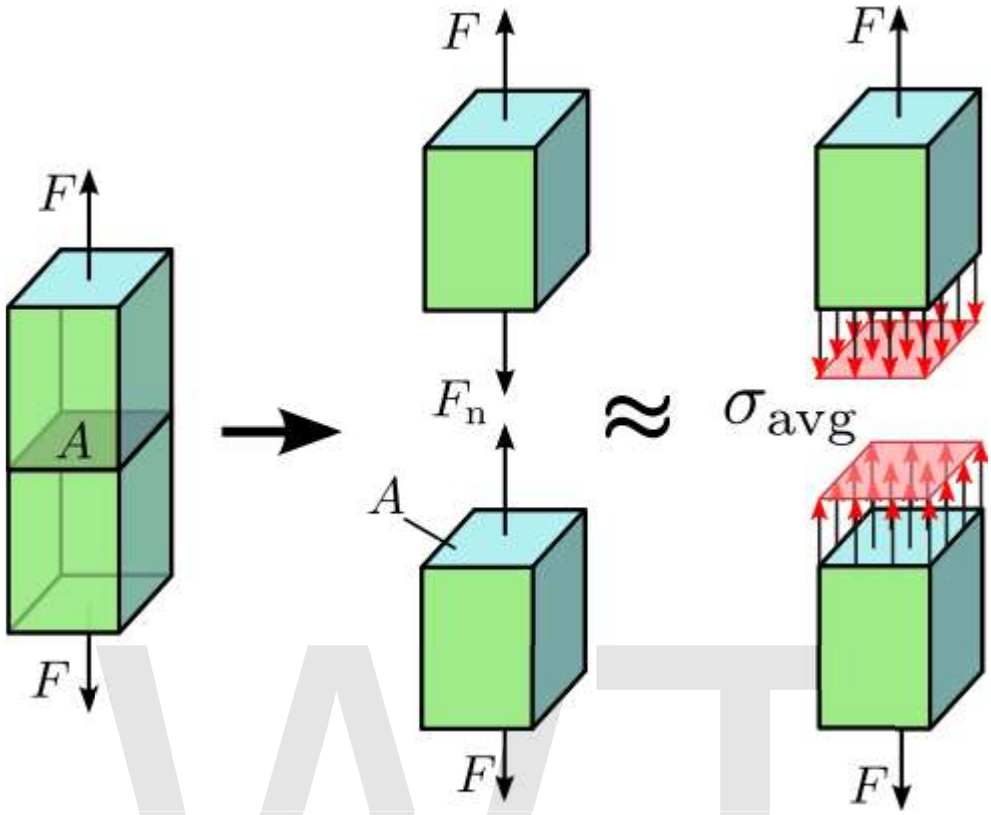

Figure 1.2 Axial stress in a prismatic bar axially loaded

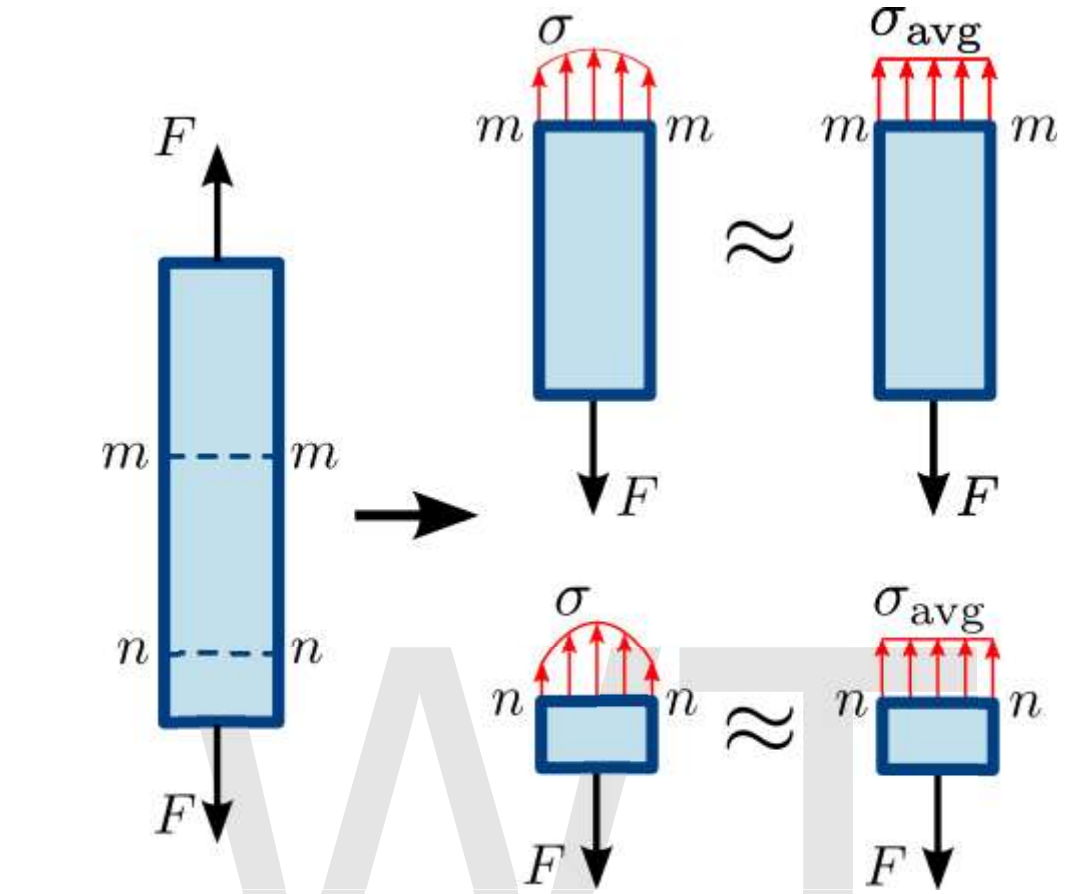

Figure 1.3 Normal stress in a prismatic (straight member of uniform cross-sectional area) bar. The stress or force distribution in the cross section of the bar is not necessarily uniform. However, an average normal stress σ_{avg} can be used

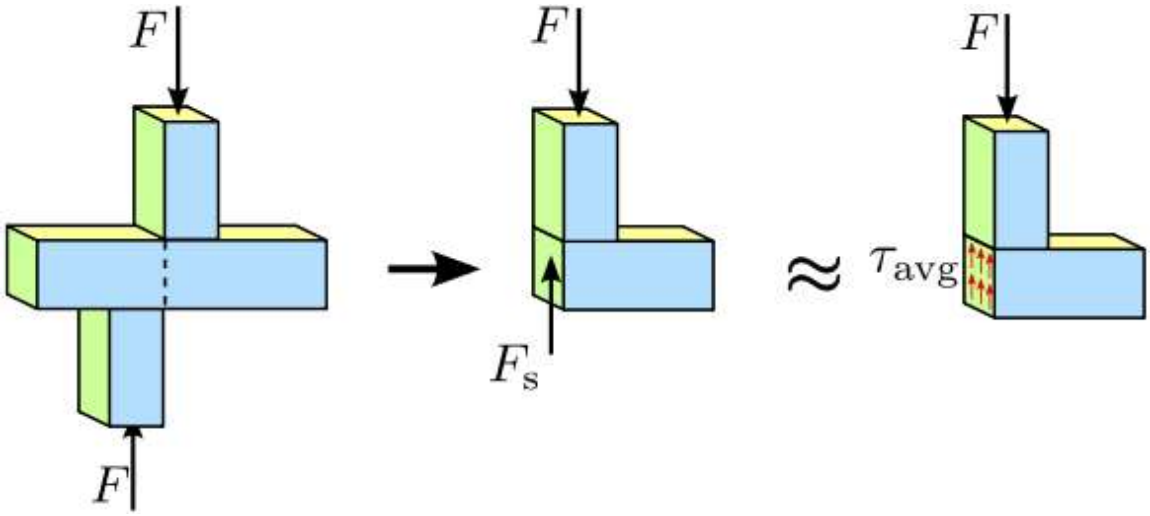

Figure 1.4 Shear stress in a prismatic bar. The stress or force distribution in the cross section of the bar is not necessarily uniform. Nevertheless, an average shear stress τ_{avg} is a reasonable approximation.

In continuum mechanics, **stress** is a measure of the internal forces acting within a deformable body. Quantitatively, it is a measure of the average force per unit area of a surface within the body on which internal forces act. These internal forces are produced between the particles in the body as a reaction to external forces applied on the body. Because the loaded deformable body is assumed to behave as a continuum, these internal forces are distributed continuously within the volume of the material body, and result in deformation of the body's shape. Beyond certain limits of material strength, this can lead to a permanent change of shape or physical failure.

However, treating physical force as a "one dimensional entity", as it is often done in mechanics, creates a few problems. Any model of continuum mechanics which explicitly expresses force as a variable generally fails to merge and describe deformation of matter and solid bodies, because the attributes of matter and solids are three dimensional. Classical models of continuum mechanics assume an average force and fail to properly incorporate "geometrical factors", which are important to describe stress distribution and accumulation of energy during the continuum.

The dimension of stress is that of pressure, and therefore the SI unit for stress is the pascal (symbol Pa), which is equivalent to one newton (force) per square meter (unit area), that is N/m^2. In Imperial units, stress is measured in pound-force per square inch, which is abbreviated as psi.

Introduction

Stress is a measure of the average force per unit area of a surface within a deformable body on which internal forces act. It is a measure of the intensity of the internal forces acting between particles of a deformable body across imaginary internal surfaces. These internal forces are produced between the particles in the body as a reaction to external forces applied on the body. External forces are either surface forces or body forces. Because the loaded deformable body is assumed to behave as a continuum, these internal forces are distributed continuously within the volume of the material body, *i.e.* the stress distribution in the body is expressed as a piecewise continuous function of space coordinates and time.

Normal , shear stresses and virial stresses

For the simple case of a body axially loaded, e.g., a prismatic bar subjected to tension or compression by a force passing through its centroid (Figures 1.2 and 1.3) the stress σ, or intensity of internal forces, can be obtained by dividing the total *normal force* F_{n}, determined from the equilibrium of forces, by the cross-sectional area A of the prism it is acting upon. The normal force can be a *tensile force* if acting outward from the plane, or *compressive force* if acting inward to the plane. In the case of a prismatic bar axially loaded, the stress σ is represented by a scalar called *engineering stress* or *nominal stress* that represents an average stress (σ_{avg}) over the area, meaning that the stress in the cross section is uniformly distributed. Thus, we have

$$\sigma_{\mathrm{avg}} = \frac{F_{\mathrm{n}}}{A} \approx \sigma$$

A different type of stress is obtained when transverse forces F are applied to the prismatic bar as shown in Figure 1.4. Considering the same cross-section as before, from static equilibrium the internal force has a magnitude equal to F_{s} and in opposite direction parallel to the cross-section. F_{s} is called the *shear force*. Dividing the shear force F_{s} by the area A of the cross section we obtain the *shear stress*. In this case the shear stress τ is a scalar quantity representing an average shear stress (τ_{avg}) in the section, *i.e.* the stress in the cross-section is uniformly distributed. In materials science and in engineering aspects the average of the ""scalar"" shear force (τ_{avg}) are true for crystallized materials during brittle fracture and operates through the fractured cross-section or stress plane.

$$\tau_{\mathrm{avg}} = \frac{F_{\mathrm{s}}}{A} \approx \tau$$

In Figure 1.3, the normal stress is observed in two planes $m - m$ and $n - n$ of the axially loaded prismatic bar. The stress on plane $n - n$, which is closer to the point of application of the load F, varies more across the cross-section than that of plane $m - m$. However, if the cross-sectional area of the bar is very small, *i.e.* the bar is slender, the variation of stress across the area is small and the normal stress can be approximated by σ_{avg}. On the other hand, the variation of shear stress across the section of a prismatic bar cannot be assumed to be uniform.

Virial stress is a measure of stress on an atomic scale. It is given by

$$\tau_{ij} = \frac{1}{\Omega} \sum_{k \in \Omega} \left(-m^{(k)} (u_i^{(k)} - \bar{u}_i)(u_j^{(k)} - \bar{u}_j) + \frac{1}{2} \sum_{\ell \in \Omega} (x_i^{(\ell)} - x_i^{(k)}) f_j^{(k\ell)} \right)$$

where

- k and ℓ are atoms in the domain,
- Ω is the volume of the domain,
- $m^{(k)}$ is the mass of atom k,
- $u_i^{(k)}$ is the i^{th} component of the velocity of atom k,
- $\bar{u}_j$ is the j^{th} component of the average velocity of atoms in the volume,
- $x_i^{(k)}$ is the i^{th} component of the position of atom k, and
- $f_i^{(k\ell)}$ is the i^{th} component of the force between atom k and ℓ.

At zero kelvin, all velocities are zero so we have

$$\tau_{ij} = \frac{1}{2\Omega} \sum_{k,\ell \in \Omega} (x_i^{(\ell)} - x_i^{(k)}) f_j^{(k\ell)}$$

.

This can be thought of as follows. The τ_{11} component of stress is the force in the 1 direction divided by the area of a plane perpendicular to that direction. Consider two adjacent volumes separated by such a plane. The 11-component of stress on that interface is the sum of all pairwise forces between atoms on the two sides....

Stress modeling (Cauchy)

In general, stress is not uniformly distributed over the cross-section of a material body, and consequently the stress at a point in a given region is different from the average stress over the entire area. Therefore, it is necessary to define the stress not over a given area but at a specific point in the body (Figure 1.1). According to Cauchy, the *stress at any point* in an object, assumed to behave as a continuum, is completely defined by the nine components σ_{ij} of a second-order tensor of type (0,2) known as the Cauchy stress tensor, $\boldsymbol{\sigma}$:

$$\boldsymbol{\sigma} = \begin{bmatrix} \sigma_{11} & \sigma_{12} & \sigma_{13} \\ \sigma_{21} & \sigma_{22} & \sigma_{23} \\ \sigma_{31} & \sigma_{32} & \sigma_{33} \end{bmatrix} \equiv \begin{bmatrix} \sigma_{xx} & \sigma_{xy} & \sigma_{xz} \\ \sigma_{yx} & \sigma_{yy} & \sigma_{yz} \\ \sigma_{zx} & \sigma_{zy} & \sigma_{zz} \end{bmatrix} \equiv \begin{bmatrix} \sigma_x & \tau_{xy} & \tau_{xz} \\ \tau_{yx} & \sigma_y & \tau_{yz} \\ \tau_{zx} & \tau_{zy} & \sigma_z \end{bmatrix}$$

The Cauchy stress tensor obeys the tensor transformation law under a change in the system of coordinates. A graphical representation of this transformation law is the Mohr's circle of stress distribution.

The Cauchy stress tensor is used for stress analysis of material bodies experiencing small deformations where the differences in stress distribution in most cases can be neglected. For large deformations, also called finite deformations, other measures of stress, such as the first and second Piola-Kirchhoff stress tensors, the Biot stress tensor, and the Kirchhoff stress tensor, are required.

According to the principle of conservation of linear momentum, if a continuous body is in static equilibrium it can be demonstrated that the components of the Cauchy stress tensor in every material point in the body satisfy the equilibrium equations (Cauchy's equations of motion for zero acceleration). At the same time, according to the principle of conservation of angular momentum, equilibrium requires that the summation of moments with respect to an arbitrary point is zero, which leads to the conclusion that the stress tensor is symmetric, thus having only six independent stress components instead of the original nine.

There are certain invariants associated with the stress tensor, whose values do not depend upon the coordinate system chosen or the area element upon which the stress tensor operates. These are the three eigenvalues of the stress tensor, which are called the principal stresses. Solids, liquids, and gases have stress fields. Static fluids support normal stress but will flow under shear stress. Moving viscous fluids can support shear stress (dynamic pressure). Solids can support both shear and normal stress, with ductile materials failing under shear and brittle materials failing under normal stress. All materials have temperature dependent variations in stress-related properties, and non-Newtonian materials have rate-dependent variations.

Stress analysis

Stress analysis means the determination of the internal distribution of stresses in a structure. It is needed in engineering for the study and design of structures such as tunnels, dams, mechanical parts, and structural frames, under prescribed or expected loads. To determine the distribution of stress in a structure, the engineer needs to solve a boundary-value problem by specifying the boundary conditions. These are displacements and forces on the boundary of the structure.

Constitutive equations, such as Hooke's Law for linear elastic materials, describe the stress-strain relationship in these calculations.

When a structure is expected to deform elastically (and resume its original shape), a boundary-value problem based on the theory of elasticity is applied, with infinitesimal strains, under design loads.

When the applied loads permanently deform the structure, the theory of plasticity is used.

The stress analysis can be simplified when the physical dimensions and the distribution of loads allow the structure to be treated as one-dimensional or two-dimensional. For a two-dimensional analysis a plane stress or a plane strain condition can be assumed. Alternatively, experimental determination of stresses can be carried out.

Approximate computer-based solutions for boundary-value problems can be obtained through numerical methods such as the Finite Element Method, the Finite Difference Method, and the Boundary Element Method. Analytical or closed-form solutions can be obtained for simple geometries, constitutive relations, and boundary conditions.

Theoretical background

Continuum mechanics deals with deformable bodies, as opposed to rigid bodies. The stresses considered in continuum mechanics are only those produced by deformation of the body, *sc.* only relative changes in stress are considered, not the absolute values. A body is considered stress-free if the only forces present are those inter-atomic forces (ionic, metallic, and van der Waals forces) required to hold the body together and to keep its shape in the absence of all external influences, including gravitational attraction.

Stresses generated during manufacture of the body to a specific configuration are also excluded.

Following the classical dynamics of Newton and Euler, the motion of a material body is produced by the action of externally applied forces which are assumed to be of two kinds: surface forces and body forces.

Surface forces, or contact forces, can act either on the bounding surface of the body, as a result of mechanical contact with other bodies, or on imaginary internal surfaces that bound portions of the body, as a result of the mechanical interaction between the parts of the body to either side of the surface (Euler-Cauchy's stress principle). When a body is acted upon by external contact forces, internal contact forces are then transmitted from point to point inside the body to balance their action, according to Newton's second law of motion of conservation of linear momentum and angular momentum (for continuous bodies these laws are called the Euler's equations of motion). The internal contact forces are related to the body's deformation through constitutive equations. This is concerned with the manner in which internal contact forces are mathematically described and how they relate to the motion of the body, independent of the body's material makeup.

The concept of stress can then be thought as a measure of the intensity of the internal contact forces acting between particles of the body across imaginary internal surfaces. In other words, stress is a measure of the average quantity of force exerted per unit area of the surface on which these internal forces act. The intensity of contact forces is related, specifically in an inverse proportion, to the area of contact. For example, if a force applied to a small area is compared to a distributed load of the same resultant magnitude applied to a larger area, one finds that the effects or intensities of these two forces are locally different because the stresses are not the same.

Body forces are forces originating from sources outside of the body that act on the volume (or mass) of the body. Saying that body forces are due to outside sources implies that the *internal forces* are manifested through the contact forces alone. These forces arise from the presence of the body in force fields, (*e.g.*, a gravitational field). As the mass of a continuous body is assumed to be continuously distributed, any force originating from the mass is also continuously distributed. Thus, body forces are assumed to be continuous over the entire volume of the body.

The density of internal forces at every point in a deformable body are not necessarily equal, *i.e.* there is a distribution of stresses throughout the body. This variation of internal forces throughout the body is governed by Newton's second law of motion of conservation of linear momentum and angular momentum, which normally are applied to a mass particle but are extended in continuum mechanics to a body of continuously distributed mass. For continuous bodies these laws are called Euler’s equations of motion. If a body is represented as an assemblage of discrete particles, each governed by Newton’s laws of motion, then Euler’s equations can be derived from Newton’s laws. Euler’s equations can, however, be taken as axioms describing the laws of motion for extended bodies, independently of any particle structure.

Euler–Cauchy stress principle

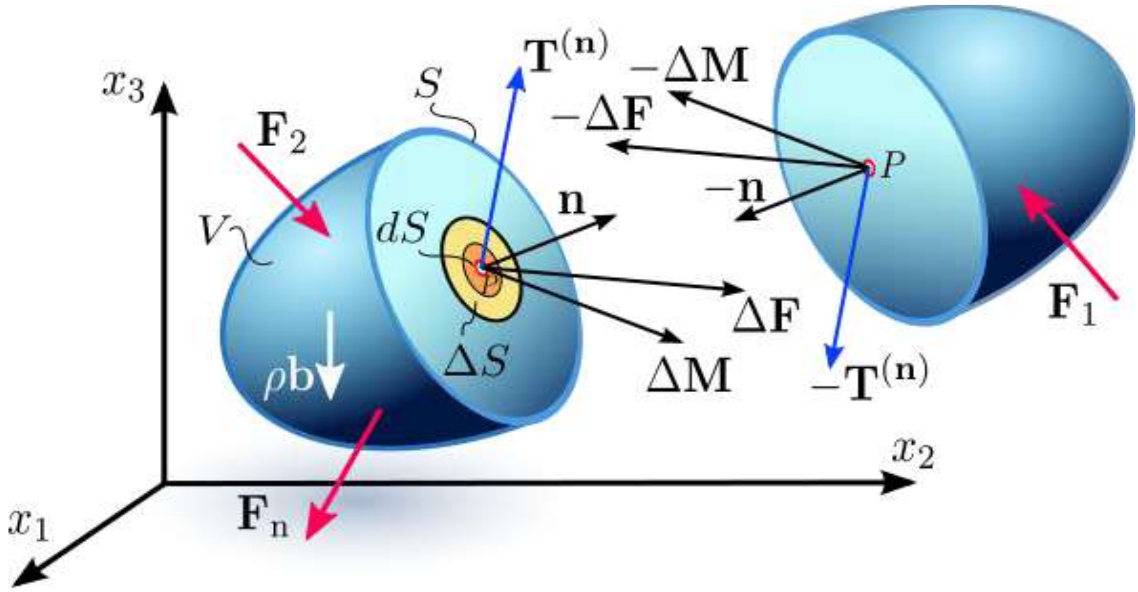

Figure 2.1a Internal distribution of contact forces and couple stresses on a differential dS of the internal surface S in a continuum, as a result of the interaction between the two portions of the continuum separated by the surface

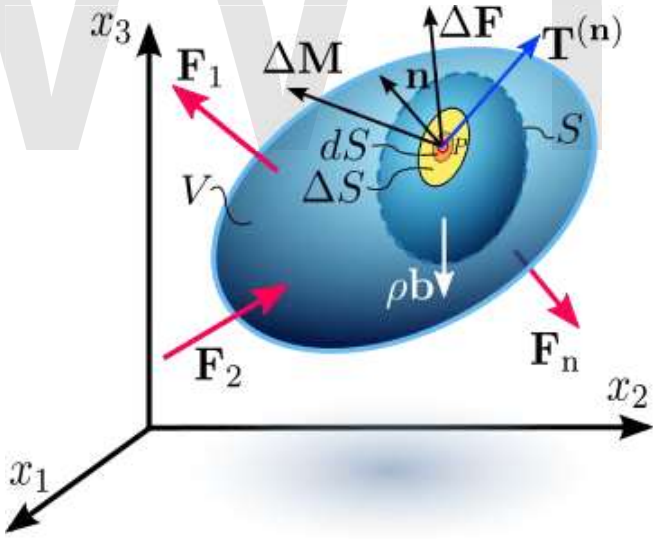

Figure 2.1b Internal distribution of contact forces and couple stresses on a differential dS of the internal surface S in a continuum, as a result of the interaction between the two portions of the continuum separated by the surface

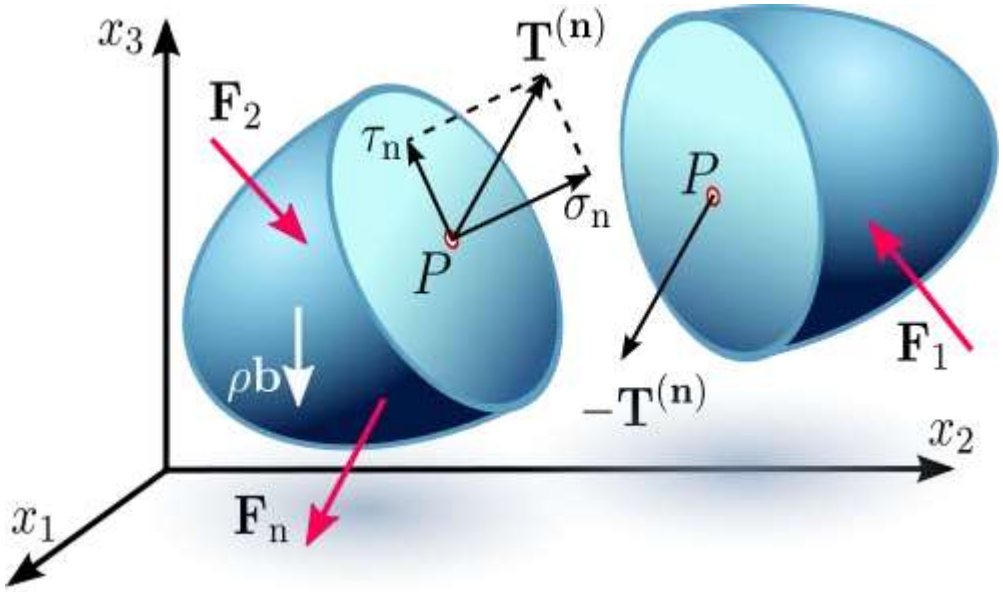

Figure 2.1c Stress vector on an internal surface S with normal vector n. Depending on the orientation of the plane under consideration, the stress vector may not necessarily be perpendicular to that plane, *i.e.* parallel to $\mathbf{n}$, and can be resolved into two components: one component normal to the plane, called *normal stress* $\sigma_\mathbf{n}$, and another component parallel to this plane, called the *shearing stress* τ.

The Euler–Cauchy stress principle states that *upon any surface (real or imaginary) that divides the body, the action of one part of the body on the other is equivalent (equipollent) to the system of distributed forces and couples on the surface dividing the body*, and it is represented by a vector field $\mathbf{T}^{(\mathbf{n})}$, called the stress vector, defined on the surface *S* and assumed to depend continuously on the surface's unit vector **n**.

To explain this principle, we consider an imaginary surface *S* passing through an internal material point *P* dividing the continuous body into two segments, as seen in Figure 2.1a or 2.1b (some authors use the cutting plane diagram and others use the diagram with the arbitrary volume inside the continuum enclosed by the surface *S*). The body is subjected to external surface forces **F** and body forces **b**. The internal contact forces being transmitted from one segment to the other through the dividing plane, due to the action of one portion of the continuum onto the other, generate a force distribution on a small area ΔS, with a normal unit vector **n**, on the dividing plane *S*. The force distribution is equipollent to a contact force $\Delta\mathbf{F}$ and a couple stress $\Delta\mathbf{M}$, as shown in Figure 2.1a and 2.1b. Cauchy's stress principle asserts that as ΔS becomes very small and tends to zero the ratio $\Delta\mathbf{F}/\Delta S$ becomes $\mathrm{d}\mathbf{F}/\mathrm{d}S$ and the couple stress vector $\Delta\mathbf{M}$ vanishes. In specific fields of continuum mechanics the couple stress is assumed not to vanish; however, as stated previously, in classical branches of continuum mechanics we deal with non-polar materials which do not consider couple stresses and body moments. The resultant vector $\mathrm{d}\mathbf{F}/\mathrm{d}S$ is defined as the *stress vector* or *traction vector* given by $\mathbf{T}^{(\mathbf{n})} = T_\mathrm{i}^{(\mathbf{n})}\,\mathbf{e}_\mathrm{i}$ at the point *P* associated with a plane with a normal vector **n**:

$$T_i^{(\mathbf{n})} = \lim_{\Delta S \to 0} \frac{\Delta F_i}{\Delta S} = \frac{dF_i}{dS}.$$

This equation means that the stress vector depends on its location in the body and the orientation of the plane on which it is acting.

Depending on the orientation of the plane under consideration, the stress vector may not necessarily be perpendicular to that plane, *i.e.* parallel to **n**, and can be resolved into two components:

- one normal to the plane, called *normal stress*

  $$\sigma_{\mathrm{n}} = \lim_{\Delta S \to 0} \frac{\Delta F_{\mathrm{n}}}{\Delta S} = \frac{dF_{\mathrm{n}}}{dS},$$
  where $\mathrm{d}F_{\mathrm{n}}$ is the normal component of the force d**F** to the differential area d*S*

- and the other parallel to this plane, called the *shear stress*

  $$\tau = \lim_{\Delta S \to 0} \frac{\Delta F_{\mathrm{s}}}{\Delta S} = \frac{dF_{\mathrm{s}}}{dS},$$
  where $\mathrm{d}F_{\mathrm{s}}$ is the tangential component of the force d**F** to the differential surface area d*S*. The shear stress can be further decomposed into two mutually perpendicular vectors.

Cauchy's postulate

According to the *Cauchy Postulate*, the stress vector $\mathbf{T}^{(\mathbf{n})}$ remains unchanged for all surfaces passing through the point *P* and having the same normal vector **n** at *P*, *i.e.* having a common tangent at *P*. This means that the stress vector is a function of the normal vector **n** only, and it is not influenced by the curvature of the internal surfaces.

Cauchy's fundamental lemma

A consequence of Cauchy's postulate is *Cauchy's Fundamental Lemma*, also called the *Cauchy reciprocal theorem*, which states that the stress vectors acting on opposite sides of the same surface are equal in magnitude and opposite in direction. Cauchy's fundamental lemma is equivalent to Newton's third law of motion of action and reaction, and it is expressed as

$$-\mathbf{T}^{(\mathbf{n})} = \mathbf{T}^{(-\mathbf{n})}.$$

Cauchy's stress theorem – stress tensor

The state of stress at a point in the body is then defined by all the stress vectors $\mathbf{T}^{(\mathbf{n})}$ associated with all planes (infinite in number) that pass through that point. However,

according to *Cauchy's fundamental theorem*, also called *Cauchy's stress theorem*, merely by knowing the stress vectors on three mutually perpendicular planes, the stress vector on any other plane passing through that point can be found through coordinate transformation equations.

Cauchy's stress theorem states that there exists a second-order tensor field $\boldsymbol{\sigma}(\mathbf{x}, t)$, called the *Cauchy stress tensor*, independent of $\mathbf{n}$, such that $\mathbf{T}$ is a linear function of $\mathbf{n}$:

$$\mathbf{T}^{(\mathbf{n})} = \boldsymbol{\sigma} \cdot \mathbf{n} \quad \text{or} \quad T_j^{(n)} = \sigma_{ij} n_i.$$

This equation implies that the stress vector $\mathbf{T}^{(\mathbf{n})}$ at any point P in a continuum associated with a plane with normal vector $\mathbf{n}$ can be expressed as a function of the stress vectors on the planes perpendicular to the coordinate axes, *i.e.* in terms of the components σ_{ij} of the stress tensor $\boldsymbol{\sigma}$.

To prove this expression, consider a tetrahedron with three faces oriented in the coordinate planes, and with an infinitesimal area dA oriented in an arbitrary direction specified by a normal vector $\mathbf{n}$ (Figure 2.2). The tetrahedron is formed by slicing the infinitesimal element along an arbitrary plane $\mathbf{n}$. The stress vector on this plane is denoted by $\mathbf{T}^{(\mathbf{n})}$. The stress vectors acting on the faces of the tetrahedron are denoted as $\mathbf{T}^{(\mathbf{e}_1)}$, $\mathbf{T}^{(\mathbf{e}_2)}$, and $\mathbf{T}^{(\mathbf{e}_3)}$, and are by definition the components σ_{ij} of the stress tensor $\boldsymbol{\sigma}$. This tetrahedron is sometimes called the *Cauchy tetrahedron*. From equilibrium of forces, *i.e.* Euler's first law of motion (Newton's second law of motion), we have

$$\mathbf{T}^{(\mathbf{n})}\, dA - \mathbf{T}^{(\mathbf{e}_1)}\, dA_1 - \mathbf{T}^{(\mathbf{e}_2)}\, dA_2 - \mathbf{T}^{(\mathbf{e}_3)}\, dA_3 = \rho \left(\frac{h}{3} dA \right) \mathbf{a},$$

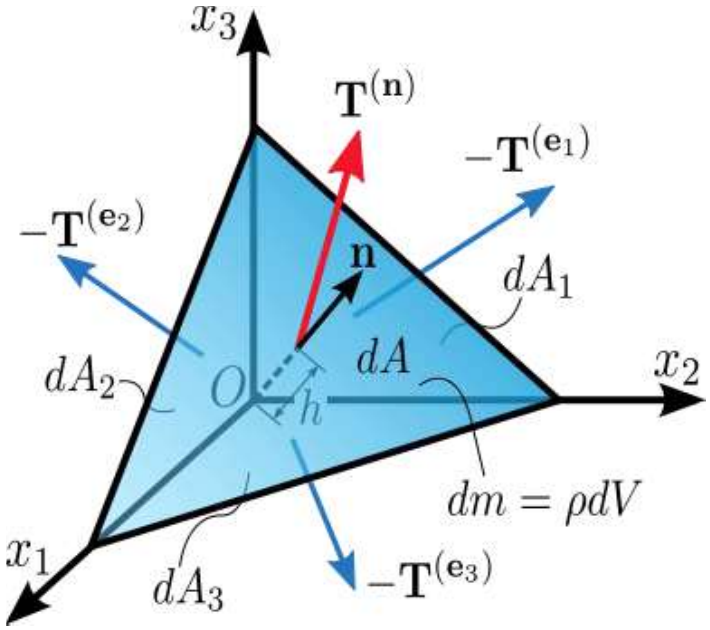

Figure 2.2. Stress vector acting on a plane with normal vector **n**.
A note on the sign convention: The tetrahedron is formed by slicing a parallelepiped along an arbitrary plane **n**. So, the force acting on the plane **n** is the reaction exerted by the other half of the parallelepiped and has an opposite sign.

where the right-hand-side of the equation represents the product of the mass enclosed by the tetrahedron and its acceleration: ρ is the density, **a** is the acceleration, and h is the height of the tetrahedron, considering the plane **n** as the base. The area of the faces of the tetrahedron perpendicular to the axes can be found by projecting dA into each face (using the dot product):

$$\begin{aligned} dA_1 &= (\mathbf{n} \cdot \mathbf{e}_1)\, dA = n_1\, dA, \\ dA_2 &= (\mathbf{n} \cdot \mathbf{e}_2)\, dA = n_2\, dA, \\ dA_3 &= (\mathbf{n} \cdot \mathbf{e}_3)\, dA = n_3\, dA, \end{aligned}$$

and then substituting into the equation to cancel out dA:

$$\mathbf{T}^{(\mathbf{n})} - \mathbf{T}^{(\mathbf{e}_1)} n_1 - \mathbf{T}^{(\mathbf{e}_2)} n_2 - \mathbf{T}^{(\mathbf{e}_3)} n_3 = \rho \left(\frac{h}{3}\right) \mathbf{a}.$$

To consider the limiting case as the tetrahedron shrinks to a point, h must go to 0 (intuitively, the plane **n** is translated along **n** toward O). As a result, the right-hand-side of the equation approaches 0, so

$$\mathbf{T}^{(\mathbf{n})} = \mathbf{T}^{(\mathbf{e}_1)} n_1 + \mathbf{T}^{(\mathbf{e}_2)} n_2 + \mathbf{T}^{(\mathbf{e}_3)} n_3.$$

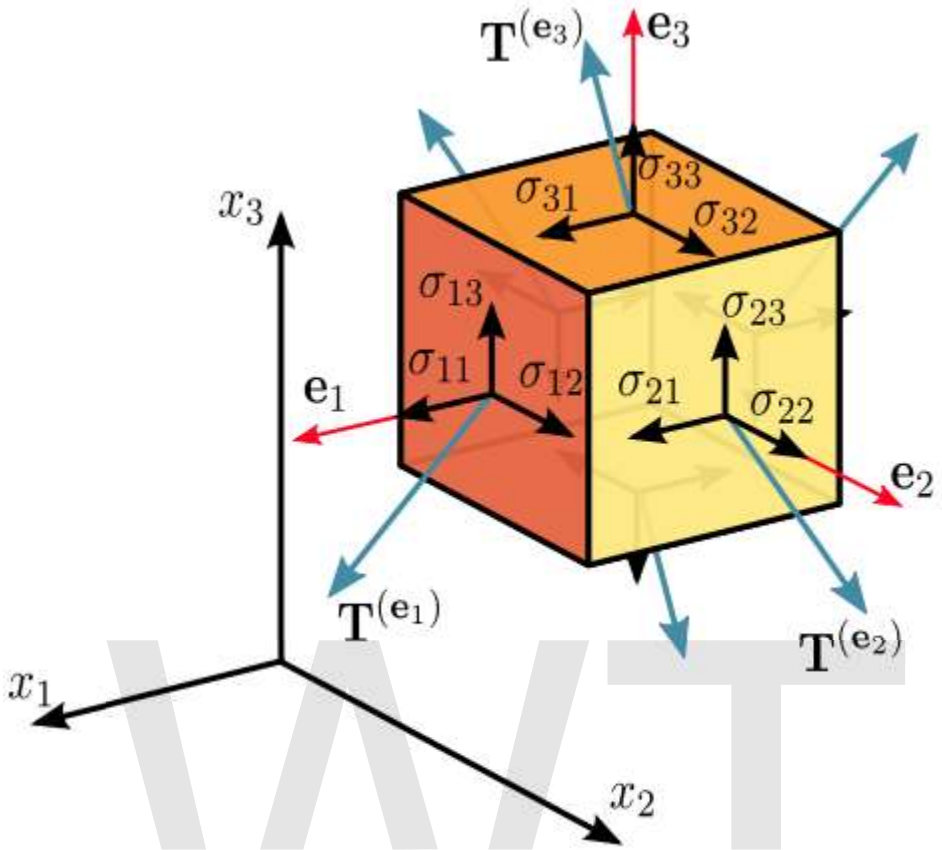

Figure 2.3 Components of stress in three dimensions

Assuming a material element (Figure 2.3) with planes perpendicular to the coordinate axes of a Cartesian coordinate system, the stress vectors associated with each of the element planes, *i.e.* $\mathbf{T}^{(\mathbf{e}_1)}$, $\mathbf{T}^{(\mathbf{e}_2)}$, and $\mathbf{T}^{(\mathbf{e}_3)}$ can be decomposed into a normal component and two shear components, *i.e.* components in the direction of the three coordinate axes. For the particular case of a surface with normal unit vector oriented in the direction of the x_1-axis, the normal stress is denoted by σ_{11}, and the two shear stresses are denoted as σ_{12} and σ_{13}:

$$\begin{aligned}
\mathbf{T}^{(\mathbf{e}_1)} &= T_1^{(\mathbf{e}_1)}\mathbf{e}_1 + T_2^{(\mathbf{e}_1)}\mathbf{e}_2 + T_3^{(\mathbf{e}_1)}\mathbf{e}_3 = \sigma_{11}\mathbf{e}_1 + \sigma_{12}\mathbf{e}_2 + \sigma_{13}\mathbf{e}_3, \\
\mathbf{T}^{(\mathbf{e}_2)} &= T_1^{(\mathbf{e}_2)}\mathbf{e}_1 + T_2^{(\mathbf{e}_2)}\mathbf{e}_2 + T_3^{(\mathbf{e}_2)}\mathbf{e}_3 = \sigma_{21}\mathbf{e}_1 + \sigma_{22}\mathbf{e}_2 + \sigma_{23}\mathbf{e}_3, \\
\mathbf{T}^{(\mathbf{e}_3)} &= T_1^{(\mathbf{e}_3)}\mathbf{e}_1 + T_2^{(\mathbf{e}_3)}\mathbf{e}_2 + T_3^{(\mathbf{e}_3)}\mathbf{e}_3 = \sigma_{31}\mathbf{e}_1 + \sigma_{32}\mathbf{e}_2 + \sigma_{33}\mathbf{e}_3,
\end{aligned}$$

In index notation this is

$$\mathbf{T}^{(\mathbf{e}_i)} = T_j^{(\mathbf{e}_i)}\mathbf{e}_j = \sigma_{ij}\mathbf{e}_j.$$

The nine components σ_{ij} of the stress vectors are the components of a second-order Cartesian tensor called the *Cauchy stress tensor*, which completely defines the state of stress at a point and is given by

$$\boldsymbol{\sigma} = \sigma_{ij} = \begin{bmatrix} \mathbf{T}^{(\mathbf{e}_1)} \\ \mathbf{T}^{(\mathbf{e}_2)} \\ \mathbf{T}^{(\mathbf{e}_3)} \end{bmatrix} = \begin{bmatrix} \sigma_{11} & \sigma_{12} & \sigma_{13} \\ \sigma_{21} & \sigma_{22} & \sigma_{23} \\ \sigma_{31} & \sigma_{32} & \sigma_{33} \end{bmatrix} \equiv \begin{bmatrix} \sigma_{xx} & \sigma_{xy} & \sigma_{xz} \\ \sigma_{yx} & \sigma_{yy} & \sigma_{yz} \\ \sigma_{zx} & \sigma_{zy} & \sigma_{zz} \end{bmatrix} \equiv \begin{bmatrix} \sigma_x & \tau_{xy} & \tau_{xz} \\ \tau_{yx} & \sigma_y & \tau_{yz} \\ \tau_{zx} & \tau_{zy} & \sigma_z \end{bmatrix},$$

where σ_{11}, σ_{22}, and σ_{33} are normal stresses, and σ_{12}, σ_{13}, σ_{21}, σ_{23}, σ_{31}, and σ_{32} are shear stresses. The first index i indicates that the stress acts on a plane normal to the x_i-axis, and the second index j denotes the direction in which the stress acts. A stress component is positive if it acts in the positive direction of the coordinate axes, and if the plane where it acts has an outward normal vector pointing in the positive coordinate direction.

Thus, using the components of the stress tensor

$$\begin{aligned} \mathbf{T}^{(\mathbf{n})} &= \mathbf{T}^{(\mathbf{e}_1)} n_1 + \mathbf{T}^{(\mathbf{e}_2)} n_2 + \mathbf{T}^{(\mathbf{e}_3)} n_3 \\ &= \sum_{i=1}^{3} \mathbf{T}^{(\mathbf{e}_i)} n_i \\ &= \left(\sigma_{ij} \mathbf{e}_j\right) n_i \\ &= \sigma_{ij} n_i \mathbf{e}_j \end{aligned}$$

or, equivalently,

$$T_j^{(\mathbf{n})} = \sigma_{ij} n_i.$$

Alternatively, in matrix form we have

$$\begin{bmatrix} T_1^{(\mathbf{n})} & T_2^{(\mathbf{n})} & T_3^{(\mathbf{n})} \end{bmatrix} = \begin{bmatrix} n_1 & n_2 & n_3 \end{bmatrix} \cdot \begin{bmatrix} \sigma_{11} & \sigma_{12} & \sigma_{13} \\ \sigma_{21} & \sigma_{22} & \sigma_{23} \\ \sigma_{31} & \sigma_{32} & \sigma_{33} \end{bmatrix}.$$

The Voigt notation representation of the Cauchy stress tensor takes advantage of the symmetry of the stress tensor to express the stress as a six-dimensional vector of the form:

$$\boldsymbol{\sigma} = \begin{bmatrix} \sigma_1 & \sigma_2 & \sigma_3 & \sigma_4 & \sigma_5 & \sigma_6 \end{bmatrix}^T \equiv \begin{bmatrix} \sigma_{11} & \sigma_{22} & \sigma_{33} & \sigma_{23} & \sigma_{31} & \sigma_{12} \end{bmatrix}^T.$$

The Voigt notation is used extensively in representing stress-strain relations in solid mechanics and for computational efficiency in numerical structural mechanics software.

Transformation rule of the stress tensor

It can be shown that the stress tensor is a contravariant second order tensor, which is a statement of how it transforms under a change of the coordinate system. From an x_i-system to an x_i'-system, the components σ_{ij} in the initial system are transformed into the components σ_{ij}' in the new system according to the tensor transformation rule (Figure 2.4):

$$\sigma'_{ij} = a_{im}a_{jn}\sigma_{mn} \quad \text{or} \quad \boldsymbol{\sigma}' = \mathbf{A}\boldsymbol{\sigma}\mathbf{A}^T,$$

where **A** is a rotation matrix with components a_{ij}. In matrix form this is

$$\begin{bmatrix} \sigma'_{11} & \sigma'_{12} & \sigma'_{13} \\ \sigma'_{21} & \sigma'_{22} & \sigma'_{23} \\ \sigma'_{31} & \sigma'_{32} & \sigma'_{33} \end{bmatrix} = \begin{bmatrix} a_{11} & a_{12} & a_{13} \\ a_{21} & a_{22} & a_{23} \\ a_{31} & a_{32} & a_{33} \end{bmatrix} \begin{bmatrix} \sigma_{11} & \sigma_{12} & \sigma_{13} \\ \sigma_{21} & \sigma_{22} & \sigma_{23} \\ \sigma_{31} & \sigma_{32} & \sigma_{33} \end{bmatrix} \begin{bmatrix} a_{11} & a_{21} & a_{31} \\ a_{12} & a_{22} & a_{32} \\ a_{13} & a_{23} & a_{33} \end{bmatrix}.$$

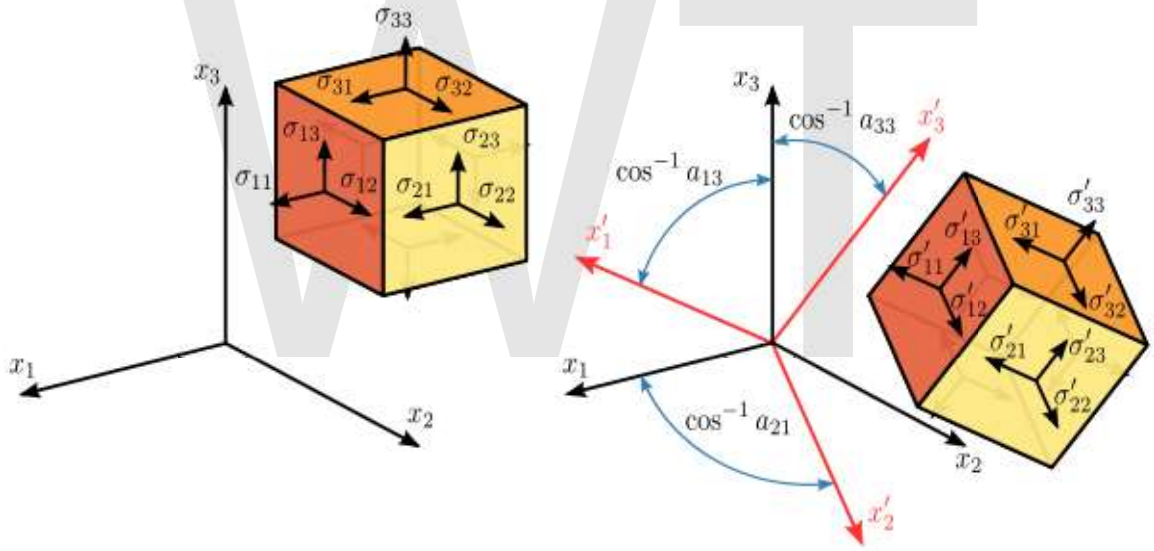

Figure 2.4 Transformation of the stress tensor

Expanding the matrix operation, and simplifying some terms by taking advantage of the symmetry of the stress tensor, gives

$$\begin{aligned}
\sigma'_{11} &= a_{11}^2\sigma_{11} + a_{12}^2\sigma_{22} + a_{13}^2\sigma_{33} + 2a_{11}a_{12}\sigma_{12} + 2a_{11}a_{13}\sigma_{13} + 2a_{12}a_{13}\sigma_{23}, \\
\sigma'_{22} &= a_{21}^2\sigma_{11} + a_{22}^2\sigma_{22} + a_{23}^2\sigma_{33} + 2a_{21}a_{22}\sigma_{12} + 2a_{21}a_{23}\sigma_{13} + 2a_{22}a_{23}\sigma_{23}, \\
\sigma'_{33} &= a_{31}^2\sigma_{11} + a_{32}^2\sigma_{22} + a_{33}^2\sigma_{33} + 2a_{31}a_{32}\sigma_{12} + 2a_{31}a_{33}\sigma_{13} + 2a_{32}a_{33}\sigma_{23}, \\
\sigma'_{12} &= a_{11}a_{21}\sigma_{11} + a_{12}a_{22}\sigma_{22} + a_{13}a_{23}\sigma_{33} \\
&\quad + (a_{11}a_{22} + a_{12}a_{21})\sigma_{12} + (a_{12}a_{23} + a_{13}a_{22})\sigma_{23} + (a_{11}a_{23} + a_{13}a_{21})\sigma_{13},
\end{aligned}$$

$$\begin{aligned}\sigma'_{23} =& a_{21}a_{31}\sigma_{11} + a_{22}a_{32}\sigma_{22} + a_{23}a_{33}\sigma_{33} \\ &+ (a_{21}a_{32} + a_{22}a_{31})\sigma_{12} + (a_{22}a_{33} + a_{23}a_{32})\sigma_{23} + (a_{21}a_{33} + a_{23}a_{31})\sigma_{13}, \\ \sigma'_{13} =& a_{11}a_{31}\sigma_{11} + a_{12}a_{32}\sigma_{22} + a_{13}a_{33}\sigma_{33} \\ &+ (a_{11}a_{32} + a_{12}a_{31})\sigma_{12} + (a_{12}a_{33} + a_{13}a_{32})\sigma_{23} + (a_{11}a_{33} + a_{13}a_{31})\sigma_{13}.\end{aligned}$$

The Mohr circle for stress is a graphical representation of this transformation of stresses.

Normal and shear stresses

The magnitude of the normal stress component σ_n of any stress vector $\mathbf{T}^{(\mathbf{n})}$ acting on an arbitrary plane with normal vector $\mathbf{n}$ at a given point, in terms of the components σ_{ij} of the stress tensor $\boldsymbol{\sigma}$, is the dot product of the stress vector and the normal vector:

$$\begin{aligned}\sigma_{\mathbf{n}} &= \mathbf{T}^{(\mathbf{n})} \cdot \mathbf{n} \\ &= T_i^{(\mathbf{n})} n_i \\ &= \sigma_{ij} n_i n_j.\end{aligned}$$

The magnitude of the shear stress component τ_n, acting in the plane spanned by the two vectors $\mathbf{T}^{(\mathbf{n})}$ and $\mathbf{n}$, can then be found using the Pythagorean theorem:

$$\begin{aligned}\tau_{\mathbf{n}} &= \sqrt{\left(T^{(\mathbf{n})}\right)^2 - \sigma_{\mathbf{n}}^2} \\ &= \sqrt{T_i^{(\mathbf{n})} T_i^{(\mathbf{n})} - \sigma_{\mathbf{n}}^2},\end{aligned}$$

where

$$\left(T^{(\mathbf{n})}\right)^2 = T_i^{(\mathbf{n})} T_i^{(\mathbf{n})} = \left(\sigma_{ij} n_j\right)\left(\sigma_{ik} n_k\right) = \sigma_{ij}\sigma_{ik} n_j n_k.$$

Equilibrium equations and symmetry of the stress tensor

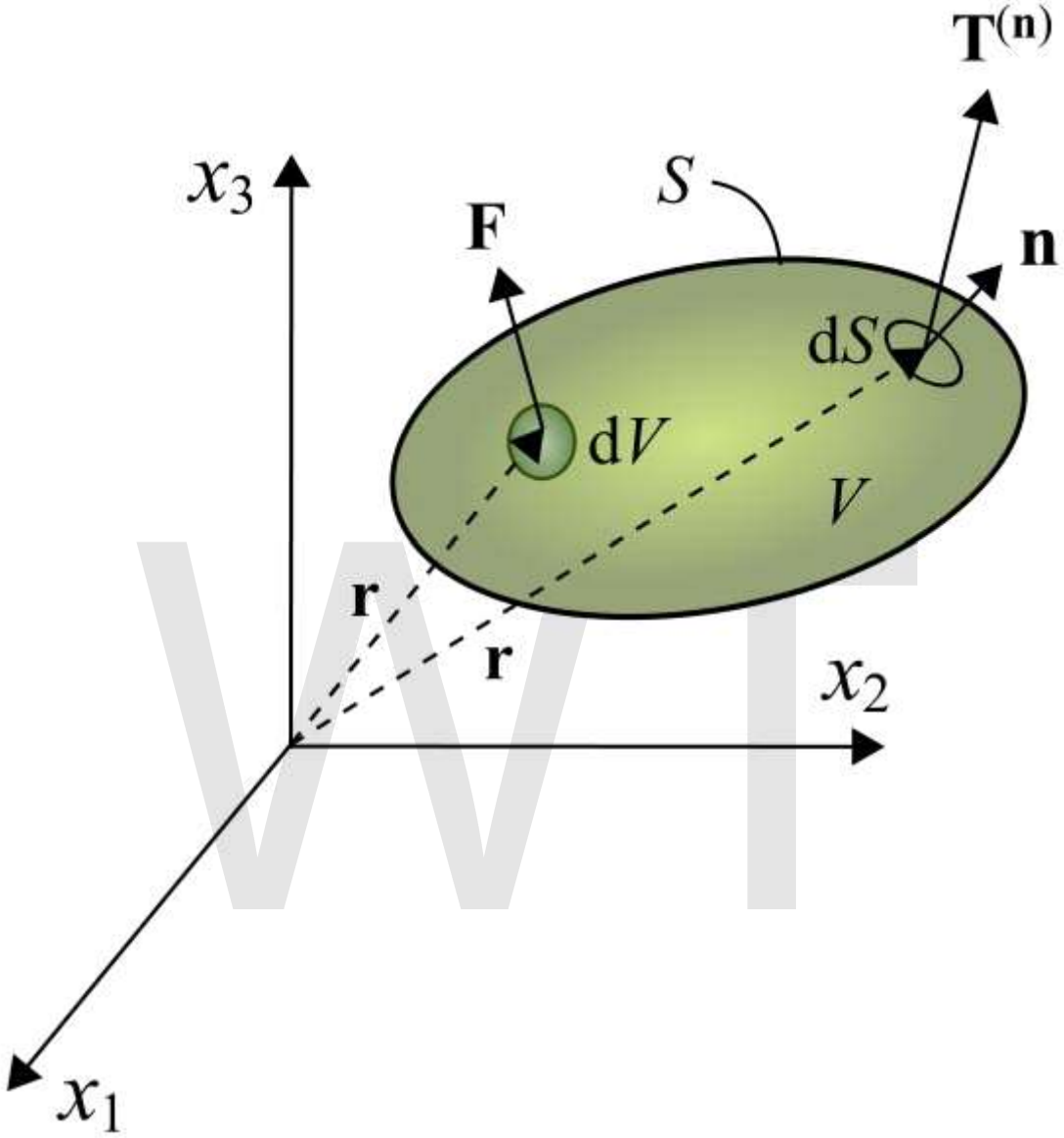

Figure 4. Continuum body in equilibrium

When a body is in equilibrium the components of the stress tensor in every point of the body satisfy the equilibrium equations,

$$\sigma_{ji,j} + F_i = 0$$

For example, for a hydrostatic fluid in equilibrium conditions, the stress tensor takes on the form:

$$\sigma_{ij} = -p\delta_{ij},$$

where p is the hydrostatic pressure, and δ_{ij} is the kronecker delta.

At the same time, equilibrium requires that the summation of moments with respect to an arbitrary point is zero, which leads to the conclusion that the stress tensor is symmetric, i.e.

$$\sigma_{ij} = \sigma_{ji}$$

However, in the presence of couple-stresses, i.e. moments per unit volume, the stress tensor is non-symmetric. This also is the case when the Knudsen number is close to one, $K_n \rightarrow 1$, or the continuum is a non-Newtonian fluid, which can lead to rotationally non-invariant fluids, such as polymers.

Principal stresses and stress invariants

At every point in a stressed body there are at least three planes, called *principal planes*, with normal vectors $\mathbf{n}$, called *principal directions*, where the corresponding stress vector is perpendicular to the plane, i.e., parallel or in the same direction as the normal vector $\mathbf{n}$, and where there are no normal shear stresses $\tau_{\mathbf{n}}$. The three stresses normal to these principal planes are called *principal stresses*.

The components σ_{ij} of the stress tensor depend on the orientation of the coordinate system at the point under consideration. However, the stress tensor itself is a physical quantity and as such, it is independent of the coordinate system chosen to represent it. There are certain invariants associated with every tensor which are also independent of the coordinate system. For example, a vector is a simple tensor of rank one. In three dimensions, it has three components. The value of these components will depend on the coordinate system chosen to represent the vector, but the length of the vector is a physical quantity (a scalar) and is independent of the coordinate system chosen to represent the vector. Similarly, every second rank tensor (such as the stress and the strain tensors) has three independent invariant quantities associated with it. One set of such invariants are the principal stresses of the stress tensor, which are just the eigenvalues of the stress tensor. Their direction vectors are the principal directions or eigenvectors.

A stress vector parallel to the normal vector $\mathbf{n}$ is given by:

$$\mathbf{T}^{(\mathbf{n})} = \lambda \mathbf{n} = \sigma_{\mathbf{n}} \mathbf{n}$$

where λ is a constant of proportionality, and in this particular case corresponds to the magnitudes $\sigma_{\mathbf{n}}$ of the normal stress vectors or principal stresses.

Knowing that $T_i^{(n)} = \sigma_{ij} n_j$ and $n_i = \delta_{ij} n_j$, we have

$$
\begin{aligned}
T_i^{(n)} &= \lambda n_i \\
\sigma_{ij} n_j &= \lambda n_i \\
\sigma_{ij} n_j - \lambda n_i &= 0 \\
\left(\sigma_{ij} - \lambda \delta_{ij}\right) n_j &= 0
\end{aligned}
$$

This is a homogeneous system, i.e. equal to zero, of three linear equations where n_j are the unknowns. To obtain a nontrivial (non-zero) solution for n_j, the determinant matrix of the coefficients must be equal to zero, i.e. the system is singular. Thus,

$$
\left|\sigma_{ij} - \lambda \delta_{ij}\right| = \begin{vmatrix} \sigma_{11} - \lambda & \sigma_{12} & \sigma_{13} \\ \sigma_{21} & \sigma_{22} - \lambda & \sigma_{23} \\ \sigma_{31} & \sigma_{32} & \sigma_{33} - \lambda \end{vmatrix} = 0
$$

Expanding the determinant leads to the *characteristic equation*

$$
\left|\sigma_{ij} - \lambda \delta_{ij}\right| = -\lambda^3 + I_1 \lambda^2 - I_2 \lambda + I_3 = 0
$$

where

$$
\begin{aligned}
I_1 &= \sigma_{11} + \sigma_{22} + \sigma_{33} \\
&= \sigma_{kk} \\
I_2 &= \begin{vmatrix} \sigma_{22} & \sigma_{23} \\ \sigma_{32} & \sigma_{33} \end{vmatrix} + \begin{vmatrix} \sigma_{11} & \sigma_{13} \\ \sigma_{31} & \sigma_{33} \end{vmatrix} + \begin{vmatrix} \sigma_{11} & \sigma_{12} \\ \sigma_{21} & \sigma_{22} \end{vmatrix} \\
&= \sigma_{11}\sigma_{22} + \sigma_{22}\sigma_{33} + \sigma_{11}\sigma_{33} - \sigma_{12}^2 - \sigma_{23}^2 - \sigma_{13}^2 \\
&= \frac{1}{2}\left(\sigma_{ii}\sigma_{jj} - \sigma_{ij}\sigma_{ji}\right) \\
I_3 &= \det(\sigma_{ij}) \\
&= \sigma_{11}\sigma_{22}\sigma_{33} + 2\sigma_{12}\sigma_{23}\sigma_{31} - \sigma_{12}^2\sigma_{33} - \sigma_{23}^2\sigma_{11} - \sigma_{13}^2\sigma_{22}
\end{aligned}
$$

The characteristic equation has three real roots λ, i.e. not imaginary due to the symmetry of the stress tensor. The three roots $\lambda_1 = \sigma_1$, $\lambda_2 = \sigma_2$, and $\lambda_3 = \sigma_3$ are the eigenvalues or principal stresses, and they are the roots of the Cayley–Hamilton theorem. The principal stresses are unique for a given stress tensor. Therefore, from the characteristic equation it is seen that the coefficients I_1, I_2 and I_3, called the first, second, and third *stress invariants*, respectively, have always the same value regardless of the orientation of the coordinate system chosen.

For each eigenvalue, there is a non-trivial solution for n_j in the equation $(\sigma_{ij} - \lambda\delta_{ij})\, n_j = 0$. These solutions are the principal directions or eigenvectors defining the plane where the principal stresses act. The principal stresses and principal directions characterize the stress at a point and are independent of the orientation of the coordinate system.

If we choose a coordinate system with axes oriented to the principal directions, then the normal stresses will be the principal stresses and the stress tensor is represented by a diagonal matrix:

$$\sigma_{ij} = \begin{bmatrix} \sigma_1 & 0 & 0 \\ 0 & \sigma_2 & 0 \\ 0 & 0 & \sigma_3 \end{bmatrix}$$

The principal stresses may be combined to form the stress invariants, I_1, I_2, and I_3. The first and third invariant are the trace and determinant respectively, of the stress tensor. Thus,

$$I_1 = \sigma_1 + \sigma_2 + \sigma_3$$
$$I_2 = \sigma_1\sigma_2 + \sigma_2\sigma_3 + \sigma_3\sigma_1$$
$$I_3 = \sigma_1\sigma_2\sigma_3$$

Because of its simplicity, working and thinking in the principal coordinate system is often very useful when considering the state of the elastic medium at a particular point.

Principal stresses are often expressed in the following equation for evaluating stresses in the x and y directions or axial and bending stresses on a part. The principal normal stresses can then be used to calculate the Von Mises stress and ultimately the safety factor and margin of safety.

$$\sigma_1, \sigma_2 = \frac{\sigma_x + \sigma_y}{2} \pm \sqrt{\left(\frac{\sigma_x - \sigma_y}{2}\right)^2 + \tau_{xy}^2}$$

Using just the part of the equation under the square root is equal to the maximum and minimum shear stress for plus and minus. This is shown as:

$$\tau_{max}, \tau_{min} = \pm\sqrt{\left(\frac{\sigma_x - \sigma_y}{2}\right)^2 + \tau_{xy}^2}$$

Maximum and minimum shear stresses

The maximum shear stress or maximum principal shear stress is equal to one-half the difference between the largest and smallest principal stresses, and acts on the plane that bisects the angle between the directions of the largest and smallest principal stresses, i.e. the plane of the maximum shear stress is oriented 45° from the principal stress planes. The maximum shear stress is expressed as

$$\tau_{\mathbf{max}} = \frac{1}{2}\left|\sigma_{\mathbf{max}} - \sigma_{\mathbf{min}}\right|$$

Assuming $\sigma_1 \geq \sigma_2 \geq \sigma_3$ then

$$\tau_{\mathbf{max}} = \frac{1}{2}\left|\sigma_1 - \sigma_3\right|$$

The normal stress component acting on the plane for the maximum shear stress is non-zero and it is equal to

$$\sigma_{\mathrm{n}} = \frac{1}{2}\left(\sigma_1 + \sigma_3\right)$$

Stress deviator tensor

The stress tensor σ_{ij} can be expressed as the sum of two other stress tensors:

1. a *mean hydrostatic stress tensor* or *volumetric stress tensor* or *mean normal stress tensor*, $p\delta_{ij}$, which tends to change the volume of the stressed body; and
2. a deviatoric component called the *stress deviator tensor*, s_{ij}, which tends to distort it.

So:

$$\sigma_{ij} = s_{ij} + p\delta_{ij},$$

where p is the mean stress given by

$$p = \frac{\sigma_{kk}}{3} = \frac{\sigma_{11} + \sigma_{22} + \sigma_{33}}{3} = \tfrac{1}{3}I_1.$$

Note that convention in solid mechanics differs slightly from what is listed above. In solid mechanics, pressure is generally defined as negative one-third the trace of the stress tensor.

The deviatoric stress tensor can be obtained by subtracting the hydrostatic stress tensor from the stress tensor:

$$s_{ij} = \sigma_{ij} - \frac{\sigma_{kk}}{3}\delta_{ij},$$

$$\begin{bmatrix} s_{11} & s_{12} & s_{13} \\ s_{21} & s_{22} & s_{23} \\ s_{31} & s_{32} & s_{33} \end{bmatrix} = \begin{bmatrix} \sigma_{11} & \sigma_{12} & \sigma_{13} \\ \sigma_{21} & \sigma_{22} & \sigma_{23} \\ \sigma_{31} & \sigma_{32} & \sigma_{33} \end{bmatrix} - \begin{bmatrix} p & 0 & 0 \\ 0 & p & 0 \\ 0 & 0 & p \end{bmatrix}$$

$$= \begin{bmatrix} \sigma_{11} - p & \sigma_{12} & \sigma_{13} \\ \sigma_{21} & \sigma_{22} - p & \sigma_{23} \\ \sigma_{31} & \sigma_{32} & \sigma_{33} - p \end{bmatrix}.$$

Invariants of the stress deviator tensor

As it is a second order tensor, the stress deviator tensor also has a set of invariants, which can be obtained using the same procedure used to calculate the invariants of the stress tensor. It can be shown that the principal directions of the stress deviator tensor s_{ij} are the same as the principal directions of the stress tensor σ_{ij}. Thus, the characteristic equation is

$$|s_{ij} - \lambda\delta_{ij}| = \lambda^3 - J_1\lambda^2 - J_2\lambda - J_3 = 0,$$

where J_1, J_2 and J_3 are the first, second, and third *deviatoric stress invariants*, respectively. Their values are the same (invariant) regardless of the orientation of the coordinate system chosen. These deviatoric stress invariants can be expressed as a function of the components of s_{ij} or its principal values s_1, s_2, and s_3, or alternatively, as a function of σ_{ij} or its principal values σ_1, σ_2, and σ_3. Thus,

$$\begin{aligned}
J_1 &= s_{kk} = 0, \\
J_2 &= \tfrac{1}{2}s_{ij}s_{ji} \\
&= -s_1s_2 - s_2s_3 - s_3s_1 \\
&= \tfrac{1}{6}\left[(\sigma_{11} - \sigma_{22})^2 + (\sigma_{22} - \sigma_{33})^2 + (\sigma_{33} - \sigma_{11})^2\right] + \sigma_{12}^2 + \sigma_{23}^2 + \sigma_{31}^2 \\
&= \tfrac{1}{6}\left[(\sigma_1 - \sigma_2)^2 + (\sigma_2 - \sigma_3)^2 + (\sigma_3 - \sigma_1)^2\right] \\
&= \tfrac{1}{3}I_1^2 - I_2, \\
J_3 &= \det(s_{ij}) \\
&= \tfrac{1}{3}s_{ij}s_{jk}s_{ki} \\
&= s_1s_2s_3 \\
&= \tfrac{2}{27}I_1^3 - \tfrac{1}{3}I_1I_2 + I_3.
\end{aligned}$$

Because $s_{kk} = 0$, the stress deviator tensor is in a state of pure shear.

A quantity called the equivalent stress or von Mises stress is commonly used in solid mechanics. The equivalent stress is defined as

$$\sigma_e = \sqrt{3\ J_2} = \sqrt{\tfrac{1}{2}\ [(\sigma_1 - \sigma_2)^2 + (\sigma_2 - \sigma_3)^2 + (\sigma_3 - \sigma_1)^2]}\,.$$

Octahedral stresses

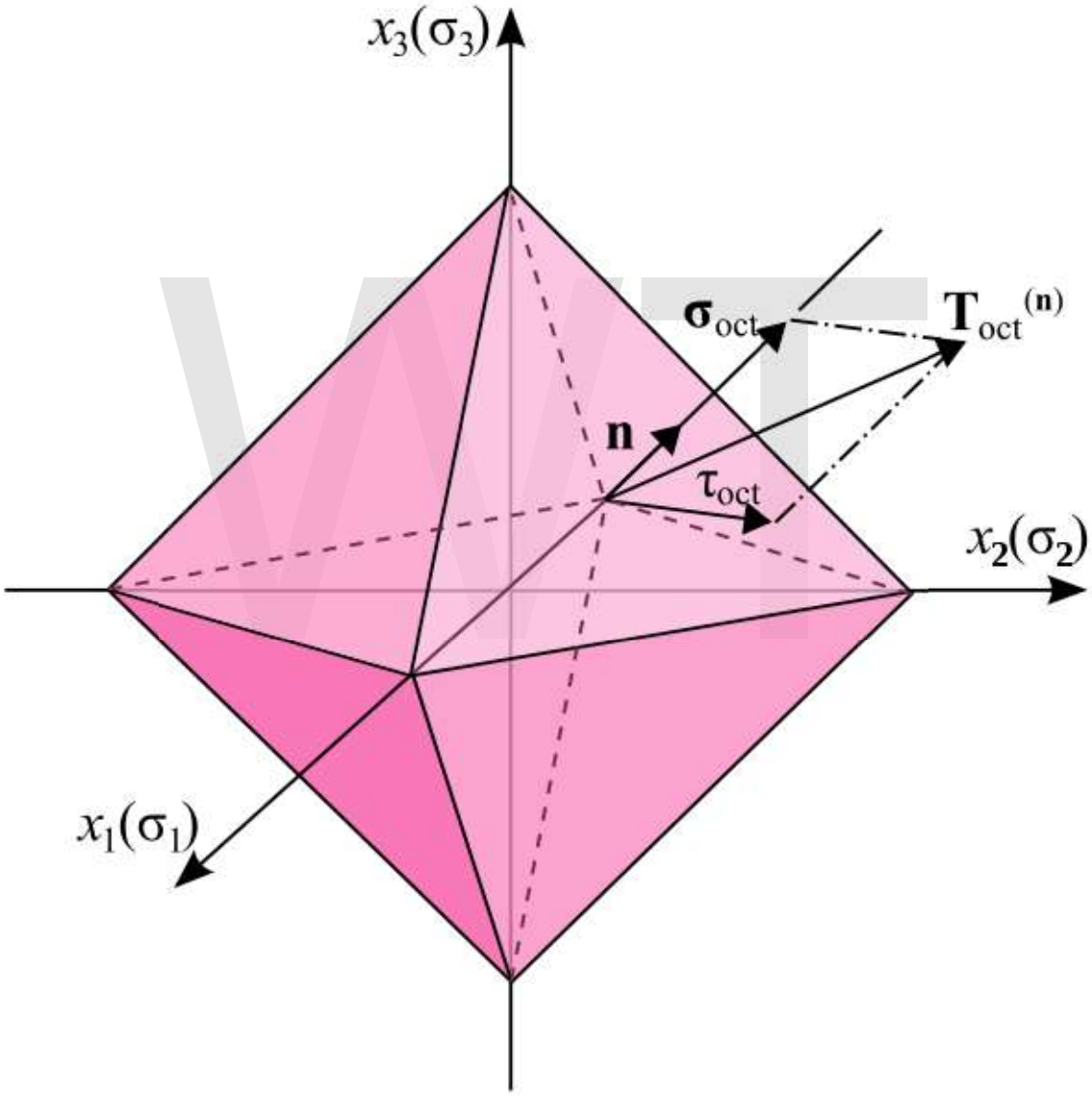

Figure 6. Octahedral stress planes

Considering the principal directions as the coordinate axes, a plane whose normal vector makes equal angles with each of the principal axes (i.e. having direction cosines equal to

$|1/\sqrt{3}|$) is called an *octahedral plane*. There are a total of eight octahedral planes (Figure 6). The normal and shear components of the stress tensor on these planes are called *octahedral normal stress* $\sigma_{\mathrm{oct}}$and *octahedral shear stress* τ_{oct}, respectively.

Knowing that the stress tensor of point O (Figure 6) in the principal axes is

$$\sigma_{ij} = \begin{bmatrix} \sigma_1 & 0 & 0 \\ 0 & \sigma_2 & 0 \\ 0 & 0 & \sigma_3 \end{bmatrix}$$

the stress vector on an octahedral plane is then given by:

$$\begin{aligned} \mathbf{T}_{\mathrm{oct}}^{(\mathbf{n})} &= \sigma_{ij} n_i \mathbf{e}_j \\ &= \sigma_1 n_1 \mathbf{e}_1 + \sigma_2 n_2 \mathbf{e}_2 + \sigma_3 n_3 \mathbf{e}_3 \\ &= \tfrac{1}{\sqrt{3}}(\sigma_1 \mathbf{e}_1 + \sigma_2 \mathbf{e}_2 + \sigma_3 \mathbf{e}_3) \end{aligned}$$

The normal component of the stress vector at point O associated with the octahedral plane is

$$\begin{aligned} \sigma_{\mathrm{oct}} &= T_i^{(n)} n_i \\ &= \sigma_{ij} n_i n_j \\ &= \sigma_1 n_1 n_1 + \sigma_2 n_2 n_2 + \sigma_3 n_3 n_3 \\ &= \tfrac{1}{3}(\sigma_1 + \sigma_2 + \sigma_3) = \tfrac{1}{3} I_1 \end{aligned}$$

which is the mean normal stress or hydrostatic stress. This value is the same in all eight octahedral planes. The shear stress on the octahedral plane is then

$$\begin{aligned} \tau_{\mathrm{oct}} &= \sqrt{T_i^{(n)} T_i^{(n)} - \sigma_{\mathrm{n}}^2} \\ &= \left[\tfrac{1}{3}(\sigma_1^2 + \sigma_2^2 + \sigma_3^2) - \tfrac{1}{9}(\sigma_1 + \sigma_2 + \sigma_3)^2\right]^{1/2} \\ &= \tfrac{1}{3}\left[(\sigma_1 - \sigma_2)^2 + (\sigma_2 - \sigma_3)^2 + (\sigma_3 - \sigma_1)^2\right]^{1/2} = \tfrac{1}{3}\sqrt{2I_1^2 - 6I_2} = \sqrt{\tfrac{2}{3} J_2} \end{aligned}$$

Alternative measures of stress

The Cauchy stress tensor is not the only measure of stress that is used in practice. Other measures of stress include the first and second Piola–Kirchhoff stress tensors, the Biot stress tensor, and the Kirchhoff stress tensor.

Piola–Kirchhoff stress tensor

In the case of finite deformations, the *Piola–Kirchhoff stress tensors* are used to express the stress relative to the reference configuration. This is in contrast to the Cauchy stress tensor which expresses the stress relative to the present configuration. For infinitesimal deformations or rotations, the Cauchy and Piola–Kirchhoff tensors are identical. These tensors take their names from Gabrio Piola and Gustav Kirchhoff.

Whereas the Cauchy stress tensor, $\boldsymbol{\sigma}$ relates stresses in the current configuration, the deformation gradient and strain tensors are described by relating the motion to the reference configuration; thus not all tensors describing the state of the material are in either the reference or current configuration. Having the stress, strain and deformation all described either in the reference or current configuration would make it easier to define constitutive models (for example, the Cauchy Stress tensor is variant to a pure rotation, while the deformation strain tensor is invariant; thus creating problems in defining a constitutive model that relates a varying tensor, in terms of an invariant one during pure rotation; as by definition constitutive models have to be invariant to pure rotations). The 1st Piola–Kirchhoff stress tensor, $\boldsymbol{P}$ is one possible solution to this problem. It defines a family of tensors, which describe the configuration of the body in either the current or the reference state.

The 1st Piola–Kirchhoff stress tensor, $\boldsymbol{P}$ relates forces in the *present* configuration with areas in the *reference* ("material") configuration.

$$\boldsymbol{P} = J\ \boldsymbol{\sigma} \cdot \boldsymbol{F}^{-T}$$

where $\boldsymbol{F}$ is the deformation gradient and $J = \det \boldsymbol{F}$ is the Jacobian determinant.

In terms of components with respect to an orthonormal basis, the first Piola–Kirchhoff stress is given by

$$P_{iL} = J\ \sigma_{ik}\ F^{-1}_{Lk} = J\ \sigma_{ik}\ \frac{\partial X_L}{\partial x_k}$$

Because it relates different coordinate systems, the 1st Piola–Kirchhoff stress is a two-point tensor. In general, it is not symmetric. The 1st Piola–Kirchhoff stress is the 3D generalization of the 1D concept of engineering stress.

If the material rotates without a change in stress state (rigid rotation), the components of the 1st Piola–Kirchhoff stress tensor will vary with material orientation.

The 1st Piola–Kirchhoff stress is energy conjugate to the deformation gradient.

2nd Piola–Kirchhoff stress tensor

Whereas the 1st Piola–Kirchhoff stress relates forces in the current configuration to areas in the reference configuration, the 2nd Piola–Kirchhoff stress tensor $\boldsymbol{S}$ relates forces in the reference configuration to areas in the reference configuration. The force in the reference configuration is obtained via a mapping that preserves the relative relationship between the force direction and the area normal in the current configuration.

$$\boldsymbol{S} = J\ \boldsymbol{F}^{-1} \cdot \boldsymbol{\sigma} \cdot \boldsymbol{F}^{-T}\ .$$

In index notation with respect to an orthonormal basis,

$$S_{IL} = J\ F^{-1}_{Ik}\ F^{-1}_{Lm}\ \sigma_{km} = J\ \frac{\partial X_I}{\partial x_k}\ \frac{\partial X_L}{\partial x_m}\ \sigma_{km}$$

This tensor is symmetric.

If the material rotates without a change in stress state (rigid rotation), the components of the 2nd Piola–Kirchhoff stress tensor will remain constant, irrespective of material orientation.

The 2nd Piola–Kirchhoff stress tensor is energy conjugate to the Green–Lagrange finite strain tensor.

Chapter 12

Shear Stress

Shear stress	
SI symbol:	τ
SI unit:	pascal
Derivations from other quantities:	$\tau = F / A$

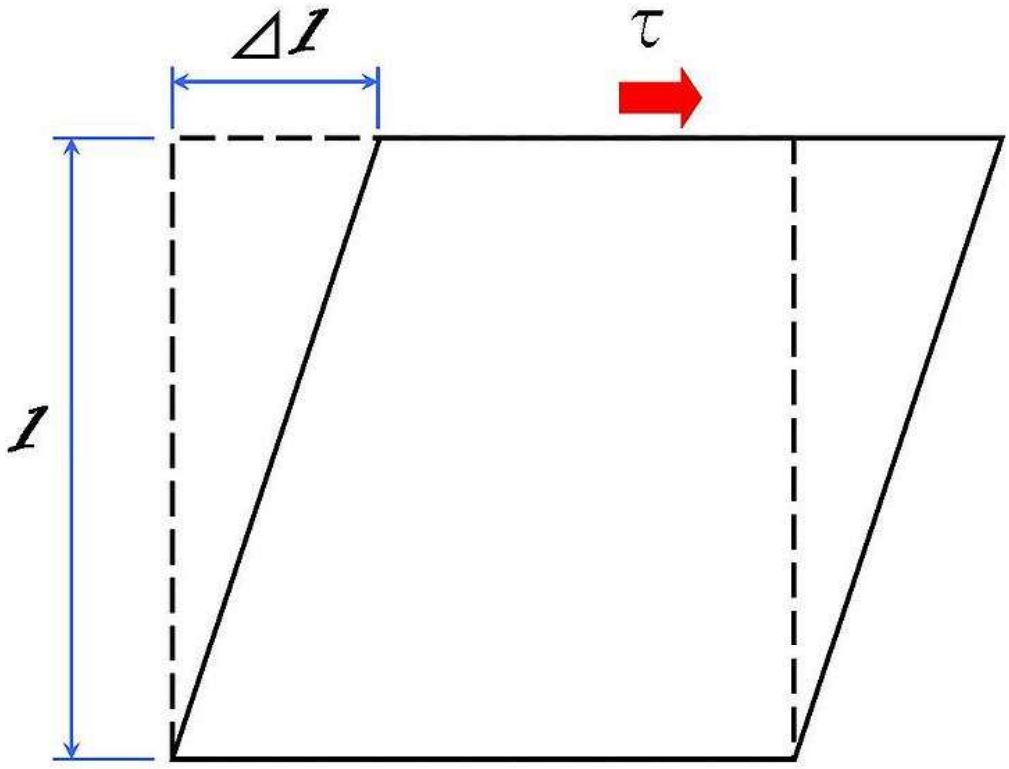

A shear stress, τ is applied to the top of the square while the bottom is held in place. This stress results in a strain, or deformation, changing the square into a parallelogram.

A **shear stress**, denoted τ (Greek: tau), is defined as a stress which is applied parallel or tangential to a face of a material, as opposed to a normal stress which is applied perpendicularly.

General shear stress

The formula to calculate average shear stress is:

$$\tau = \frac{F}{A},$$

where

τ = the shear stress;
F = the force applied;
A = the cross sectional area.

Other forms of shear stress

Beam shear

Beam shear is defined as the internal shear stress of a beam caused by the shear force applied to the beam.

$$\tau = \frac{VQ}{It},$$

where

V = total shear force at the location in question;
Q = statical moment of area;
t = thickness in the material perpendicular to the shear;
I = Moment of Inertia of the entire cross sectional area.

This formula is also known as the Jourawski formula.

Semi-monocoque shear

Shear stresses within a semi-monocoque structure may be calculated by idealizing the cross-section of the structure into a set of stringers (carrying only axial loads) and webs (carrying only shear flows). Dividing the shear flow by the thickness of a given portion of the semi-monocoque structure yields the shear stress. Thus, the maximum shear stress will occur either in the web of maximum shear flow or minimum thickness.

Also constructions in soil can fail due to shear; e.g., the weight of an earth-filled dam or dike may cause the subsoil to collapse, like a small landslide.

Impact shear

The maximum shear stress created in a solid round bar subject to impact is given as the equation:

$$\tau = 2\left(\frac{UG}{V}\right)^{\frac{1}{2}},$$

where

U = change in kinetic energy;
G = shear modulus;
V = volume of rod;

and

$$U = U_{rotating} + U_{applied};$$
$$U_{rotating} = \frac{1}{2} I\omega^2;$$
$$U_{applied} = T\theta_{displaced};$$
I = mass moment of inertia;
ω = angular speed.

Shear stress in fluids

Any real fluids (liquids and gases included) moving along solid boundary will incur a shear stress on that boundary. The no-slip condition dictates that the speed of the fluid at the boundary (relative to the boundary) is zero, but at some height from the boundary the flow speed must equal that of the fluid. The region between these two points is aptly named the boundary layer. For all Newtonian fluids in laminar flow the shear stress is proportional to the strain rate in the fluid where the viscosity is the constant of proportionality. However for Non Newtonian fluids, this is no longer the case as for these fluids the viscosity is not constant. The shear stress is imparted onto the boundary as a result of this loss of velocity. The shear stress, for a Newtonian fluid, at a surface element parallel to a flat plate, at the point y, is given by:

$$\tau(y) = \mu\frac{\partial u}{\partial y},$$

where

μ is the dynamic viscosity of the fluid;
u is the velocity of the fluid along the boundary;
y is the height above the boundary.

Specifically, the wall shear stress is defined as:

$$\tau_w \equiv \tau(y=0) = \mu \left.\frac{\partial u}{\partial y}\right|_{y=0} .$$

In case of wind, the shear stress at the boundary is called wind stress.

Measurement by shear stress sensors

Diverging fringe shear stress sensor

This relationship can be exploited to measure the wall shear stress. If a sensor could directly measure the gradient of the velocity profile at the wall, then multiplying by the dynamic viscosity would yield the shear stress. Such a sensor was demonstrated by A. A. Naqwi and W. C. Reynolds. The interference pattern generated by sending a beam of light through two parallel slits forms a network of linearly diverging fringes that seem to originate from the plane of the two slits. As a particle in a fluid passes through the fringes, a receiver detects the reflection of the fringe pattern. The signal can be processed, and knowing the fringe angle, the height and velocity of the particle can be extrapolated.

Micro-pillar shear-stress sensor

A further technique recently proposed is that of slender wall-mounted micro-pillars made of the flexible polymer PDMS, which bend in reaction to the applying drag forces in the vicinity of the wall. The deflection of the pillar tips from a reference position is detected optically and serves as a representative of the wall-shear stress. It allows the instantaneous detection of the streamwise and spanwise wall-shear stress distribution in turbulent flow up to high Reynolds numbers.

Chapter 13

Timoshenko Beam Theory

The **Timoshenko beam theory** was developed by Ukrainian-born scientist Stephen Timoshenko in the beginning of the 20th century. The model takes into account shear deformation and rotational inertia effects, making it suitable for describing the behaviour of short beams, sandwich composite beams or beams subject to high-frequency excitation when the wavelength approaches the thickness of the beam. The resulting equation is of 4^{th} order, but unlike ordinary beam theory - i.e. Bernoulli-Euler theory - there is also a second order spatial derivative present. Physically, taking into account the added mechanisms of deformation effectively lowers the stiffness of the beam, while the result is a larger deflection under a static load and lower predicted eigenfrequencies for a given set of boundary conditions. The latter effect is more noticeable for higher frequencies as the wavelength becomes shorter, and thus the distance between opposing shear forces decreases.

If the shear modulus of the beam material approaches infinity - and thus the beam becomes rigid in shear - and if rotational inertia effects are neglected, Timoshenko beam theory converges towards ordinary beam theory.

Governing equations

Quasistatic Timoshenko beam

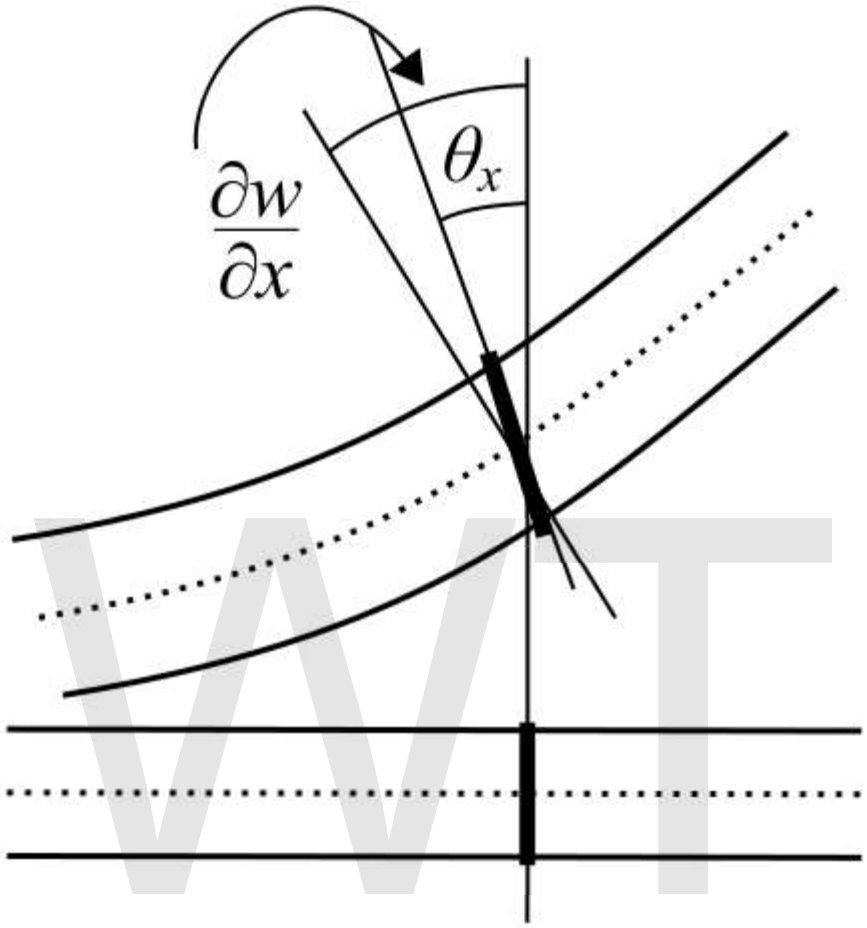

Deformation of a Timoshenko beam. The normal rotates by an amount $\theta_x = \varphi(x)$ which is not equal to dw / dx.

In static Timoshenko beam theory without axial effects, the displacements of the beam are assumed to be given by

$$u_x(x, y, z) = -z\ \varphi(x)\ ;\quad u_y(x, y, z) = 0\ ;\quad u_z(x, y) = w(x)$$

where (x,y,z) are the coordinates of a point in the beam, u_x, u_y, u_z are the components of the displacement vector in the three coordinate directions, φ is the angle of rotation of the normal to the mid-surface of the beam, and w is the displacement of the mid-surface in the z-direction.

The governing equations are the following uncoupled system of ordinary differential equations:

$$\frac{\mathrm{d}^2}{\mathrm{d}x^2}\left(EI\frac{\mathrm{d}\varphi}{\mathrm{d}x}\right) = q(x,t)$$
$$\frac{\mathrm{d}w}{\mathrm{d}x} = \varphi - \frac{1}{\kappa AG}\frac{\mathrm{d}}{\mathrm{d}x}\left(EI\frac{\mathrm{d}\varphi}{\mathrm{d}x}\right)$$

The Timoshenko beam theory for the static case is equivalent to the Euler-Bernoulli theory when the last term above is neglected, an approximation that is valid when

$$\frac{EI}{\kappa L^2 AG} \ll 1$$

where L is the length of the beam.

Combining the two equations gives, for a homogeneous beam of constant cross-section,

$$EI\,\frac{\mathrm{d}^4 w}{\mathrm{d}x^4} = q(x) - \frac{EI}{\kappa AG}\,\frac{\mathrm{d}^2 q}{\mathrm{d}x^2}$$

Dynamic Timoshenko beam

In Timoshenko beam theory without axial effects, the displacements of the beam are assumed to be given by

$$u_x(x,y,z,t) = -z\ \varphi(x,t)\ ;\quad u_y(x,y,z,t) = 0\ ;\quad u_z(x,y,z) = w(x,t)$$

where (x,y,z) are the coordinates of a point in the beam, u_x,u_y,u_z are the components of the displacement vector in the three coordinate directions, φ is the angle of rotation of the normal to the mid-surface of the beam, and w is the displacement of the mid-surface in the z-direction.

Starting from the above assumption, the Timoshenko beam theory, allowing for vibrations, may be described with the coupled linear partial differential equations :

$$\rho A\frac{\partial^2 w}{\partial t^2} - q(x,t) = \frac{\partial}{\partial x}\left[\kappa AG\left(\frac{\partial w}{\partial x} - \varphi\right)\right]$$
$$\rho I\frac{\partial^2 \varphi}{\partial t^2} = \frac{\partial}{\partial x}\left(EI\frac{\partial \varphi}{\partial x}\right) + \kappa AG\left(\frac{\partial w}{\partial x} - \varphi\right)$$

where the dependent variables are $w(x,t)$, the translational displacement of the beam, and $\varphi(x,t)$, the angular displacement. Note that unlike the Euler-Bernoulli theory, the angular deflection is another variable and not approximated by the slope of the deflection. Also,

- ρ is the density of the beam material (but not the linear density).
- A is the cross section area.
- E is the elastic modulus.
- G is the shear modulus.
- I is the second moment of area.
- κ, called the Timoshenko shear coefficient, depends on the geometry. Normally, κ = 5 / 6 for a rectangular section.
- $q(x,t)$ is a distributed load (force per length).

These parameters are not necessarily constants.

For a linear elastic, isotropic, homogeneous beam of constant cross-section these two equations can be combined to give

$$EI\,\frac{\partial^4 w}{\partial x^4}+m\,\frac{\partial^2 w}{\partial t^2}-\left(\rho I+\frac{EIm}{kAG}\right)\frac{\partial^4 w}{\partial x^2\,\partial t^2}+\frac{Jm}{kAG}\,\frac{\partial^4 w}{\partial t^4}=q(x,t)+\frac{\rho I}{kAG}\,\frac{\partial^2 q}{\partial t^2}-\frac{EI}{kAG}\,\frac{\partial^2 q}{\partial x^2}$$

Axial effects

If the displacements of the beam are given by

$$u_x(x,y,z,t)=u_0(x,t)-z\;\varphi(x,t)\;;\quad u_y(x,y,z,t)=0\;;\quad u_z(x,y,z)=w(x,t)$$

where u_0 is an additional displacement in the x-direction, then the governing equations of a Timoshenko beam take the form

$$m\frac{\partial^2 w}{\partial t^2}=\frac{\partial}{\partial x}\left[\kappa AG\left(\frac{\partial w}{\partial x}-\varphi\right)\right]+q(x,t)$$

$$J\frac{\partial^2 \varphi}{\partial t^2}=N(x,t)\,\frac{\partial w}{\partial x}+\frac{\partial}{\partial x}\left(EI\frac{\partial \varphi}{\partial x}\right)+\kappa AG\left(\frac{\partial w}{\partial x}-\varphi\right)$$

where $J=\rho I$ and $N(x,t)$ is an externally applied axial force. Any external axial force is balanced by the stress resultant

$$N_{xx}(x,t)=\int_{-h}^{h}\sigma_{xx}\,dz$$

where σ_{xx} is the axial stress and the thickness of the beam has been assumed to be $2h$.

The combined beam equation with axial force effects included is

$$EI\,\frac{\partial^4 w}{\partial x^4}+N\,\frac{\partial^2 w}{\partial x^2}+m\,\frac{\partial^2 w}{\partial t^2}-\left(J+\frac{mEI}{\kappa AG}\right)\,\frac{\partial^4 w}{\partial x^2\partial t^2}+\frac{mJ}{\kappa AG}\,\frac{\partial^4 w}{\partial t^4}=q+\frac{J}{\kappa AG}\,\frac{\partial^2 q}{\partial t^2}-\frac{EI}{\kappa AG}\,\frac{\partial^2 q}{\partial x^2}$$

Damping

If, in addition to axial forces, we assume a damping force that is proportional to the velocity with the form

$$\eta(x)\,\frac{\partial w}{\partial x}$$

the coupled governing equations for a Timoshenko beam take the form

$$m\frac{\partial^2 w}{\partial t^2}+\eta(x)\,\frac{\partial w}{\partial x}=\frac{\partial}{\partial x}\left[\kappa AG\left(\frac{\partial w}{\partial x}-\varphi\right)\right]+q(x,t)$$
$$J\frac{\partial^2 \varphi}{\partial t^2}=N\frac{\partial w}{\partial x}+\frac{\partial}{\partial x}\left(EI\frac{\partial \varphi}{\partial x}\right)+\kappa AG\left(\frac{\partial w}{\partial x}-\varphi\right)$$

and the combined equation becomes

$$EI\,\frac{\partial^4 w}{\partial x^4}+N\,\frac{\partial^2 w}{\partial x^2}+m\,\frac{\partial^2 w}{\partial t^2}-\left(J+\frac{mEI}{\kappa AG}\right)\,\frac{\partial^4 w}{\partial x^2\partial t^2}+\frac{mJ}{\kappa AG}\,\frac{\partial^4 w}{\partial t^4}-\frac{J\eta(x)}{\kappa AG}\,\frac{\partial^3 w}{\partial t^3}$$
$$+EI\,\frac{\partial^2}{\partial x^2}\left(\eta(x)\frac{\partial w}{\partial t}\right)-\eta(x)\frac{\partial w}{\partial t}=q+\frac{J}{\kappa AG}\,\frac{\partial^2 q}{\partial t^2}-\frac{EI}{\kappa AG}\,\frac{\partial^2 q}{\partial x^2}$$

Shear coefficient

Determining the shear coefficient is not straightforward (nor are the determined values widely accepted, ie there's more than one answer), generally it must satisfy:

$$\int_A \tau dA=\kappa AG\varphi$$